RESERVOIR CHARACTERISTICS OF BOKA BIL AND BHUBAN FORMATIONS OF NEOGENE SURMA GROUP, SRIKAIL GAS FIELD, BENGAL BASIN, BANGLADESH

BY

KAZI FAIZ ALAM

A Thesis Presented to the
DEANSHIP OF GRADUATE STUDIES

KING FAHD UNIVERSITY OF PETROLEUM & MINERALS

DHAHRAN, SAUDI ARABIA

In Partial Fulfillment of the
Requirements for the Degree of

MASTER OF SCIENCE

In

GEOLOGY

December 2019

KING FAHD UNIVERSITY OF PETROLEUM & MINERALS

DHAHRAN- 31261, SAUDI ARABIA

DEANSHIP OF GRADUATE STUDIES

This thesis has been written by KAZI FAIZ ALAM under the direction of his thesis advisor and approved by his thesis committee. This work has been presented and accepted by the Dean of Graduate Studies, in partial fulfillment of the requirements for the degree of **MASTER OF SCIENCE IN GEOLOGY.**

Dr. Oman M. Abdullatif
(Advisor)

Dr. Abdullatif Abdulrahman Al-Shuhail
Department Chairman

Dr. Ammar El-Husseiny
(Member)

Dr. Salam A. Zummo
Dean of Graduate Studies

Dr. Lamidi Olabode Babalola
(Member)

25/12/09

Date

To

my parents Kazi Firoz Alam and Kazi Faizunnahar Alam, my wife Mousona Islam, my only daughter Kazi Fatima Faiz Farista, my brother Kazi Kais Alam and sister Kazi Farhana Sharmin.

ACKNOWLEDGMENTS

All the admiration and glory are due to Almighty Allah (Subhanahu wa tala) for his unlimited blessings and direction. May Allah grant his peace on the prophet, Muhammad (Peace be upon him). I sincerely acknowledge for the support provided by King Fahd University of Petroleum and Minerals (KFUPM) for completing my study in such a conducive environment. I am also grateful to Bangladesh Petroleum Exploration and Production Company Limited (BAPEX), PETROBANGLA where I am working for providing me the samples and data for my current research. The core plugs and thin section for petrographic study were made in Center for integrative Petroleum Research Laboratories. Porosity and permeability measurements, QEMSCAN analysis, SEM analysis were also done in CIPR as well. XRD analysis and clay separation was done in the laboratories of Geoscience Department. All manager and operators of this laboratories are highly acknowledged for their kind support.

I would like to express by gratitude to my thesis advisor, Dr. Osman Mahmoud Abdullatif for his kind support for bringing data from my company, his effort and guidance for doing this research. My committee members, Dr. Ammar El-Hussainy and Dr. Lamidi Olabode Babalola are highly appreciated for their support and guidance during this research work.

I would like to thank the chairman, Dr. Abdullatif Abdulrahman Al-Shuhail, all the faculty members of Geoscience Department and my colleagues Md. Saleh Ahmed, Muhammad Monirul Islam, Md. Pavel Khan, Abdullah Alqubalee, Septriandi Chan, Ahmed A. Shaheen, Argo and Hasan M. H Alsaihati for their supports and encouragements.

TABLE OF CONTENTS

LIST OF TABLES

LIST OF FIGURES

LIST OF ABBREVIATIONS

XRD	:	X-Ray Diffraction
QEMSCAN	:	Quantitative Evaluation of Minerals by Scanning Electron Microscopy
SEM	:	Scanning Electron Microscopy
EDS	:	Energy-dispersive X-ray Spectrometry
V_{sh}	:	Volume of Shale
S_w	:	Water Saturation

ABSTRACT

Full Name : [Kazi Faiz Alam]

Thesis Title : [Reservoir Characteristics of Boka Bil and Bhuban Formations of Neogene Surma Group, Srikail Gas Field, Bengal Basin, Bangladesh]

Major Field : [Geology]

Date of Degree : [December 2019]

Reservoir characterization is very important to develop the suitable and sustainable exploration and production plan. This study aimed to characterize the producing gas bearing sandstone zones and investigate controls on reservoir heterogeneity and quality of the Miocene Bhuban Formation of Neogene Surma Group at the Srikail gas field, Bengal basin, Bangladesh. The study integrated wireline logs and core samples' data collected from three gas bearing zones of Srikail gas field (well-3 and 4) to achieve the research objectives. Methodology used in the study includes lithofacies and electro-facies identification from core and gamma ray log respectively, their association as well as determination of depositional environment. Petrophysical, petrographic and geochemical analyses were also carried out on the core samples. Three gas bearing zones D-upper, D-lower and E-sand were identified from wireline log interpretation. Different electro-facies have been identified from the gamma ray log analysis. Three main lithofacies associations with their depositional environments have also been identified from the core analysis of the above zones and finally a conceptual depositional model was constructed. According to the wireline log and core analyses, the D-lower and E-sands are characterized by higher porosity and permeability values than the D-upper sand. These sandstones are medium to fine grained, moderate to well sorted and were deposited in a fluvial to deltaic environment.

Based on the Folk's sandstone classification scheme, the sandstones were classified as subarkosic arenites. The medium to coarse grain facies association shows are of better reservoir quality than the fluvial channel sands. These sands have up to 15-20% porosity and 30-100 mD permeability with low ductile mineral content and less interbedded clay layers. The same reservoirs in the other field at shallower depth shows higher porosity and permeability. Depositional environments and diagenetic processes controlled the reservoir quality in the studied field. Mechanical compaction plays a major role on the reservoir quality regionally. Its effect on reservoir quality increases with increasing proportions of ductile grains in the samples. Authigenic clays like illite, kaolinite and chlorite also play an important role in reservoir quality reduction. Illite reduced the porosity and permeability by blocking pore throats, kaolinite occludes the intergranular space and chlorite fills the secondary porosity created by feldspar dissolution. Quartz overgrowth also reduced the porosity and permeability of the examined core samples by lining the pore throats. As studied formation is the main producing reservoir in Bangladesh, the outcomes of this study can be integrated with further studies, such as pore size distribution, same studies on the other gas fields to evaluate the Boka Bil and Bhuban formation in other areas. The results of this study might also enhance an understanding and prediction of other reservoir targets for exploration and development. The determination of pore size distribution and integration of other sub-surface data of the Boka Bil and Bhuban Formations of Surma group sediments on a regional scale, can help to predict the reservoir quality and architecture in Bengal basin.

ملخص الرسالة

الاسم الكامل: كازي فايز علام

عنوان الرسالة: خصائص مكامن تكوينات بوكا بيل وبوبان من مجموعة سورما ذات العمر النيوجين، حقل غاز سريكيل، حوض البنغال، بنغلاديش

التخصص: الجيولوجيا

تاريخ الدرجة العلمية: ديسمبر 2019

الدراسة إلى دراسة المكامن البترولية مهم جداً لتطوير خطة الاستكشاف والإنتاج المناسبة والمستدامة. تهدف هذه دراسة مناطق الحجر الرملي الحامل للغاز والتحقق من الأسباب المتحكمة في عدم تجانس المكمن وجودته في تكوين بوبان من العصر الميوسين التابع لمجموعة سورما في حقل غاز سريكيل، حوض البنغال، بنغلاديش. ضمت الدراسة سجلات قياسات الآبار وبيانات العينات الصخرية التي تم جمعها من ثلاث تكوينات تحمل الغاز من حقل غاز سريكيل (بئر 3 و4) لتحقيق أهداف البحث. تشتمل طريقة الدراسة على تحديد السحنات الصخرية والكهربائية من العينات الصخرية وسجلات اشعة غاما على الترتيب، دراسة تجمعاتها وكذلك تحديد بيئة الترسب. وأجريت أيضا التحليلات هي د- البتروفيزيائية والبتروغرافية والجيوكيميائية على العينات الصخرية. وقد تم تحديد ثلاث مناطق تحمل الغاز من تفسير سجلات الآبار. تم التعرف على مختلف السحنات الكهربائية من تحليل سجل العلوي، د-السفلي وي-الرمل كما تم تحديد ثلاث مجموعات رئيسية من السحنات الصخرية مع بيئات ترسبها من تحليل العينات الصخرية .أشعة جاما للنطاقات المذكورة أعلاه، وأخيراً تم عمل نموذج تصوري للترسيب. وفقًا لسجلات الابار وتحليل العينات الصخرية، هذه الأحجار الرملية متوسطة إلى بقيم مسامية ونفاذية أعلى من رمل د-العلوي. وي-الرمل تتميز نطاقات د-السفلي دقيقة الحبيبات، معتدلة إلى جيدة الفرز وترسبت في بيئة نهرية إلى بيئة دلتا. استنادًا إلى مخطط تصنيف الحجر الرملي من فولك، تم تصنيف الأحجار الرملية على أنها أرينات تحت الاركوزية. تظهر السحنات ذات الحبيبات المتوسطة إلى الخشنة جودة خزان أفضل من رمال القنوات النهرية. هذه الرمال لها ما يصل إلى 15-20 ٪ من المسامية ونفاذية 30-ملي دارسي مع محتوى منخفض من المعادن المرنة وطبقات الطين المتداخلة. نفس هذه المكامن موجودة في 100 حقل آخر على عمق ضحل وتظهر مسامية ونفاذية اعلى. تسيطر البيئات الترسبية وعمليات ما بعد الترسيب على جودة الخزان في الحقل المدروس. يلعب الضغط الميكانيكي دورًا رئيسيًا في جودة الخزان على المستوى الإقليمي. يزداد الايلايت تأثيره على جودة الخزان مع زيادة نسبة الحبيبات المرنة في العينات. كما يلعب الطين مكاني النشأة مثل دورًا مهمًا في تقليل جودة المكامن. خفض طين الايلايت من المسامية والنفاذية عن طريق والكلورايت والكاولينايت غلق المسام، كما يقفل الكاولينايت الفضاء بين الحبيبات ويملأ الكلورايت المسامية الثانوية الناتجة عن تحلل الفلسبار. قلل نمو الكوارتز أيضًا من مسامية ونفاذية العينات الصخرية التي تم فحصها عن طريق ملأ المسام. نظرًا لأن التكوين المدرسي هو المكمن الرئيسي المنتجة في بنغلاديش، يمكن دمج نتائج هذه الدراسة مع مزيد من الدراسات، مثل توزيع حجم المسام، ومع دراسات مشابهة على حقول الغاز الأخرى لتقييم تكوين بوكا بل وبوبان في مناطق أخرى. قد تعزز نتائج هذه الدراسة أيضًا فهم وتوقع الأهداف في الخزانات الأخرى من اجل الاستكشاف والتطوير. يمكن أن يساعد تحديد توزيع حجم المسام وتجميع البيانات التحت السطحية الأخرى لتشكيلات بوكا بل وبوبان من مجموعة سورما على نطاق إقليمي، على التنبؤ بجودة الخزان وبنيته في حوض البنغال.

CHAPTER 1

INTRODUCTION

1.1 Introduction

Bengal Basin is the most prolific petroleum basin with 14.16 TCF recoverable reserve in the Southeast Asia in particular, Bangladesh. To meet the increasing energy demand for the sustainable economy and development of Bangladesh, geological investigation of the Bengal Basin has drawn considerable interest due to its hydrocarbon potentials. Bengal Basin contains about 22 km of sediments from Cretaceous to Holocene age (Alam et al., 2003). An ~4000 to 5000 m thick sediments of Neogene Surma Group, the most petroliferous, occur within this huge sedimentary succession.

Total twenty-seven large to small gas fields discovered in Bangladesh, are located mainly in the north eastern part of the country (PETROBANGLA, 2018). Most of these gas fields are producing from the Boka Bil and Bhuban formations of the Neogene Surma Group. The top depth of Boka Bil and Bhuban formation increases from north to south of the Bengal basin. The lithologies of the Boka Bil Formation are comprised of an alternation of sandstone and shale sequence with shale being more dominant. On the other hand, sandstone is more dominant than shale in Bhuban Formation. Both formations host important reservoir zones in the Srikail gas Field. Reservoir zones within the Bhutan formation is the focus of this study.

1.2 Study Area

Study area includes Srikail gas field, which is a sub-surface anticline and located on the western part of thefolded belt of Bengal Foredeep within Tripura Uplift of the Bengal Basin, Bangladesh. Srikail is surrounded by few buried anticlinal structures like the Bakhrabad gas field to the south-west, Saldanadi gas field to the east, Lalmai to the South and one of the largest gas field (Titas gas field) in Bangladesh Titas to the north-east (Figure 1.1).

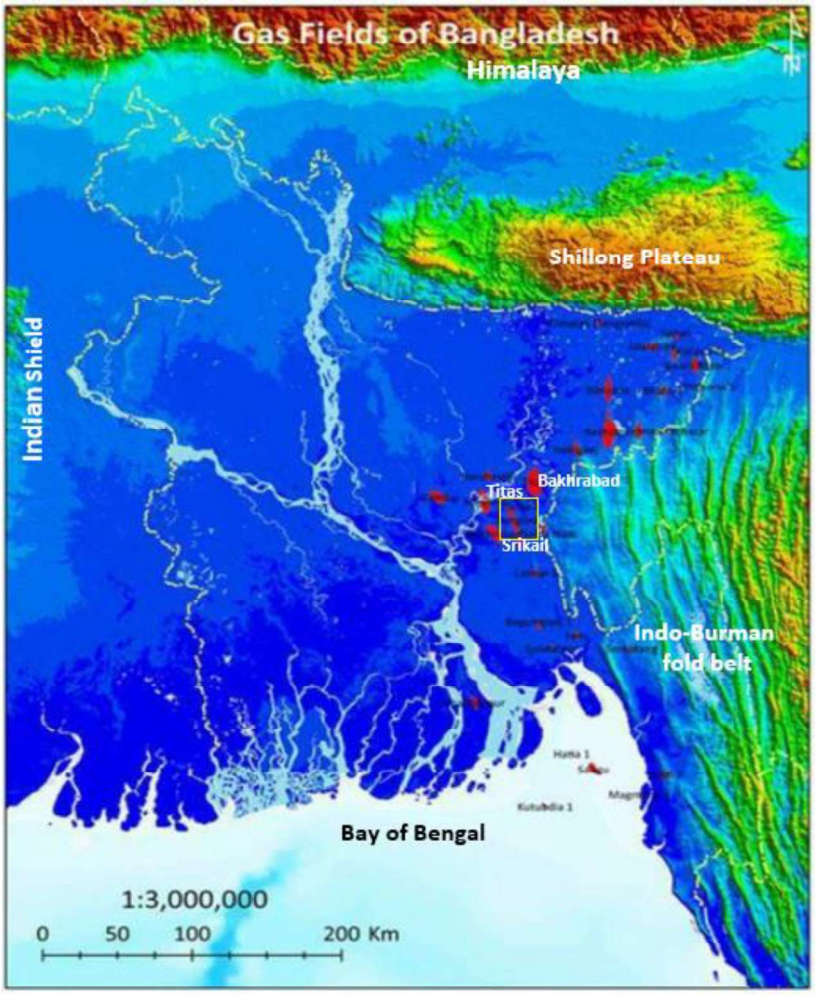

Figure 1.1 Onshore gas fields of Bangladesh and location of Srikail gas field in marked rectangle modified after (Bowles et al., 2015).

Stratigraphy of Bengal Basin has been developed under three main stratigraphic zones; NW, NE and SE Bengal Basin. The studied gas field area belongs to NE Bengal Basin (Figure 1.2). Gas is being produced by Bangladesh Petroleum Exploration and Production Company (BAPEX) from three wells-2, 3 and 4 (Figure 1.3). Well-1 which was placed in a paleochannel is a dry well. Srikail gas field has gas bearing horizons named from A-F. Gas is being produced from D-upper (Figure 1.4) and D-lower sands (Figure 1.5). The E-horizon has been tested and a commercial flow of more than 22 mmscfd has been recorded (Figure 1.6). Stratigraphically these horizons belong to Miocene Boka Bil and Bhuban formations of Neogene Surma group (Table 1.1).

Table 1.1 Stratigraphic succession of Srikail gas field based on well data and developed from published regional stratigraphy.

Depth (M)	Formation	Age	Lithology
Surface - 50	Alluvium		Alluvial covers with clay, silt & sand.
50- 400	Dupi Tila	Pleistocene	Predominantly sandstone with thin clay layers and quartzite pebbles.
400- 780	Tipam	Pliocene	Predominantly sandstone interbedded with thin layer of lignite, clay and slightly carbonaceous sand/ clay.
780- 900	UMS		Shale with occasional intercalation of sandstone and siltstone
900-1950	Bokabil	Miocene	Alternation of sandstone and shale sequence
1950- 2350			Predominantly shale interbedded with siltstone and of sandstone.
2350-3200	Bhuban		Alternation of sandstone and shale sequence with minor calcareous siltstone bands.

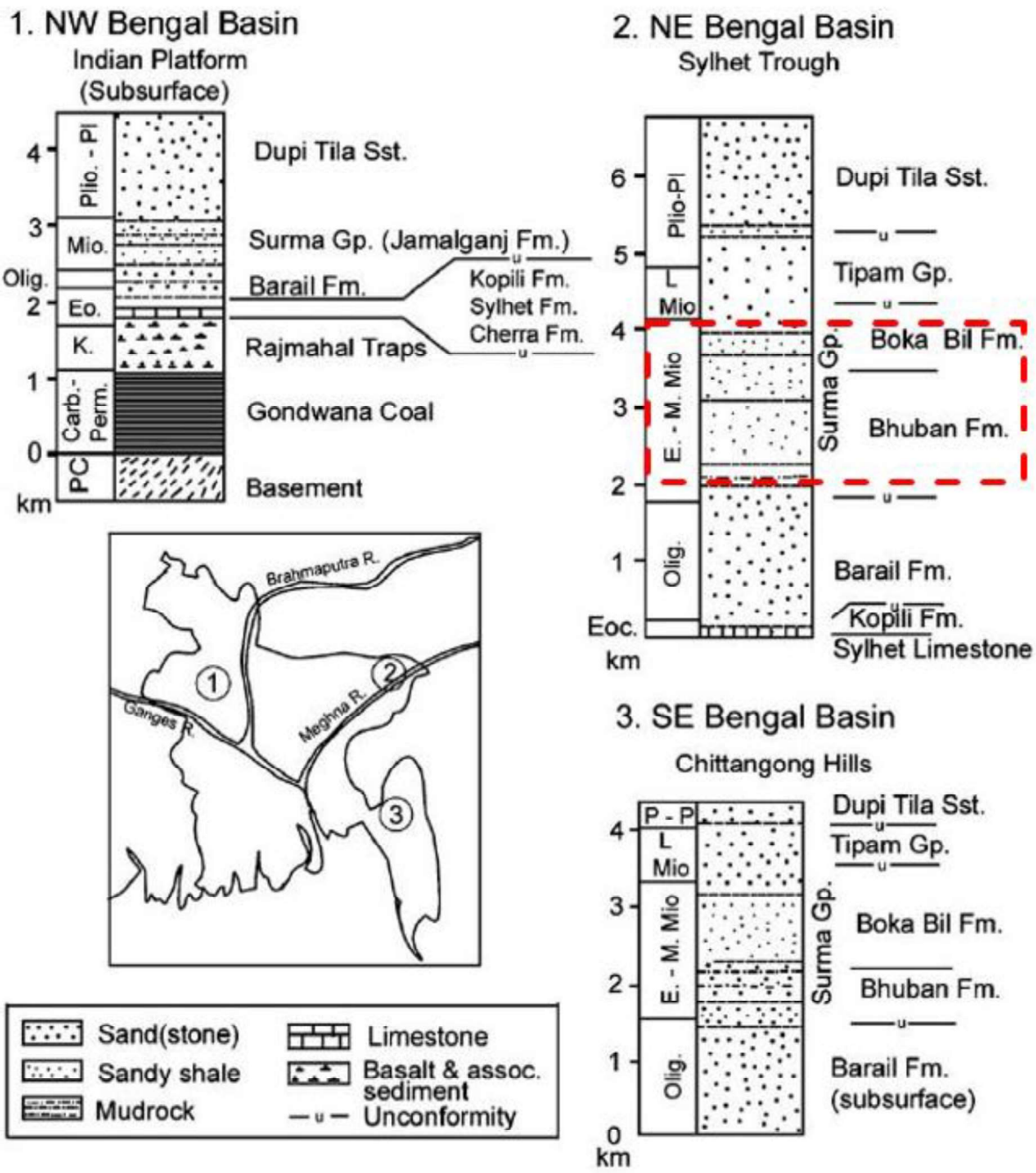

Figure 1.2 Stratigraphy of Bengal Basin developed under three main stratigraphic zones; NW, NE and SE Bengal Basin. They study area belongs to NE Bengal Basin. The red rectangular red marked is Boka Bil and Bhuban formations within the Surma Group. (after Uddin & Lundberg, 2004).

Table 1.2 Stratigraphy of Bengal Basin developed after (after Rahman and McCann, 2012)

Approximate Age	Formation (Fm.)	Lithologic Description	Depositional Environment
Pliocene to Pleistocene	Dihing Formation	Predominantly sandstone with silt size particle, clay layers, pebble beds and boulders.	Fluvial channel
	DupiTila Formation	Predominantly sandstone with thin clay layers.	
Pliocene	Tipam Group	Predominantly cross bedded Sandstone, interbedded thin coal layer, clay and minor shale.	Fluvial channel
Miocene	Surma Group		Shallow marine-deltaic
	BokaBil Formation	Predominantly shale interbedded with siltstone and sandstone. Sandy shale.	Shallow marine-deltaic
	Bhuban Formation.	Sandstone with alternating siltstone and shale. Depositional gap/Unconformity.	Shallow marine-deltaic
Oligocene	Barail Group	Mostly sandstone with some shale and coal layer.	Deltaic-shallow marine
Paleocene-Eocene	Jaintia Group	Mostly Limestone with some sandstone and shale layer.	Open Marine

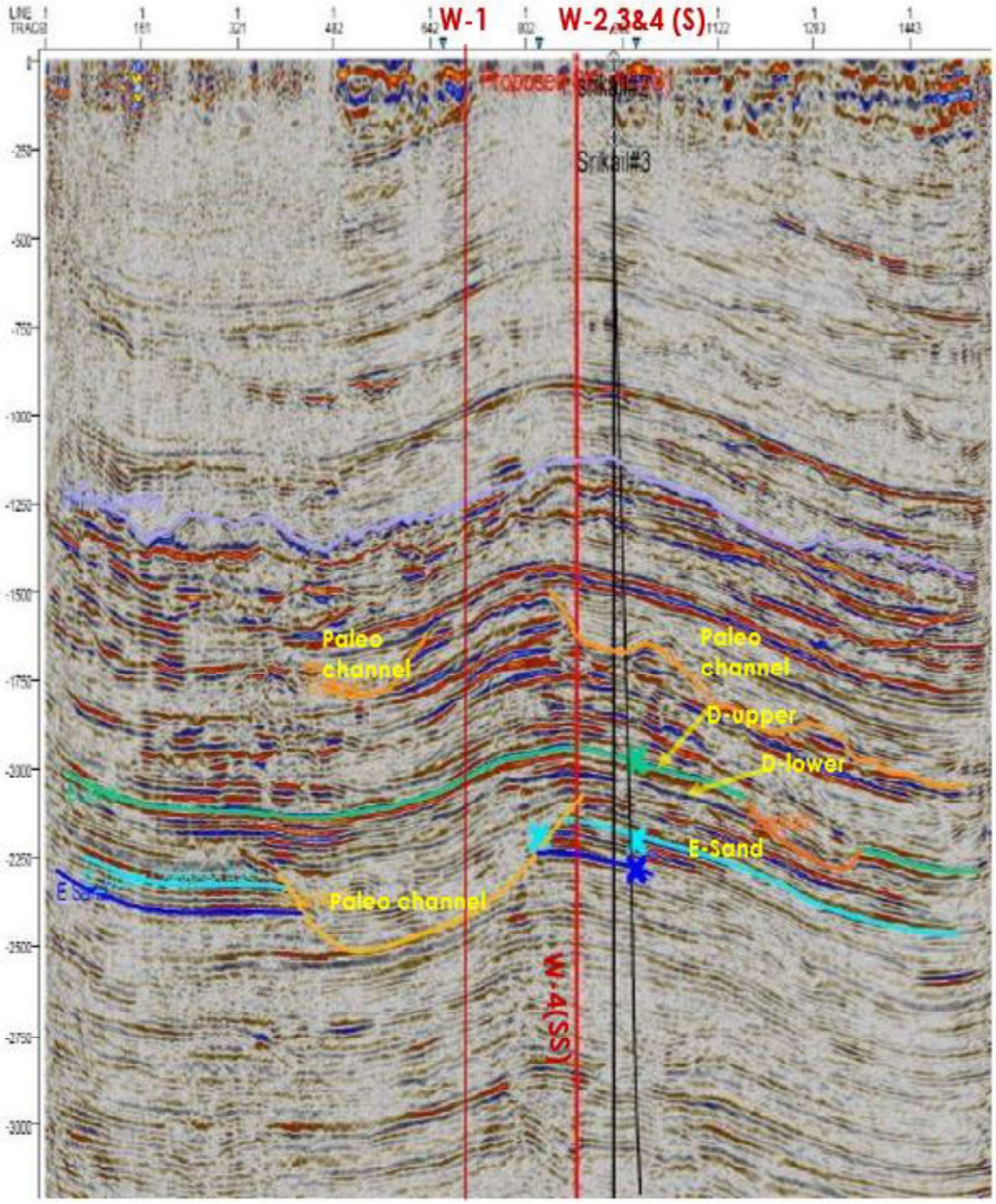

Figure 1.3 Well locations, erosional channel, and reflectors for the interpreted horizons (D-upper, D-lower and E-sand) on seismic section (Source BAPEX).

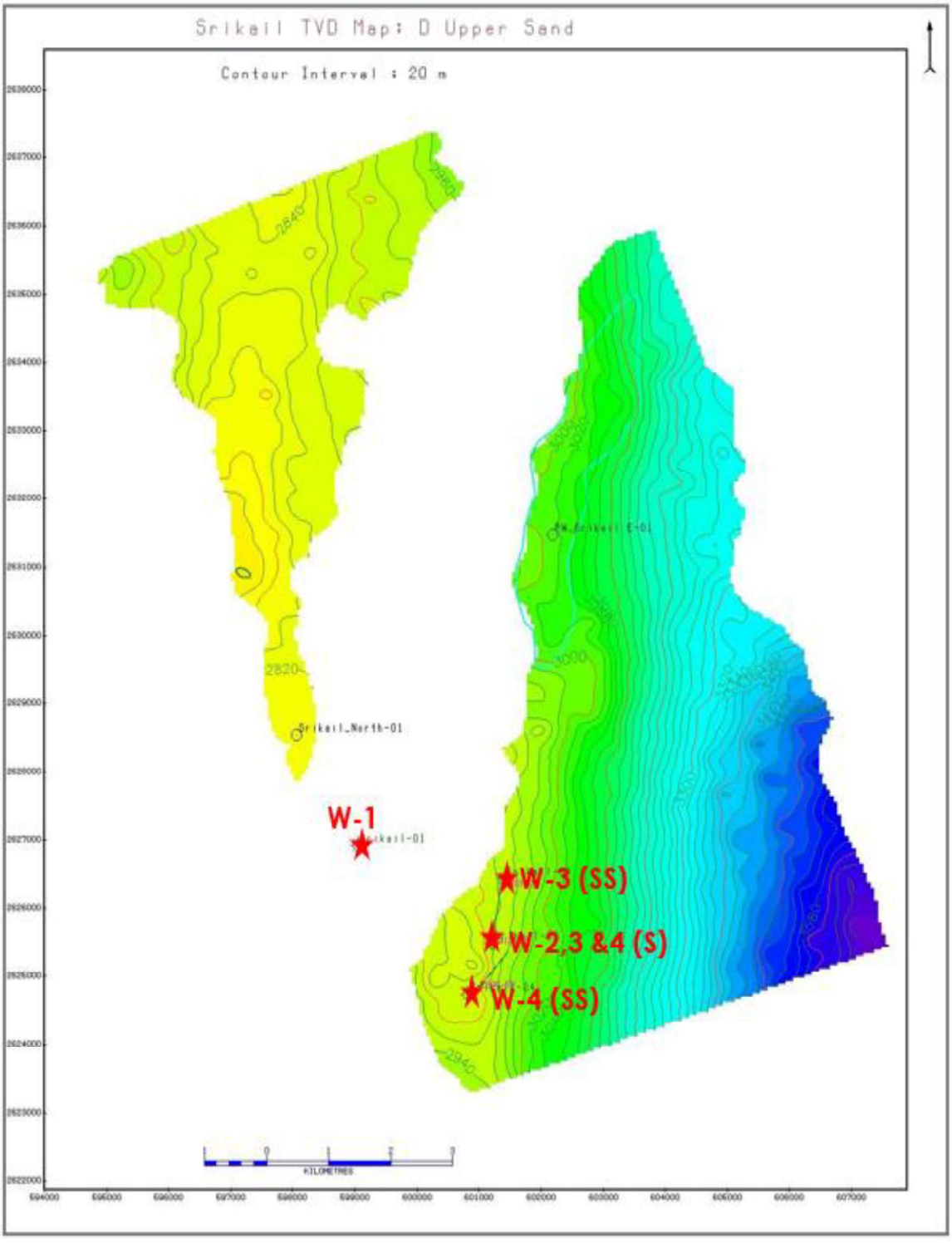

Figure 1.4 Well location (S-surface location, SS-subsurface location) on depth contour map of producing D-upper sand (Source: BAPEX).

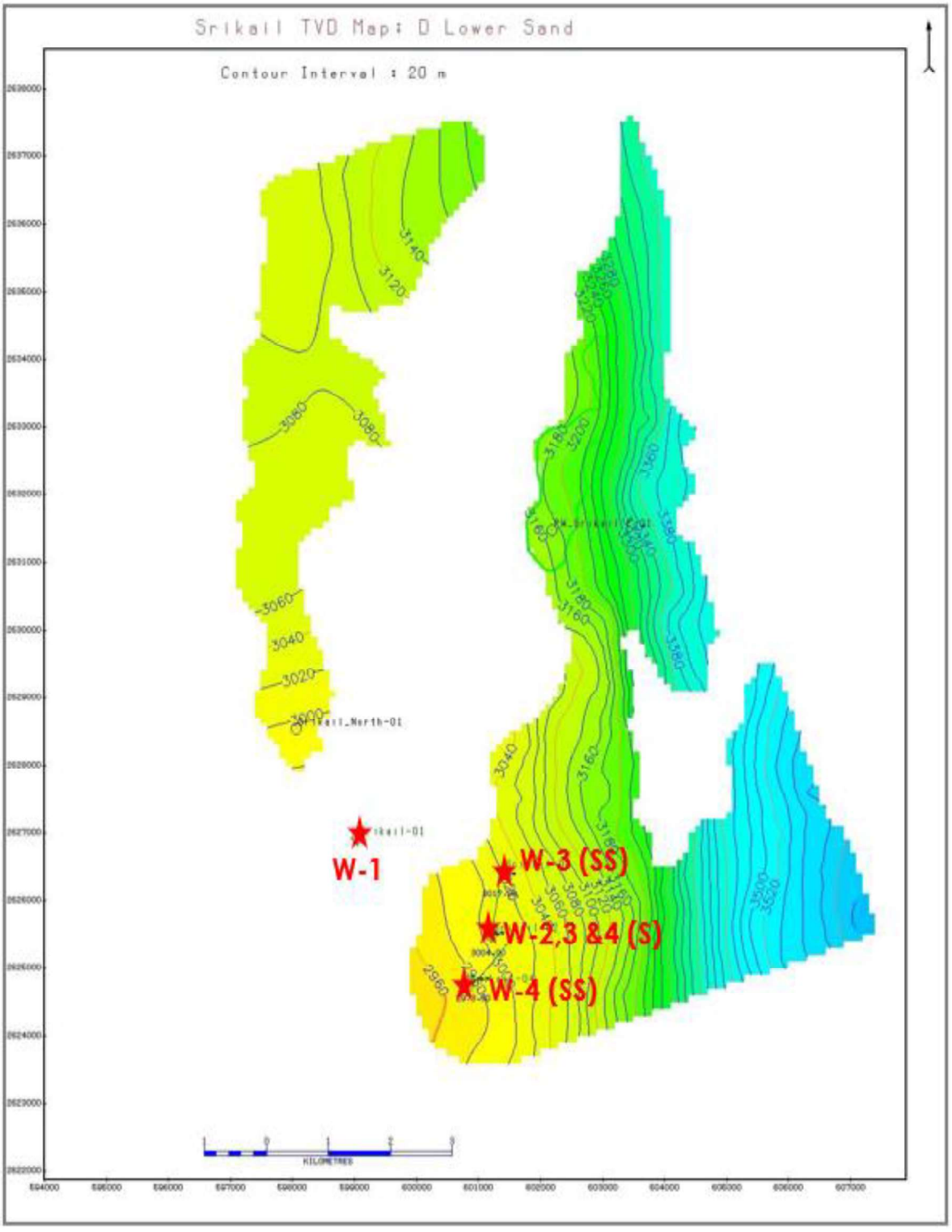

Figure 1.5 Well locations (S-surface location, SS-subsurface location) on depth contour map of the "D lower" producing horizon (Source BAPEX).

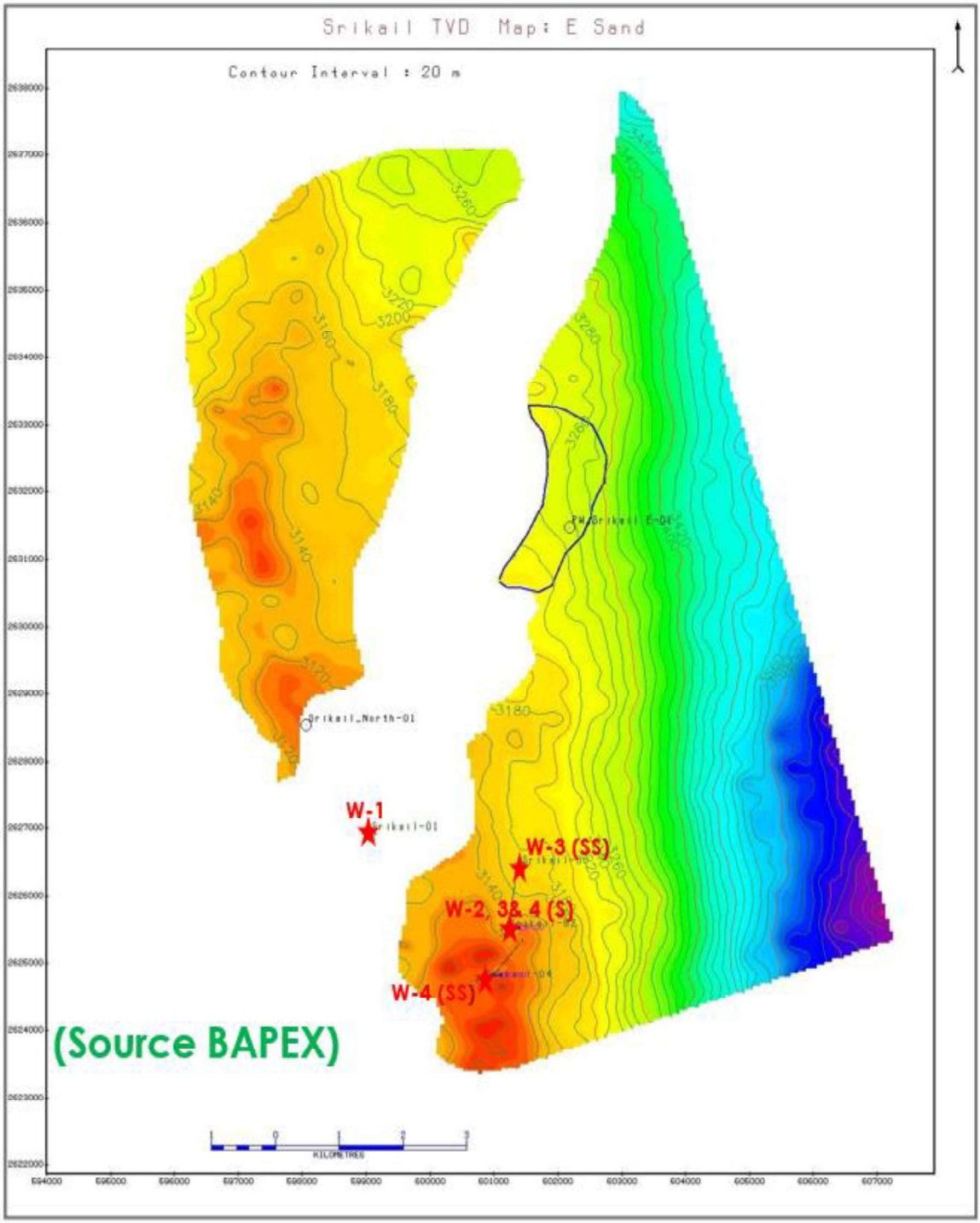

Figure 1.6 Well locations (S-surface location, SS-subsurface location) on depth contour map of the "E" producing horizon (Source BAPEX).

1.3 Objectives

The hydrocarbon discoveries that have been made in the Bengal basin so far, are hosted by the Boka Bil and Bhuban formations of the Neogene Surma group. 10.7 TCF recoverable natural gas reserve has been estimated in the Surma Basin (Curiale et al., 2002). Only a limited amount of studies has been conducted the reservoir properties and quality of these formation. The lack of extensive studies on their reservoir properties can limit the efficiency of development and exploration plans. The current study aims to:

- Determine the lithofacies and their depositional environments to create a depositional model.
- Characterize the reservoir sands of the studied gas field through facies analysis, petrophysical, petrographical and geochemical analyses.
- Evaluate reservoir heterogeneity, quality and architecture.
- Controls on the reservoir heterogeneity and quality of Bika Bil and Bhuban formations.

1.4 Previous Study

The regional geology, petroleum geology, prospects evaluation, sedimentology and tectonic evolution of the Bengal basin and its adjacent areas have been extensively studied and documented in the literature (Alam et al., 2003; Curiale et al., 2002; Gani and Alam, 2003; Johnson and Alam, 1991; Lietz, 1982; Uddin and Lundberg, 2004).

Several studies have been carried out on the Neogene Surma Group based on both out crop and subsurface data in the Bengal basin, Bangladesh. Imam and Shaw (1987) discussed the diagenesis and its control on reservoir properties of Surma Group sandstone, Bengal Basin

Bangladesh. The work was done on petrological analysis which includes fifty core samples of four onshore wells. The study suggested principal causes of producing low porosity in the sandstone of Surma Group are mechanical compaction, quartz overgrowths and the presence of carbonate cement. Effects on porosity and permeability reduction is less due to presence of clay minerals. Moreover, the formation of thick continuous chlorite rims prevented porosity reduction through inhibiting later stage quartz overgrowth. On the other hand, organic acidic solution generated from the adjacent source rock is helping to produce the secondary porosity in Surma Group sandstone by dissolution of feldspar and calcite cement. Similar type work was conducted by Rahman et al. (2016). In this study, geochemical, petrophysical and petrographic methods were used to determine and predict the controls on the reservoir quality of the Surma Group sandstones in six exploratory wells drilled in the Jalalabad, Meghna, Narshindhi and Titas gas fields. The main findings of the study include that porosity decreases mainly due to compaction process although growth of calcite cement has local effect on reduction of porosity in some sandstone. Samad et al. (2015) used wireline log data of 10 wells from five gas fields located from north to south of Bangladesh to identify reservoir characteristics. The study suggested that gamma ray value increased from wells in the north to those in the south, and also that a decrease in DPHI and NPHI in the southern gas fields leads to higher Vp due to high clay content. (Khanam et al. (2017) used core samples and gamma ray log of two wells from Jalalabad gas field to characterize the facies of the Surma Group. Miah (2014) also used wireline log data to assess the porosity in well-11 of the Titas gas field.

1.5 Problem Statement

All the previous studies were carried out on Surma group either based on core data and log data separately. A combination of wireline log data and core data is hard to find. Cores from a part of the reservoir can only cover limited portion of that reservoir and hence, cannot provide the details about the whole reservoir or the formation. To bridge this gap, the current study has incorporated both core data taken from the reservoir interval and wireline log data from two producing wells of Srikail gas field covering reservoir and prospective intervals. This gas field has multiple gas bearing zones (A-F), but gas is being produced only from the D-upper and D-lower gas sands. Pressure depletes with the time and water production also increases but at different rates in the three gas producing wells (wells-2, 3 and 4). This study integrates results obtained from conventional core and well log data analyses through petrophysical, petrographic and geochemical analyses to investigate the reservoir properties, heterogeneity, quality and controls on the Boka Bil and Bhuban formations in Srikail gas field. Specifically, the effects of facies, depositional environment, detrital composition and diagenesis on the reservoir quality and mechanism were examined. The outcomes of this study will help to determine the reservoir quality for the development of prospective gas bearing zones. The results from the study have been integrated, compared and corelated to the other studies to better understand the overall reservoir quality and heterogeneity of Boka Bil and Bhuban formations throughout the Bengal basin.

CHAPTER 2

LITERATURE REVIEW

2.1 Introduction

The literature review of this study consists of four parts. The first part focuses on the geological setting of the study area, the tectonic setting and evolution of Bengal basin. The second part reviews several studies conducted on Miocene Boka Bil and Bhuban formations of the Neogene Surma group. The third part encompasses the reviews on previous studies on reservoir description and quality of these formation. The last subsection of this chapter focuses on relevant literature on the research techniques used in this study.

2.2 Geological Settings

Bengal Basin is surrounded to the west and north by the Indian shield. The Himalaya is located the further north. The Indo-Burmese fold belt is situated in the east of the basin and to the south of the Bay of Bengal. The basin occupies most of Bangladesh and Tripura state of India as well as Bay of Bengal (Alam et al., 2003; Figure 2.1). The Bengal Basin was formed as result of the collision between the Indian and the Eurasian plates to the north, and the collision between Indian and Burmese plates in the east. The building of the Himalayan and Indo-Burmese ranges caused the formation of the Bengal sedimentary basin (Uddin and Lundberg, 2004). Bengal Basin forms a “remnant ocean basin” at the juncture

of the Burmese platelet and Indian plate during the Cretaceous to Holocene time (Alam et al., 2003).

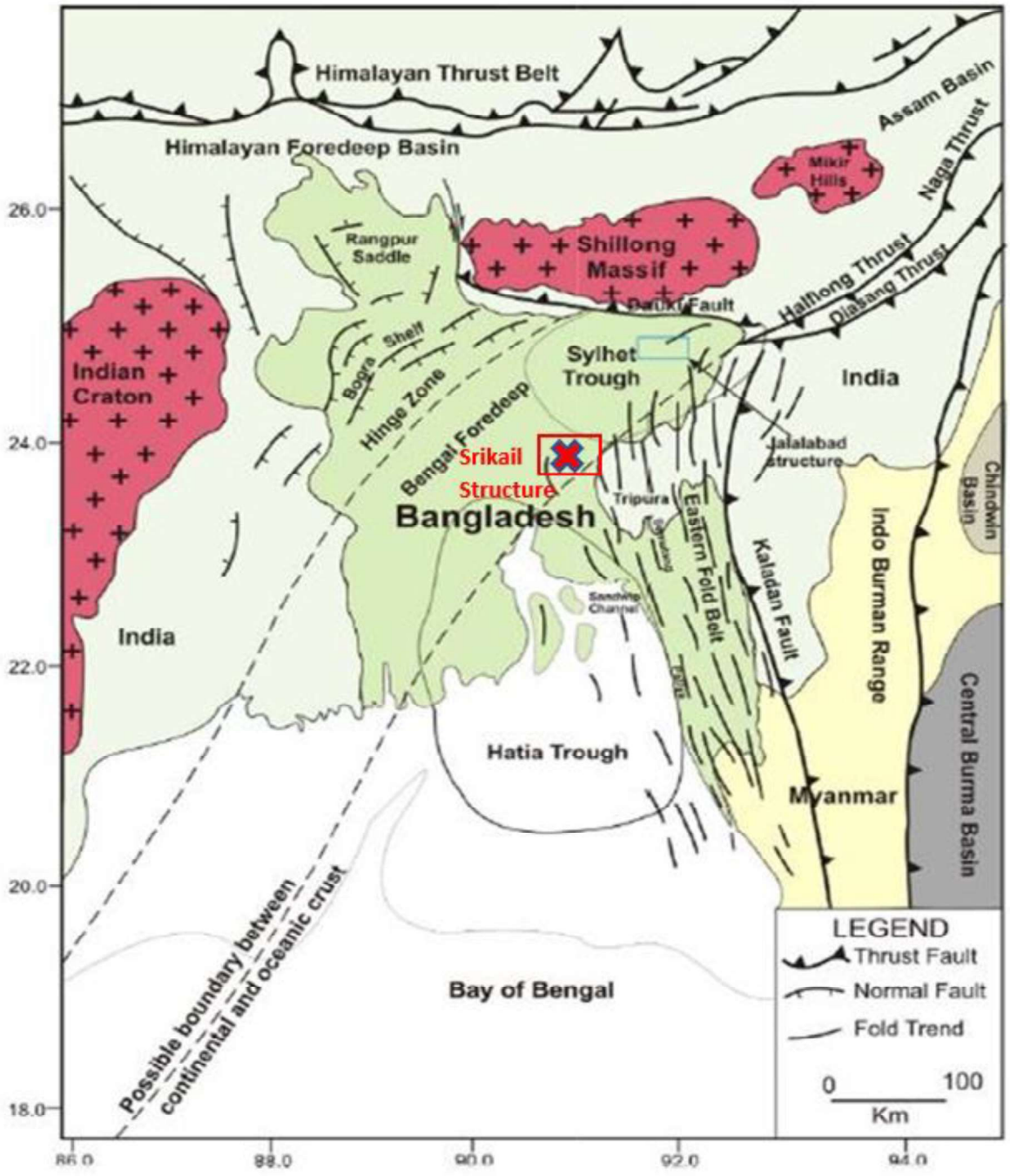

Figure 2.1 Structural elements and tectonic settings of Bengal basin and adjacent area, modified after (Khanam et al., 2017); Rectangular marked area shows the location of Srikail structure.

The initiation of the Bengal Basin building process was started by the drifting of Indian plate from the Antarctica in early Cretaceous. At the beginning of Miocene, the basin became a remnant basin because of continuous oblique subduction of the Indian plate under the Burmese plate. The three main distinct geo-technical provinces of the Bengal Basin are stable shelf, central deep basin and the Chittagong-Tripura fold belt (CTFB) (Alam et al., 2003). On-shore part of the basin is subdivided into basinal, the platform (shelf) and slope (hinge) zone (Figure 2.1).

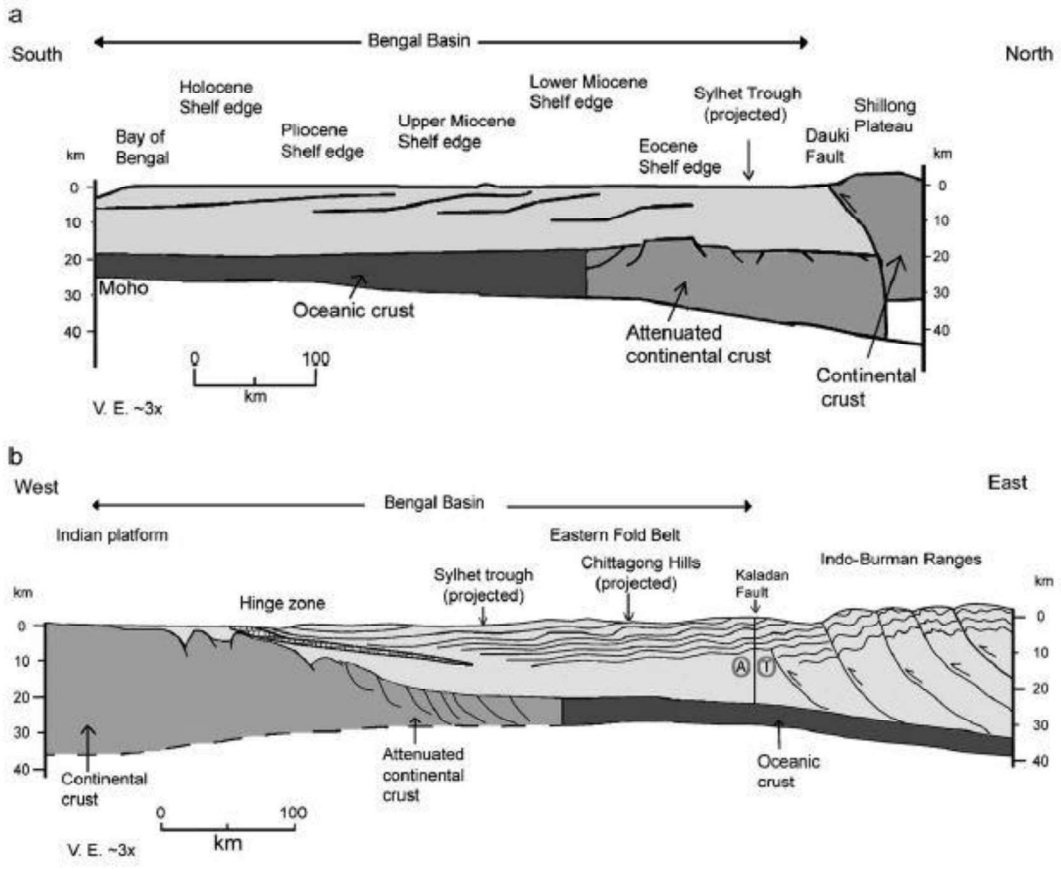

Figure 2.2 Schematic cross-section of the Bengal basin from north to south and east to west (Alam et al., 2003). Sediments thickness increases towards the south and east.

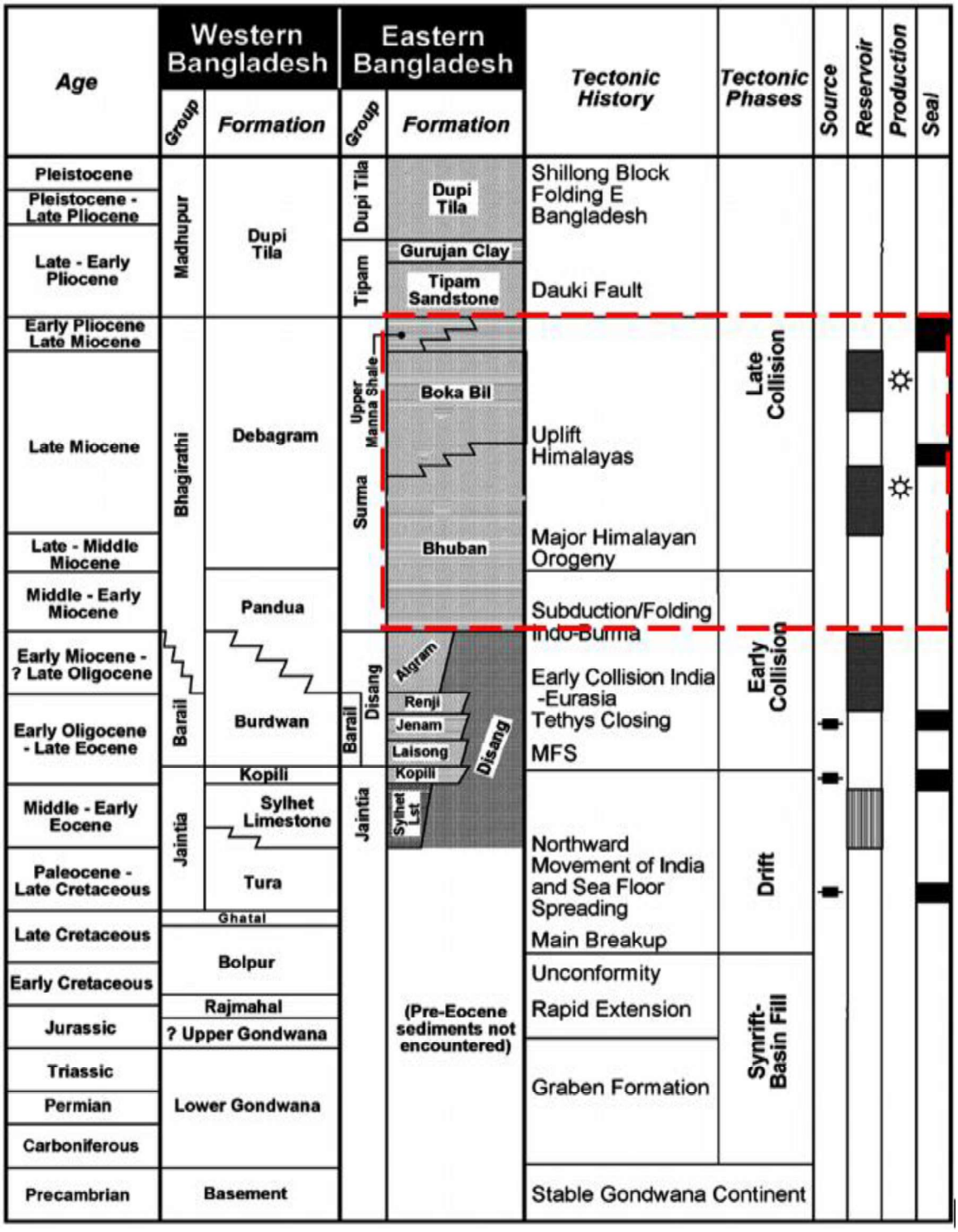

Figure 2.3 Stratigraphy of eastern and western side of Bangladesh. Figure shows the tectonic movement, phases, megasequences and elements of petroleum system. Marked area shows the stratigraphic position of Boka Bil and Bhuban formation of Surma Group (Curiale et al., 2002).

Bengal Basin covers an area of more than 200,000 km^2 and is the largest delta in the world. Clastic sediments derived from the eastern Himalaya to the north and the Indo-Burmese fold belt in the east were transported and deposited in the Bengal Basin (Uddin and Lundberg, 2004). The basin contains about 22 km of thick Cretaceous to recent sediments (Alam et al., 2003). The thickness increases from north to south as well as to the east (Figure 2.2). Miocene to recent deltaic sediments occur within this huge volume of sediments in the basin.

Early Miocene sediments which include those of the early to middle Miocene Bhuban and Boka Bil formations are called the Surma Group (Figure 2.3). The formations contain sub-equal proportion of alternation sandstones and shales. The sediments of Surma Group were deposited in a fluvio-deltaic to marine environments. The sediments are prodelta and delta front deposits of a large mud rich delta system (Johnson and Alam, 1991).

2.3 Boka Bil and Bhuban Formation (Surma Group)

Thick sequence of alluvial cover and fossils scarcity have hindered the complete understanding of the Bengal Basin's stratigraphy. Lithologic characteristics are the basis of the development of the stratigraphy of the Bengal Basin. The nomenclature of the groups and formations has been adopted from the exposed type sections in Assam basin, northeast India (Lietz, 1982). Boka Bil formation is overlain by a regional shale called the Upper Marine Shale (UMS) (Figure 2.3). It represents a regional marine transgression in this region. In the north eastern side of Bangladesh, Boka Bil formation is unconformably overlain by lower Miocene Tipam group and the Miocene Bhuban formation is on top of

the Oligocene Barail Formation (Figure 2.3). Outcrop of Boka Bil and Bhuban formations are available in the Chittagong hills and in the flank of Sylhet trough (Figure 2.4).

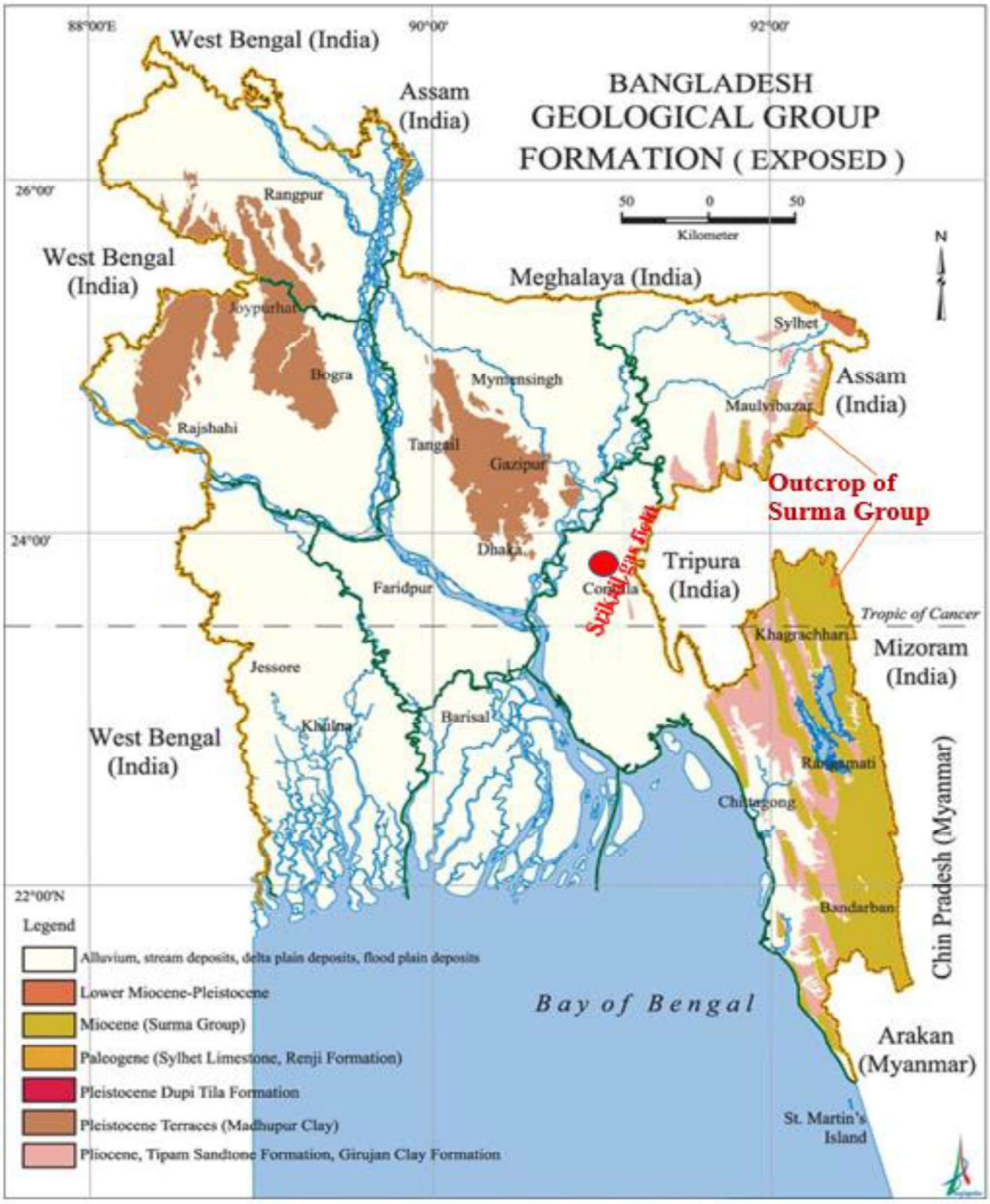

Figure 2.4 Shows the exposed geological formations in Bangladesh. (Source: Bangla pedia).

In the northwestern side of Bangladesh, the Surma Group is named as Jamalganj Formation and is characterized by less thickness compared to southeast side. Variation in thickness and depth was also found in wells drilled in Bangladesh (Uddin and Lundberg, 2004) (Figure 2.5 & Figure 2.6). The thickness and depth of Boka Bil and Bhuban formation are illustrated in Table 2.1. The Surma group has been penetrated from approximately 900m to total drilling depth (3350 m) by the wells drilled within the Srikail gas field. The formations within this group contain the main gas reservoir of this gas field like the other gas fields in Bangladesh.

Table 2.1 Thickness of Bhuban and Boka Bil Formations (Surma Group) encountered in different wells of Bangladesh (Uddin and Lundberg, 2004).

Tectonic location		Wells	Thickness of Boka Bil Formation (in meters)			Thickness of Bhuban Formation (in meters)		
Major	Important subdivision		From	To	Total	From	To	Total
Shelf		Bogra-1	217	782	565	782	1593	811
		Kuchma-X1	340	1090	750	1090	1606	516
		Singra-IX	1290	1600	310	1600	1880	280
Hinge zone		Hazipur-1	1393	2247	854	2247	3130	883
Deeper basin	Surma basin (=Sylhet trough)	Chattak-1	626	1081	456	1082	2134	1052
		Sylhet-2	1240	1915	675	1915	2818	903
		Atgram-IX	1085	2256	1171	2256	4178	1920
		Kailastila-1	2150	2900	750	2290	4138	1238
		Beani Bazar-IX	2631	3640	1009	3640	4109	469
		Rashidpur-2	1036	2710	1674	2710	3851	1141
		Habiganj	1165	2326	1161	2326	3506	1180
		Kamta-1	1030	2740	1710	2740	3614	874
		Titas-1	832	2362	1531	2362	3758	1396
		Bakhrabad-1	560	1770	1210	1770	2838	1068
		Begumganj-1	1480	2580	1100	2580	3656	1076
		Muladi-1	750	2590	1840	2590	4395	1805
		Feni-1	1300	2440	1140	2440	3200	760
	Folded belt	Semutang-1	250	1530	1280	1530	3500	1970
		Jaldi-3	500	1380	880	1380	2930	1550
	Offshore	Kutubdia	1713	3606	1792	not drilled		

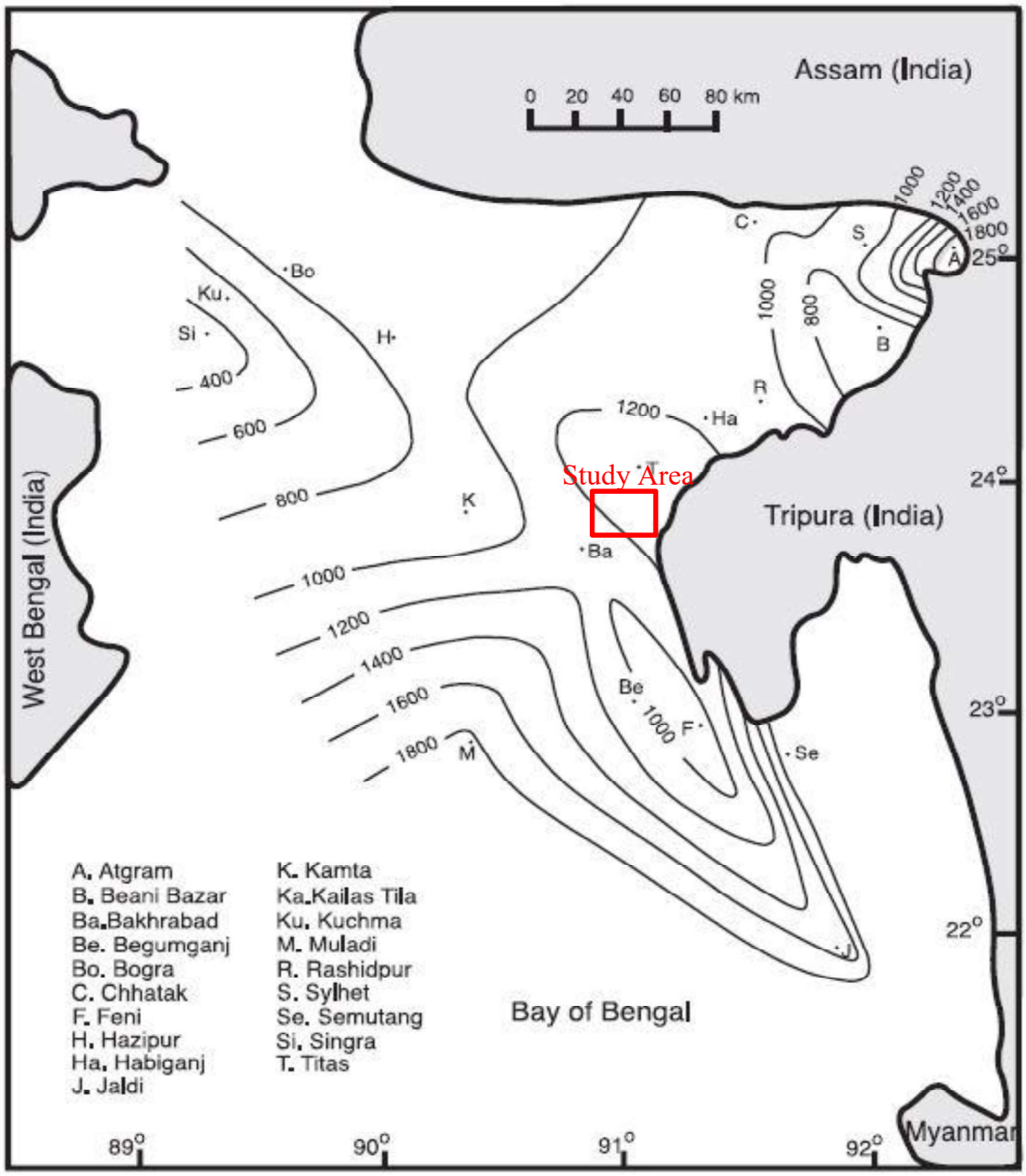

Figure 2.5 Thickness map of the lower Miocene Bhuban Formation based on well data. Index shows the well name and rectangular marked is the study area (Uddin and Lundberg, 2004).

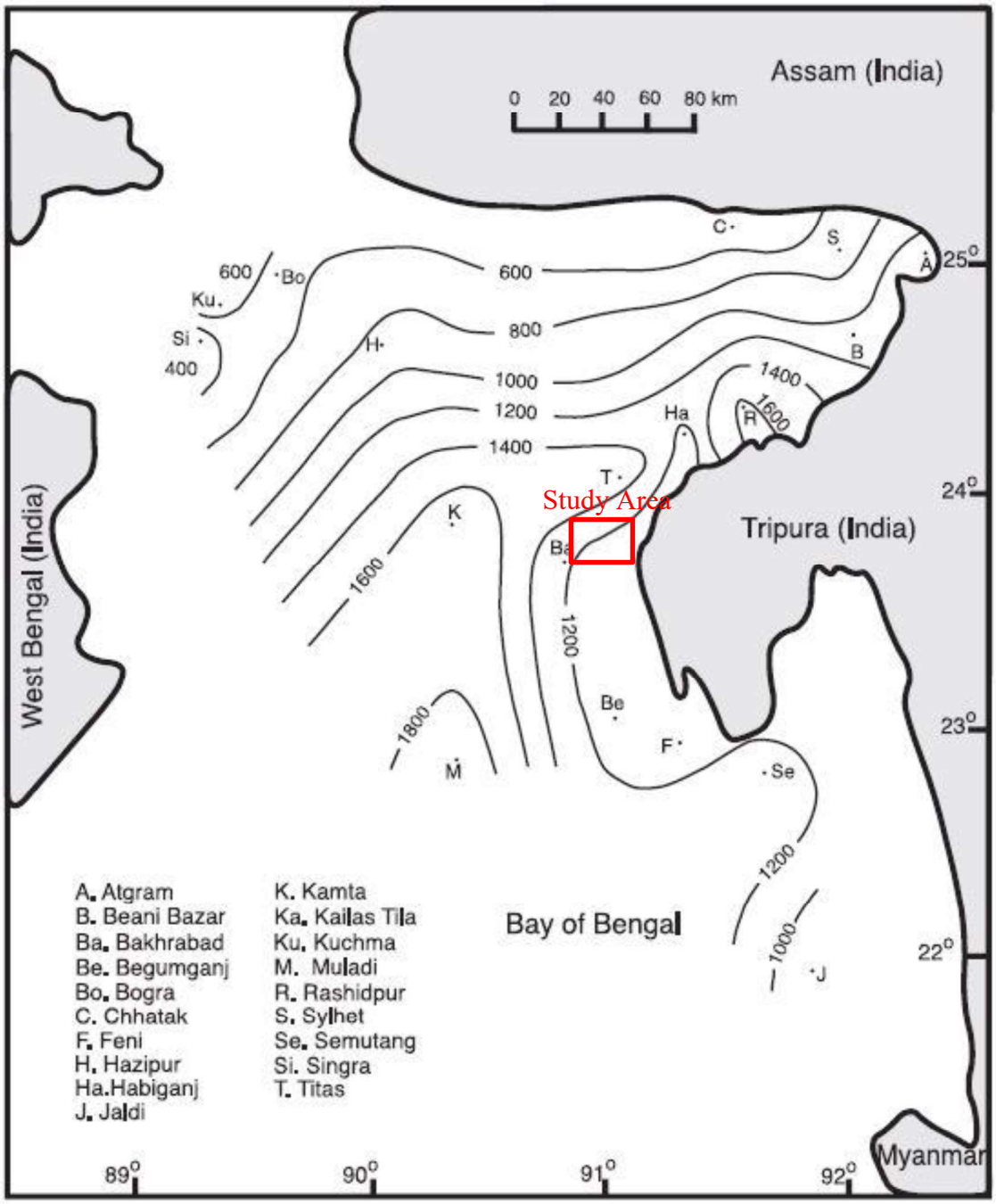

Figure 2.6 Thickness of the Middle to Upper Miocene Boka Bil Formation based on well data. The well names are given in the index and rectangular marked is the study area (Uddin and Lundberg, 2004).

2.4 Reservoir Description and Quality of Boka Bil and Bhuban Formation (Surma Group)

A large amount of literature was reviewed on reservoir description and characterization. Imam and Shaw (1987) suggested that compaction due to burial depth is the main factor that reduces porosity and permeability of Boka Bil and Bhuban formations. Various diagenetic processes including clay minerals formation, quartz overgrowth and feldspar dissolution also control the porosity and permeability variation in the formations. Core analysis of the Titas gas field indicates that the Bhuban Formation is composed of mainly quartz, feldspar and rock fragments. The formation's porosity-permeability ranges from 5-28% and 0.5-490 mD (Islam, 2009). The initial porosity was decreased primarily by the compaction and later enhanced by the dissolution of feldspar creating secondary porosity. Porosity is also affected by the formation of authigenic clay minerals like kaolinite, illite, chlorite etc. Petrophysical and petrographical analyses of core samples from Fenchuganj and Shahabazpur gas field revealed that the formation's porosity and permeability values are 20%-30% and 34-3200 mD respectively (Rahman et al., 2016). These core samples were collected at a depth interval of 2300-3200 m from the northeastern side of Bangladesh. The best reservoir quality has been found in medium to fine grained sandstone. Locally few sandstones are compartmentalized and highly cemented. Eight lithofacies were identified from core sample analysis from this formation, and were interpreted to have been deposited in tide dominated deltaic setting (Rahman et al., 2009). Khanam et al. (2017) has identified three lithofacies association from core analysis of Jalalabad gas field. According this study, medium to coarse grained facies deposited in the deltaic fluvial channel, were identified as a better-quality bearing reservoir.

2.5 Techniques Applied for Reservoir Characterization

El-Deek et al. (2017) used thin section petrography, XRD and SEM (Scanning Electron Microscopy) analyses to measure porosity and identify sandstone lithofacies to investigate reservoir heterogeneity in the Ordovician Sarah Formation in Saudi Arabia. Mahgoub et al. (2016) analyzed subsurface facies from core and wireline logs. The study which also involved also petrographic analysis aimed at assessing reservoir quality of the Paleocene fluvial/lacustrine Yabus Sandstone, Melut Basin, Sudan. Yassin et al. (2018) studied seismic data, core and wireline log data to characterize the Early Cretaceous, upper Abu Gabra sandstones, Sufyan Sub-basin, Muglad Basin, Sudan. Hippler et al. (2013) discussed the importance of using microscopic tools to identify pore types. El Hajj et al. (2015) highlighted the significance of classifying clay minerals using advanced X-ray powder diffraction, XRF and SEM techniques. Harrison (1991) integrated petrographic and petrophysical studies on frontier tight sand formation in the Green River Basin, Wyoming. He validated log data by core-to-log comparison. Zhang and Zhang (2015) conducted sedimentologic and petrographic studies on the tight sand strata in 24 cores obtained from eight wells that penetrated the Lower Cretaceous Dalaoyefu Formation, NE of China. Islam (2009) and Rahman et al. (2017a) applied clay separation technique through XRD analysis to identify the clay minerals in Surma group sandstone. Rahman and Worden (2016) used core data from three gas fields to determine the diagenetic control on the reservoir quality of Surma group sandstone. Khanam et al. (2017) has done facies analysis of Surma group sediments using GR log and core sample of Jalalabad gas field, Bengal basin Bangladesh. Their study was aimed at understanding the facies distribution, depositional environments, reservoir architecture and diagenetic processes and their effects on reservoir quality. Most

of reviewed studies, were performed on Miocene Surma Group and the study area are in the Bengal basin, hence several concepts contained in them are adopted in the current work.

CHAPTER 3

DATA SET AND METHODS

3.1 Introduction

The datasets used in this study, were provided by Bangaldesh Petroleum Exploration and Production Company Limited (BAPEX), PETROBANGLA. The datasets consist of wireline log data from two wells, namely well-3 and 4 covering all prospective reservoir zones (Table 3.1). A total of 29 core samples covering 27 m of reservoir zones were collected from the reservoir zones D-Upper and D-lower in well-3, and E-sand from well 4 that was identified from the wireline log and drilling data analysis (Table 3.2). A flowchart of research methodology started with wireline log and core analysis and ended with identification of reservoir quality and heterogeneity is presented in Figure 3.8. The details about research methodology are described in the subsequent section.

Table 3.1 Wire line logs, used for the study.

Well	Logs	Depth
Srikail-3	GR, Resistivity, Neutron porosity and Density, Sonic, Resistivity Image.	Covering all reservoir zones.
Srikail-4	GR, Resistivity, Neutron porosity and Density, Sonic, Resistivity Image.	Covering all reservoir zones.

Table 3.2 Studied core sample information.

Well	Depth Range (m)	Thickness (m)	No of Sample (Core Slab)
Srikail-3 (Core-1)	3083-3092	9	10
Srikail-3 (Core-2)	3178-3186	9	9
Srikail-4 (Core-3)	3228-3236	9	9

3.2 Core Description

A total of 29 core samples were collected from three producing zones in two wells (Well-3 and 4) within the Srikail gas field. The interval of the producing zones (D-Upper, D-Lower of well-3 and E-sand of well-4) ranges from 3075-3250 m. The core samples were sedimentologically described and subsampled for further analyses. The core description was performed following the idealized core description sheet suggested by Diana Morton-Thompson (1993) with minor modifications. Core description includes documenting all textural features (e.g., grain size, sorting), sedimentary structures and lithological identification. Easy core software has been used for the graphical display of features.

3.3 Facies Analysis

The cyclicity of sedimentation of the Surma Group was described from the gamma ray log motif of well-4. Different types of facies and their associations, depositional environments and sub-environments have been identified following Reading (1986). The contribution of individual facies association was determined, and their controls of reservoir quality were

also explained. Finally, a conceptual depositional model has been constructed depending on the analysis.

3.4 Wireline Log Interpretation

All the basic wireline logs of Srikail-3 and Srikail-4 were analyzed to characterize the three prospective gas bearing zones: D-Upper, D-Lower and E-sand. Wireline log data includes caliper, gamma ray (GR), resistivity, neutron porosity, density and sonic. Gamma Ray log was used to identify the lithology as well as to compute the shale volume. Resistivity, and density logs were used for determination of porosity and gas saturation (using Archie's equation). Techlog software has been used for wireline log display and interpretation.

3.5 Thin section Petrography

Petrographic thin section study was conducted at Center for integrative Petroleum Research (CIPR) using Olympus petrographic microscope. A total number of 24 thin sections prepared in CIPR were studied in terms of mineralogical composition, grains texture (size, roundness, sphericity, sorting, contact and packing), matrix, and cement types. Following Gazzi-Dickinson point-counting method, about three-hundred quartz, feldspar and lithic rock fragments grains were counted. The data was used to derive the quartz-feldspar-lithic rock fragments (QFL) relation for sandstone classification and provenance interpretations. The sandstone provenance follows Dickinson (1985) and the sandstone classification of Folk (1980) was established using the spreadsheet suggested by Zahid and Barbeau (2012).

3.6 XRD, XRF and SGR Analysis

Twenty-nine samples taken from the core samples were powdered and analyzed using EMPYREAN PAN analytical X-ray diffractometer (XRD) at Geosciences Department Laboratories (Figure 3.2) for their bulk mineralogical composition. Ten of the powdered samples were analyzed using Rigaku, Ultima IV X-ray diffractometer in the Engineering Research Center (ERC to validate the results.

Additionally, XRD analysis was carried out on clay fractions from five samples to identify and quantify the clay mineral types determine in the samples. The samples were disaggregated in distilled water using an agate mortar then kept for 48 hours in different dishes. Suspended fraction from the sample was separated by decanting method. The 2 μm fraction was separated from clay by centrifuge at 3000 rpm for 15 minutes and was spread on glass slide for analysis (Figure 3.1a). XRD analysis was carried out for air dried, glycolated (Figure 3.1b) and heated at 550 ºC.

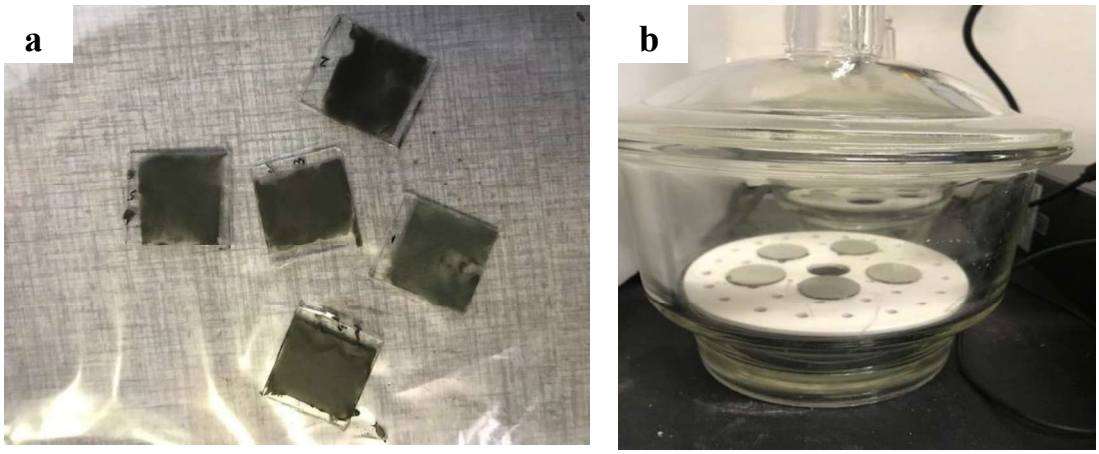

Figure 3.1 Separated clay sample pasted on the slide and kept in desiccator for glycoaltion.

Figure 3.2 EMPYREAN PAN analytical X-ray diffractometer (XRD) at Geosciences Department Laboratory.

Same powdered samples that were prepared for XRD analysis were used for XRF elemental analysis. The analysis was done in Geosciences Laboratory using M4-Tornado micro XRF analyzer (Figure 3.3). The analysis was done to determine the major and minor rock forming elements in the samples.

Figure 3.3 M4-Tornado micro XRF analyzer at Geosciences Department Laboratory.

Spectral Gamma Ray (SGR) analysis was done using Spectral Core Gamma (Core lab instrument) in CIPR (Figure 3.4). The core was scanned for quantitative analysis of potassium (K), uranium (U) and thorium concentrations in the core sample. Ten data points acquired from every sample, were averaged to quantify the elemental concentrations in each sample.

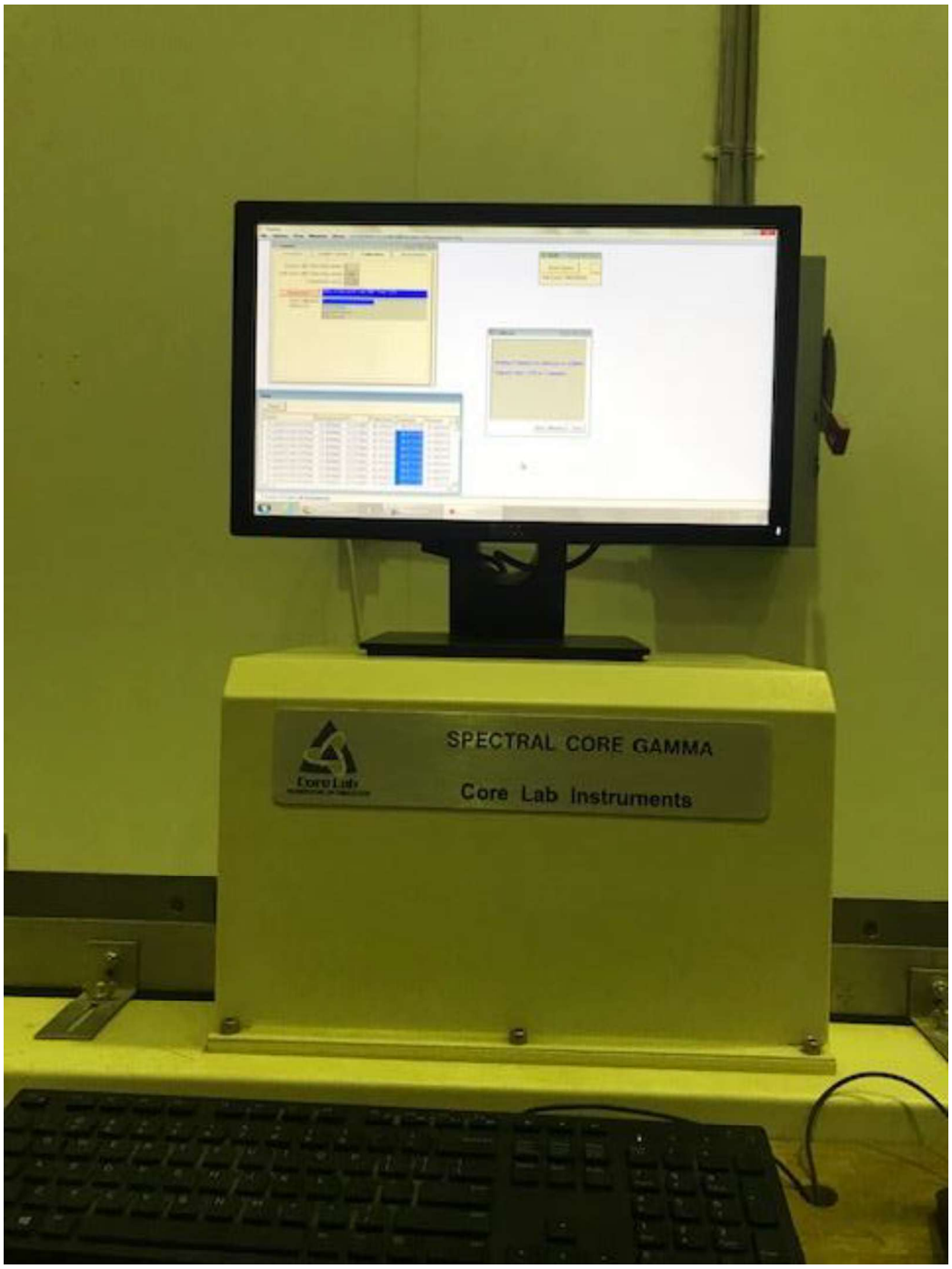

Figure 3.4 Spectral Core Gamma (Core lab instrument) in CIPR deployed for SGR analysis.

3.7 Core Porosity and Permeability

A total of 24 core samples were collected from D-Upper and D-lower in well-3, and from E-sand in well 4. Core plugs of one-inch diameter were drilled for porosity and permeability measurement. Porosity and permeability were measured from 24 core plugs taken form 27 m cored intervals to characterize the transport properties of the reservoir. Measurements were done using AP-608 automated permeameter/porosimeter (Figure 3.5).

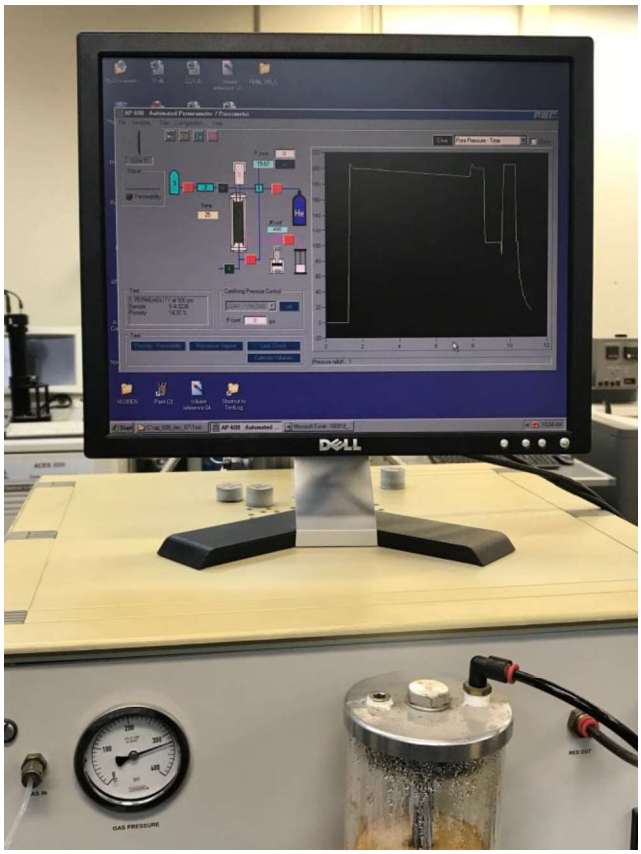

Figure 3.5 AP-608 automated permeameter/porosimeter in CIPR.

The petrophysical data was integrated with petrographical and geochemical data to investigate the reservoir heterogeneity, quality and their controlling factors.

3.8 SEM and QEMSCAN Analysis

Based on low, medium and high core porosity and permeability values, 10 samples were selected for Scanning Electron Microscopy (SEM). Less than 1 cm diameter of rock fragments with fresh surfaces were prepared for SEM analysis. They were analyzed using JEOL JSM-6610LV (SEM) fitted with BSE (backscattered electron detector) and EDX (Energy dispersive X-ray spectrometry) detector to identify pore filling, pore lining clay minerals, their morphology and diagenetic features like quartz over growth, and feldspar dissolution (Figure 3.6).

Figure 3.6 JEOL JSM-6610LV Scanning Electron Microscope (SEM) at the Material Characterization Laboratory, Research Institute, was used to identify pore filling, pore lining clay minerals, their morphology and diagenetic features like quartz over growth, and feldspar dissolution.

QEMSCAN 650F combined with field emission gun-scanning electron microscope (FEG-SEM), high resolution BSE (Back scattered electron) and a Spectral Analysis Engine

(SAE) was employed for quantitative analysis of rock forming minerals, authigenic clay minerals and cements in 10 thin section of sandstone samples (Figure 3.7).

Figure 3.7 QEMSCAN 650F was used for quantitative mineralogical analysis.

\

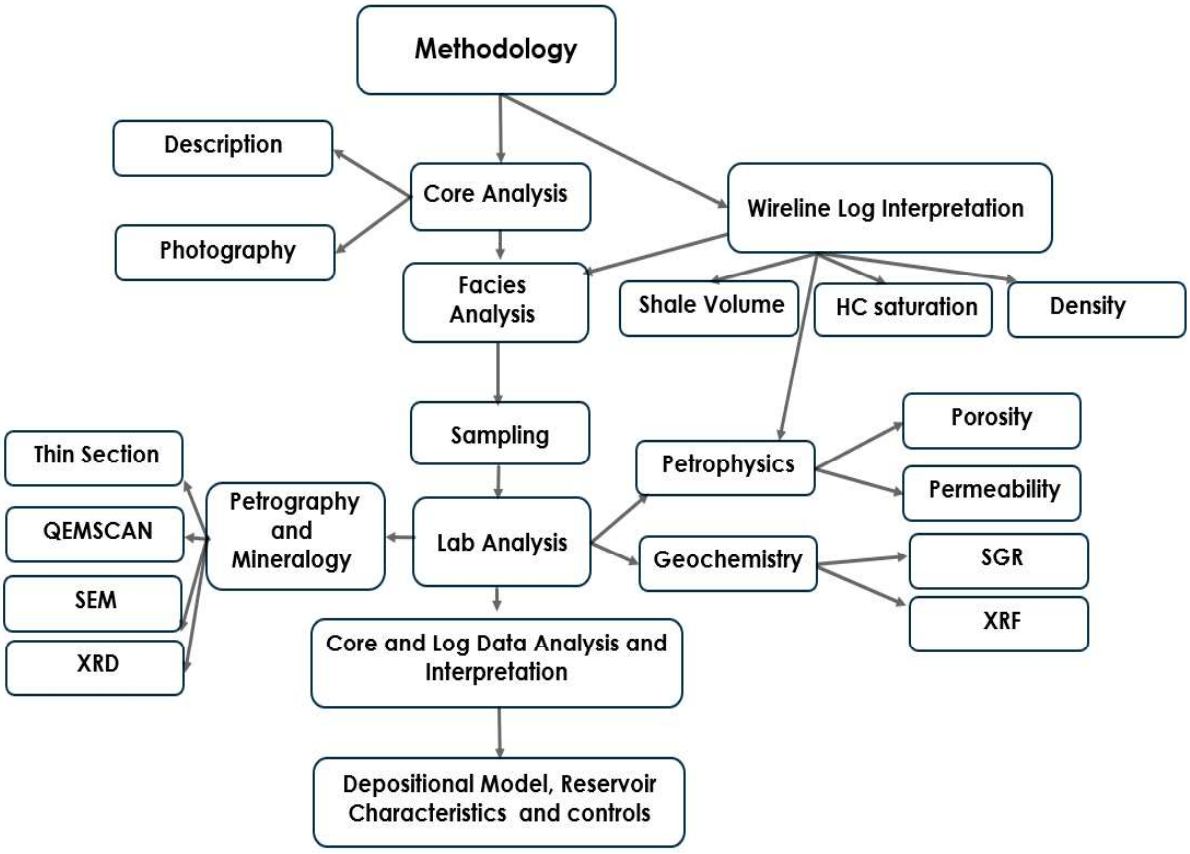

Figure 3.8 Research methodology.

CHAPTER 4

SEDIMENTOLOGY AND FACIES ANALYSIS

4.1 Introduction

The core samples collected from three producing zones of two wells (Well-3 and 4) from the Srikail gas field were sedimentologically described. For the identification of facies, direct observation and analysis of the core sample is the best but core is not always available in all wells and coring cannot be done all through the wells. As core cannot cover all the reservoir zones, wireline log can be used to study facies and identify the depositional environments. Application of wireline log is not limited to the reservoir identification and hydrocarbon estimation, it is also a very powerful tool for identifying stratigraphy and paleo-environment (Murkute Y., 1991). Core samples taken from D-upper and D-lower of Srikail well-3 and from E-sand of well-4 as well as gamma ray log from 2650-3260 m depth of the well-4 have been used for facies analysis in this study.

4.2 Core Description

Core-1 (3083-3092) penetrated by the D-upper sand in well-3, is composed of alternation of sandstone and sandy shale beds (Figure 4.1a). Sandstones are characterized by medium to fine grained sandstone, sandstone-siltstone interbeds and laminated sandy shale with thickness of millimeter to centimeter. Sandstones are moderate to well sorted, subangular to sub-rounded and micaceous. Wavy bedding, lenticular bedding, flaser bedding, planner and trough cross beddings are present.

Core-2 (3178-3186 m) retrieved from D-lower sand strata of the same well, is characterized by parallel and trough cross bedded sandstone, wavy bedded sandstone and massive sandstone with thinly laminated sandy shale. Sandstones are medium to fine grained, moderate to well sorted, rounded to sub-rounded and micaceous (Figure 4.1b).

Core-3 (3228-3236 m) was collected from E sand of well-4. It is mainly composed of cross bedded sandstone, wavy and flaser bedded, cross bedded sandstone with clay flakes and local thinly laminated shale (Figure 4.2). According to Johnson and Nur Alam (1991), Boka Bil and Bhuban Formations of the Surma Group are deposited in a deltaic environment.

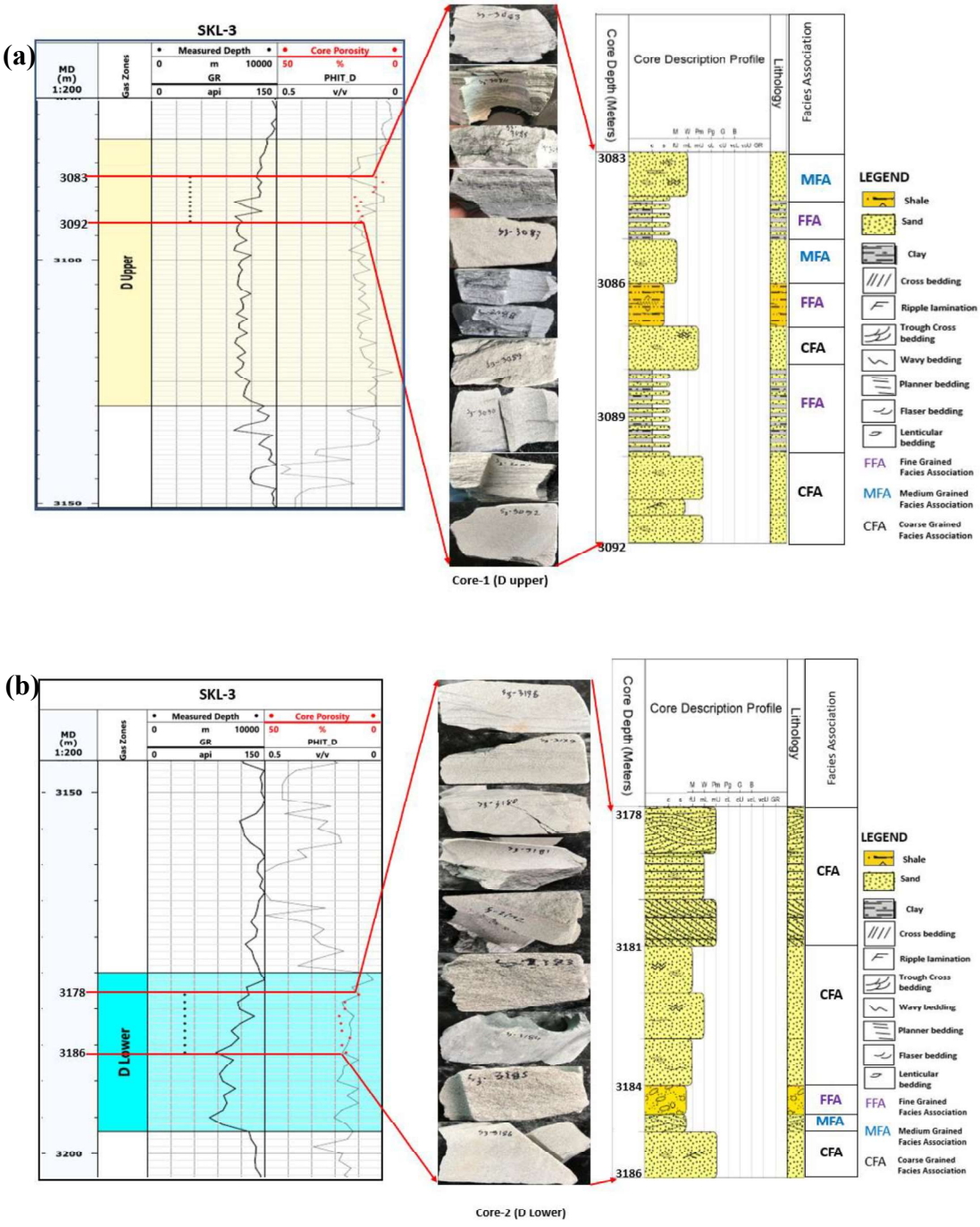

Figure 4.1 Shows Gamma ray log with porosity determined from density porosity, core porosity with core photographs, litholog and facies association of (a) core-1 (3083-3192 m); (b) core-2 (3178-3186 m) from D-upper and D-lower sand of well-3(here, FFA-Fine grained Facies Association, MFA-Medium grained Facies Association and CFA-Coarse grained Facies Association); GR log shows fining upward sequence for both of the core.

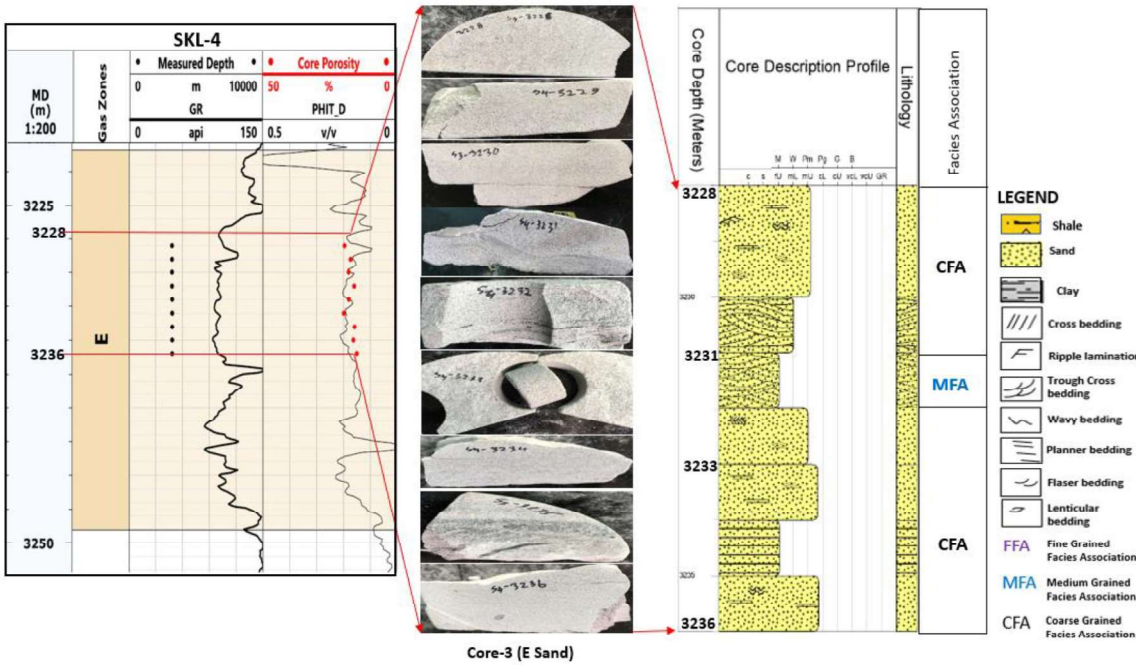

Figure 4.2 Shows Gamma ray log with porosity determined from density porosity, core porosity with core photographs, litholog and facies association of core-3 (3228-3236 m) from E-sand of well-4 (here, FFA-Fine grained Facies Association, MFA-Medium grained Facies Association and CFA-Coarse grained Facies Association). GR log response shows fining upward sequence.

4.3 Facies Association and Lithofacies

Based on grain texture and sedimentary structure examined from the core samples, eight lithofacies and three distinct facies associations have been identified in the studied field. In the studied wells (well-3 & 4), these facies and facies associations have been identified in different proportions. Individual facies and the relationships between the facies association were identified, and their depositional environment were interpreted by integrating their grain sizes, sedimentary structures and architecture.

Table 4.1 Different types of litho-facies and facies associations identified from the core of Srikail gas field, Bengal basin, Bangladesh.

Facies	Facies Association	Percentage %
a) Shale or claystone (Fm) b) Sandstone or siltstone with shale (F1) c) Shale with lenticular bedding (Ln)	Fine grained Facies Association (FFA)	15
d) Sandstone with wavy bedding (Wb) e) Flaser-bedded sandstone, Ripple laminated sandstone (Srm).	Medium grained Facies Association (MFA)	24
f) Sandstone with parallel lamination (Sh) g) Trough (St) and planner (Sp) cross bedded sandstone. h) Massive sandstone with lag mud clasts (Ms).	Coarse grained Facies Association (CFA)	61

Fine grained Facies Association (FFA):

Interbedded shale/claystone (Fm), sandstone or siltstone with shale (F1) and shale with lenticular bedding are the main facies of this facies association. The interbedded shale or claystone facies is composed of mainly minor claystone and very thinly laminated shale. The shales are sometimes silty, and their color is grey to dark grey or blackish. They are common in core-1of well-3 from 3084-3085 m, 3086-3087 m and their thickness vary from few millimeters to centimeter (Figure 4.3a, b). Sandstone or siltstone with shale facies (F1) and shale with lenticular bedding (Ln) were also identified in core-1 of well-3. They are very common from 3084-3084.5 m and 3085-3085.03 m core intervals (Figure 4.3a, b). This facies association is rich in claystone and shale. They are compacted and with low porosity and permeability. In this facies association, fine sandstone or siltstone lenses are

well preserved and they are sometimes connected or isolated. When this lenses are isolated and show internal microlamination, they are called starved ripple (Reineck and Singh, 1980). This facies association occurs in quiet and calm depositional environment. They represents the rhythmic depositional pattern due to the repetitive tidal effect (Rahman et al., 2009). The siltstone or sandstone streaks might have been deposited during storm of high tides period. Mainly, this facies association represents a weak hydrodynamic energy condition. This lithofacies association contributes 15% of total lithofacies in the examined core (Figure 4.6).

Medium grained Facies Association (MFA):

Medium gained facies association is composed of wavy bedded (Wb) and ripple laminated sandstone. Flaser bedding (Srm) is also common is this facies association (Figure 4.3a, b, c ; Figure 4.4a and Figure 4.5b). Alternating mudstone and sandstone as a continuous layer are the characteristics of wavy bedded facies. It is formed when ripple troughs are filled by mudstone and making thin layer of mud on the crest of the ripple. They are isolated and discontinuous vertically. The mudstone layers are bluish grey, and the sandstone layers are grey Figure 4.3a. These wavy bedded facies usually indicate the deposition under non-uniform and bidirectional current. They are common in intervals 3085-3085.5m, and 3089-3089.3 m in core-1, from 3178-3179 m in core-2, from 3228-3236 in core-3 in the studied well-3. They also occur from 3231-3231.3 m core interval in the studied well-4. Structures created by the soft sediment deformation have been also observed. Flaser bedded facies are associated with light grey and medium to fine grained sandstone. The thickness of this facies varies form 3-5 centimeters. Mud flasers usually formed on the troughs of the ripple

and occasionally continues up to the lower part of the ripple. The flasers thickness varies sometimes from millimeters to centimeters.

Figure 4.3 Figure shows, (a) Wavy beded sandstone (Wb), lenticular bedded facies (Ln) and flaser bedded sandstone (Srm) in core-1 from 3083-3086 m; (b) Thinly laminate sand and shale facies (Sm), cross and flaser bedded sandstone (Srm) in core-1 from 3085-3090 m depth; (c) Flaser bedded (Srn) and cross bedded sandstone (St) in core-1from 3090-3093 m depth in Srikail well-3.

This type of facies is observed from 3085-3085.03 m, 3089-3089.5 m, and 3090-3090.5 m intervals in core-1 of well-3, as well as from 3232-3232.5 m in core-3 of well-4. The wavy bedded facies in the fine grained facies association is thought to have been deposited under moderate to low energy condition between the middle portion of intertidal zone but ripple laminated sandstone and flaser bedded sandstone facies might have been deposited in the lower intertidal to upper subtidal zone (Raaf and Boersma, 1971). Sedimentary structures found in this facies association indicate that they might me generated into the intertidal zone by progradation of tidal flats within the tidal depositional setting. This lithofacies association contributes 24% of total lithofacies (Figure 4.6).

Coarse grain Facies Association (CFA):

This facies association consists of sandstone with parallel lamination (Sh), trough cross bedded sandstone (St), sandstone with planner cross bedding (Sp) and massive sandstone with mud clasts facies (Ms). In the parallel laminated sandstone facies (Sh), the beds are horizontally laminated. It consists of grey to light grey, medium to coarse grained sandstone. This sandstone is moderately porous, permeable and compacted. The beds thickness varies from 5 to 20 centimeters and shows textural and mineralogical variation. They are encountered from intervals 3090-3091 m in core-1 and from 3178-3179 m in core-2 in well-3 (Figure 4.3c & Figure 4.4a).The cross bedded sandstone facies consists of planner cross bedded (Sp) and trough cross bedded (St) facies where lower bounded surface of this facies is curved, suggesting an erosional surface (Figure 4.3b, Figure 4.5a). These facies are dominant in the studied core samples. They have been encountered from intervals 3087-3088 m, 3090-3091 m, and 3091-3092 m in core-1, from 3178-3180 m in core-2 of well-3 and from 3228-3229 m, 3233-3234 m & 3234-3235 m in core-3 of well-4.

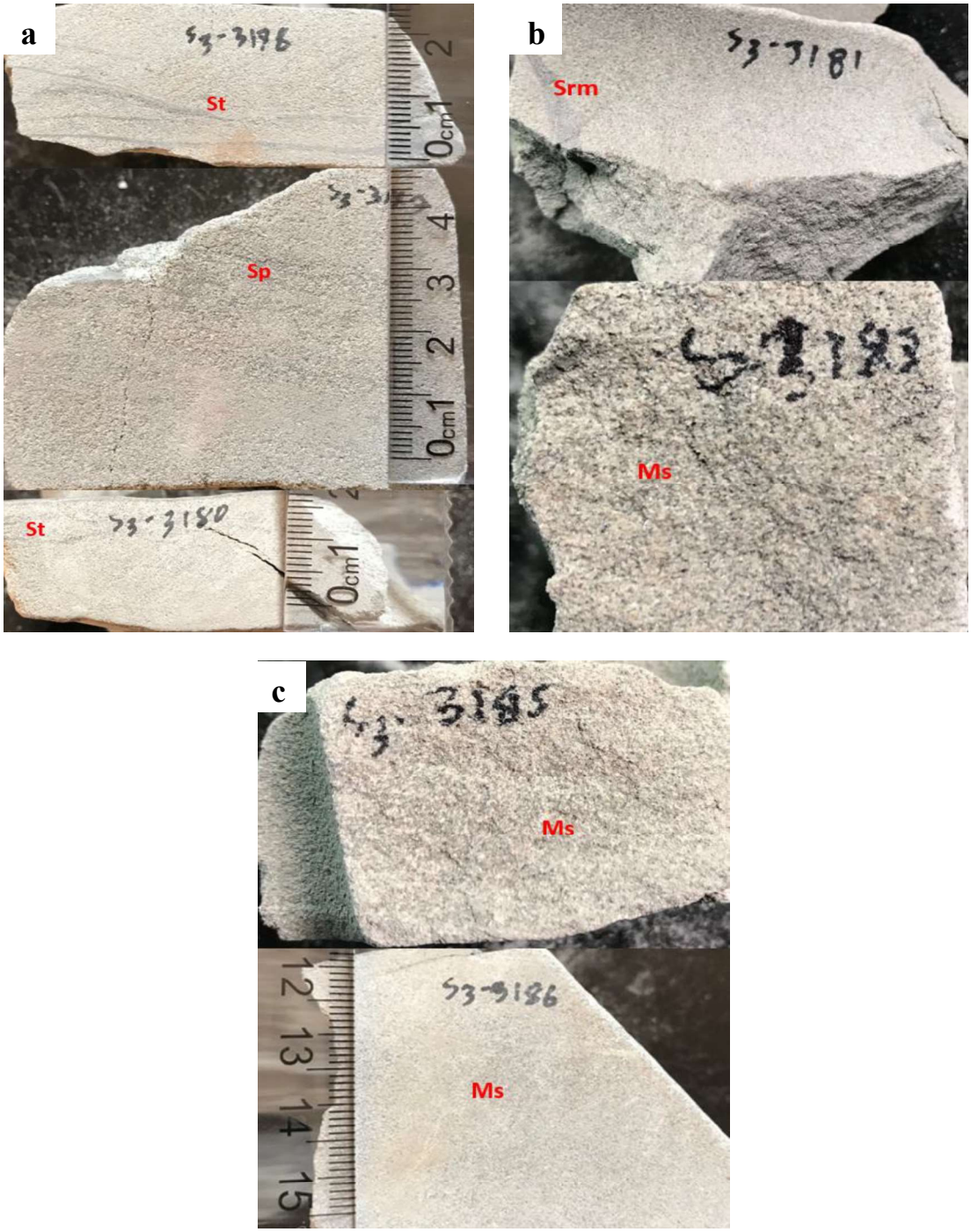

Figure 4.4 Shows (a) Parallel (Sp) and trough cross bedded sandstone (St) (3178-3180 m) ; (b) Flaser bedding (Srm) and massive sandstone facies (Ms) with enormous mica (3181-3183 m) and (c) massive sandstone facies (Ms) (3185-3187 m) in core-2 of Srikail well-3.

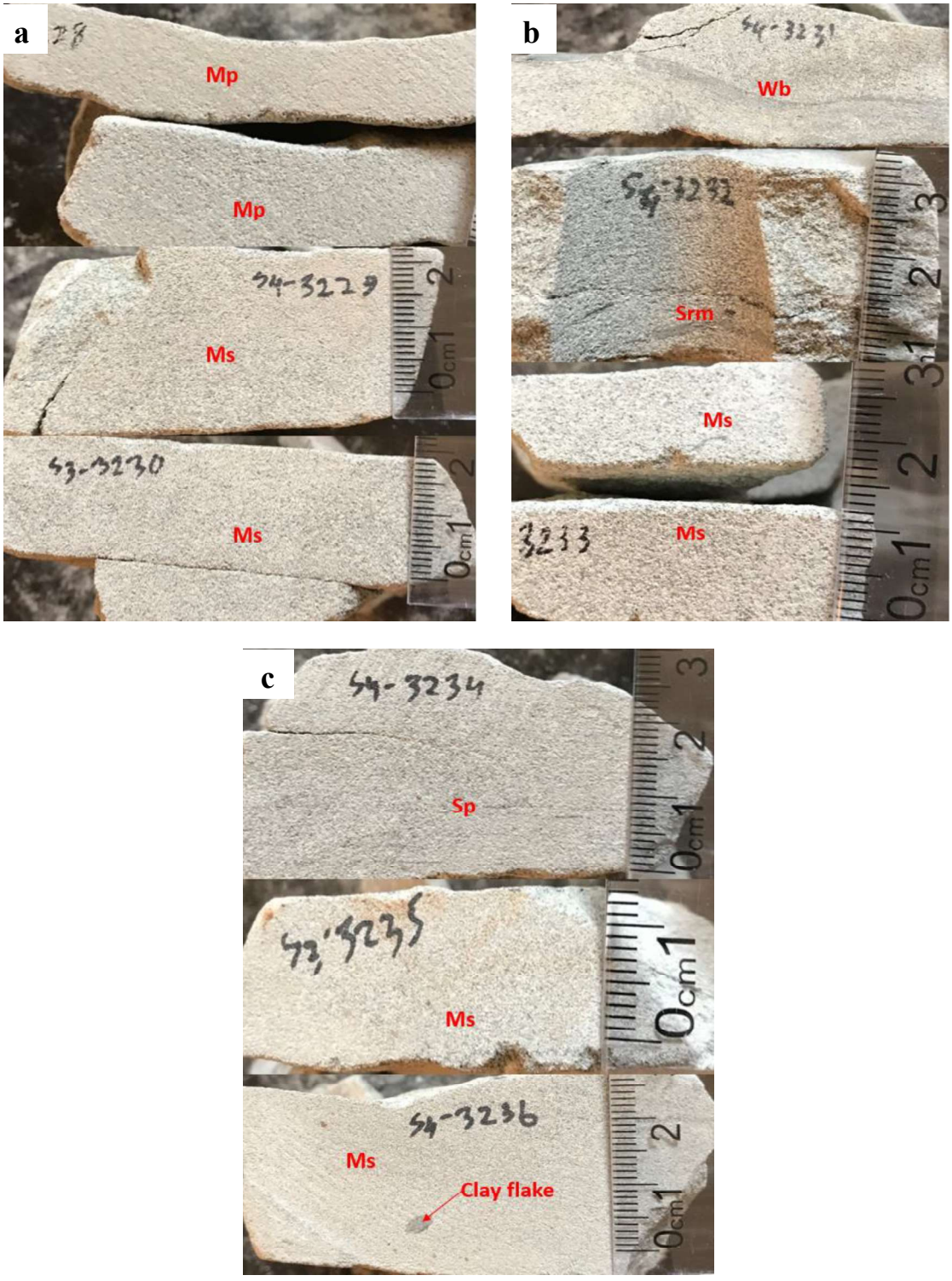

Figure 4.5 Shows (a) Cross bedded and massive sandstone facies (3228-3231 m); (b) Wavy and flaser bedded sandstone (3231-3233 m) and (c) Cross bedded and massive sandstone with clay flakes facies in core-3 of Srikail well-4.

Other than cross bedded sandstone facies and massive sandstone facies are also common in the studied core samples. The sandstone of these facies is grey to light grey color, coarse to medium grained and occasionally clay flakes are observed (Figure 4.5c). Enormous mica is present in this sandstone facies. They have been encountered from 3092-3093 m in core-1, from 3183-3186 m in core-2 of well-3 and from 3229-3231 m, 3235-3236 m in core-3 of well-4.

The coarse-grained facies association consisting of parallel and trough cross bedded facies as well as massive sandstone facies indicates that the sediments have been transported by strong traction current. Parallel cross bedded sandstones are deposited in high energy condition within the upper flow regime in shallow tidal channel, high velocity turbulent flow is also responsible for this deposits (Rahman et al., 2009). Cross bedded sandstone might be deposited in a broad subtidal environment by large migrating bedform influenced by high tidal energy. Massive sandstone with clay flakes reflects channel fill deposits. This lithofacies association contributes 61% of total lithofacies (Figure 4.6).

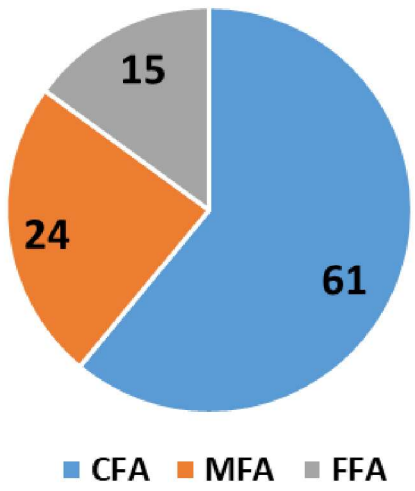

Figure 4.6 Lithofacies distribution among the studied reservoir sandstone of Srikail gas field, where Coarse grained Facies association (CFA) contribute 61%, Medium grained Facies Association (MFA) 24% and Fine grained Facies Association 15% of total lithofacies.

4.4 Electro Facies Analysis

Core study and wireline log response unveiled the cyclic sedimentation character of the Surma Group in the study area (Srikail Gas Field). Two prominent sedimentation cycles were recognized: (a) Cycle of small-scale and (b) Cycle of large-scale. The small-scale cycle was identified from the gamma ray log response and from the core. These cycles arefew centimeters to meters in thickness. These stratigraphic accumulations are the representation of asymmetric cycles which can be represented as coarsening-upward sequence (CU), fining upward sequence (FU), random sequence (RD). They are assumed to have been created by lateral migration of the elements of depositional environments and sub-environments according to Walter's (1894) 'Law of Facies' in response to autogenic mechanism (Reading, 1986). On the other hand, electro-facies analyzed from the wireline log of studied well allowed the possibility to identify the large-scale cycles or sequences which are few meters to hundreds of meters in thickness. They are characterized by para-sequences (PS), (either fining upward or coarsening upward) and para-sequence set these are the episodic stratigraphic accumulations (Wagoner et al.,1990). According to Grotzinger (1986), the generation of para-sequences are related to the allogenic mechanisms due to the eustatic sea-level changes that is transgression and regression, subsidence due to tectonic activity and sediment accumulation rate. From the gamma ray log response of the studied well, different log motifs have been identified; these are (1) funnel shape (2) bell shape (3) bow or egg shape (4) cylinder shape and (5) linear shape (Figure 4.7).

Total of six para-sequence sets (basin wide), twenty-five para-sequence (local changes in the environments) and different bounding discontinuities have been identified from the

gamma ray response of the studied well-4 covering 2650-3260 m depth. These para-sequence sets, and para-sequences reflects different cycles of deposition related to the gross and minor environmental changes. All the para-sequence sets are described below:

Parasequence set-1 (3260-3220 m): This sedimentation cycle shows an overall, coarsening upward (CU) sequence which is consist of three para-sequences (Figure 4.9). In between three para-sequences, 3260-3254 m is coarsening then fining upward cycle (overall funnel shape), 3254-3247 m is also coarsening upward sequence (with bow shape motif) and 3247-3220 m is overall a RD sequence with funnel shape. This para-sequence is bounded by a regressive erosional surface (RES) at 3223m and a marine flooding surface at 3220m which reflects changes in sea-level. The funnel shape reflects the coarsening upward sequence of sand and shale lithofacies which are deposited in prograding tidal flat and prograding deltaic environments. The shale lithofacies represents decreasing hydrodynamic condition and sand represents increasing hydrodynamic condition. The coarsening and fining upward cycle of deposition indicates the subtidal channel, intertidal, floodplain and tidal flat deposits.

Parasequence set-2 (3222-3127 m): This sedimentary sequence (parasequence set) extends from 3222-3127 m and consists of three parasequences Figure 4.9. Above para-sequence set is represented mostly by shaly lithofacies with minor sand facies. It consists of two RD sequences from 3222-3171 m and 3158-3126 m, and one coarsening then fining upward (CUFU) sequence from 3171-3158 m. This parasequence set reflects the transgressive event between parasequence sets-1 and 3. This shale sequence has possibly been deposited in a depositional sub-environment as channel-tidal flat deposit. This

sequence is bounded by marine flooding surface (MFS) in the bottom at 3219 m and regressive erosional surface (RES) on the top at 3125 m.

Parasequence set-3 (3127-3000 m): This sedimentary cycle set represents an overall fining upward (FU) sequence with six small parasequences and it is occurring within 3127-3000 m core interval (Figure 4.9). The sequence set consists of six parasequences with different log motif. Three of the parasequences found at core intervals 3127-3118 m, 3128-3105 m and 3054-3000 m are characterized by fining upward (FU) trend and are delineated bell shape motifs. The three sequences occur as RD sequence (3105-3085 m), coarsening then fining upward sequence (CUFU) (3085-3075 m) and coarsening upward (CU) sequence (3075-3054 m). This parasequence set is composed of sand facies in the bottom and an alteration of sand and shale facies at the top. The sand sequences were likely deposited in fluvial channels or in distributary channels and the shale sequence was deposited under a stable condition where hydrodynamic energy was relatively low. The bottom part of the parasequence set is bounded by a regressive (RES) erosional surface which represents progradation and decreasing sea-level. But the upper part represents the transgressive event which may be because of increasing sea-level or low sedimentation rate.

Parasequence set-4 (3000-2850 m): Para-sequence set-4 is extended from 3000-2850 m with an RD sequence in the bottom and an overall coarsening upward sequence at the top (Figure 4.9). This sequence consists of six parasequences in which core interval 3000-2942 m, representing RD sequence consists of shale facies which is the continuation of transgressive event of para-sequence set-3, and stable low hydrodynamic condition was revealed by minor tidal effect. Core interval 2942-2920 m with bell shape motif represents

fining upward sequence (FU), 2920-2900 m is coarsening upward then fining upward (CUFU) sequence and core intervals 2900-2864 m, 2868-2861 m and 2861-2850 m characterized by funnel shape represent coarsening upward (CU) sequence part of the sequence set. A regressive erosional surface (RES) present at 2942 m depth, reflects a sharp change from high to low sea-level. The upper portion of this parasequence set is sand dominated which reflect the high sedimentation rate and increasing hydrodynamic condition. This sediment might have been deposited in fluvial channel, distributary channel and sub-tidal to intertidal channel.

Parasequence set-5 (2850-2706 m): This overall coarsening para-sequence set consists of four parasequences in which core interval 2850-2790 m with minor change in motif in-between represents RD sequence and fining upward sequence (FU) is found at intervals 2791-2728 m and 2719-2706 m. The core interval from 2778-2719 m represents the coarsening then fining upward (CUFU) sequence (Figure 4.9). This parasequence set is overall rich in sand facies, but the lower portion of this cycle is a bit shaley. This sequence was likely deposited in a tidal or subtidal distributary channel. The sediments can also be deposited in channel tidal flat environment following progradation. A transgressive erosional surface (TES) marked at 2706 m which reflects the sea level change and decreasing sediment supply.

Parasequence set-6 (2706-2685 m): This parasequence set which extends from 2706-2685 m, is dominated by shale facies (Figure 4.9). The sequence is composed of three parasequences where core interval 2706-2685 m is fining upward sequence, 2685-2662 m and 2662-2650 m with funnel shape log motifs, are the coarsening upward sequence.

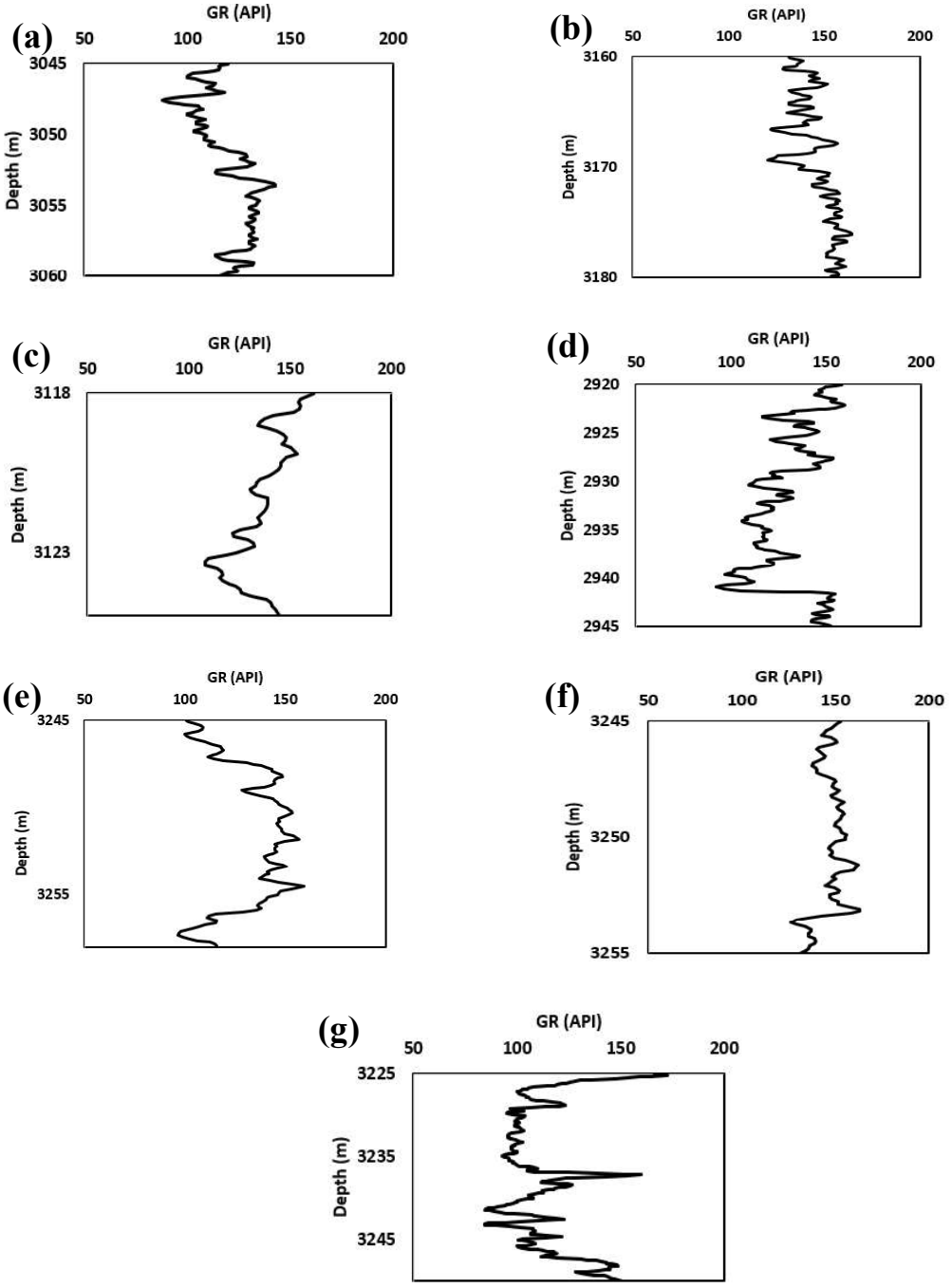

Figure 4.7 Gamma ray log motif of Surma Group sediments encountered in Srikail well-4; (a) & (b) Funnel shape & Serrated funnel shape, represent coarsening upward (CU) sequence, deposits of crevasse splay, mouth bar and delta front; (c) & (d) Bell shape and Serrated bell shape, represents fining upward sequence (FU), deposited in deltaic distributaries and mixed tidal flat (e) Bow of Egg shape, represents coarsening then fining upward sequence (CUFU), deposited in mixed tidal flat (f) Linear shape, deposits of fluvial flood plain and mixed tidal flat (g) Cylinder shape, represents aggradation and deposits of fluvial channel sands and prograding delta.

This parasequence set can be deposited in sub-tidal distributary channel or in shallow marine depositional environment where hydrodynamic power was low. It also reflects a transgressive event of relatively low sediment supply.

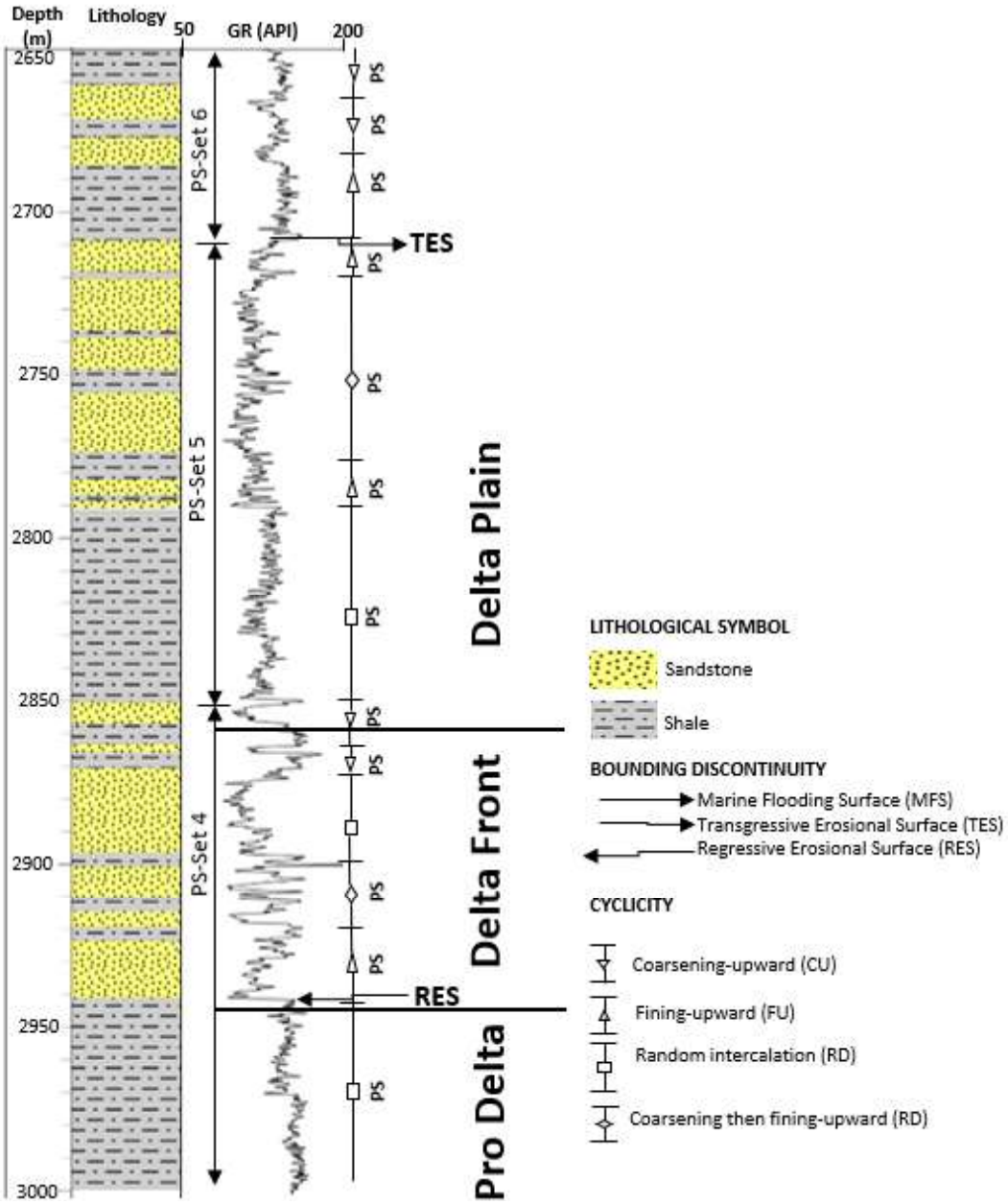

Figure 4.8 Different types of bounding discontinuities, para-sequence set, para sequence have been identified from the gamma ray log response in Srikail-4 well ranges from 2650-3000 m depth. (Here MFS-Marine flooding surface, TES-Transgressive erosional surface, RES-Regressive erosional surface, PS-Set-Para sequence Set and PS-Para sequence).

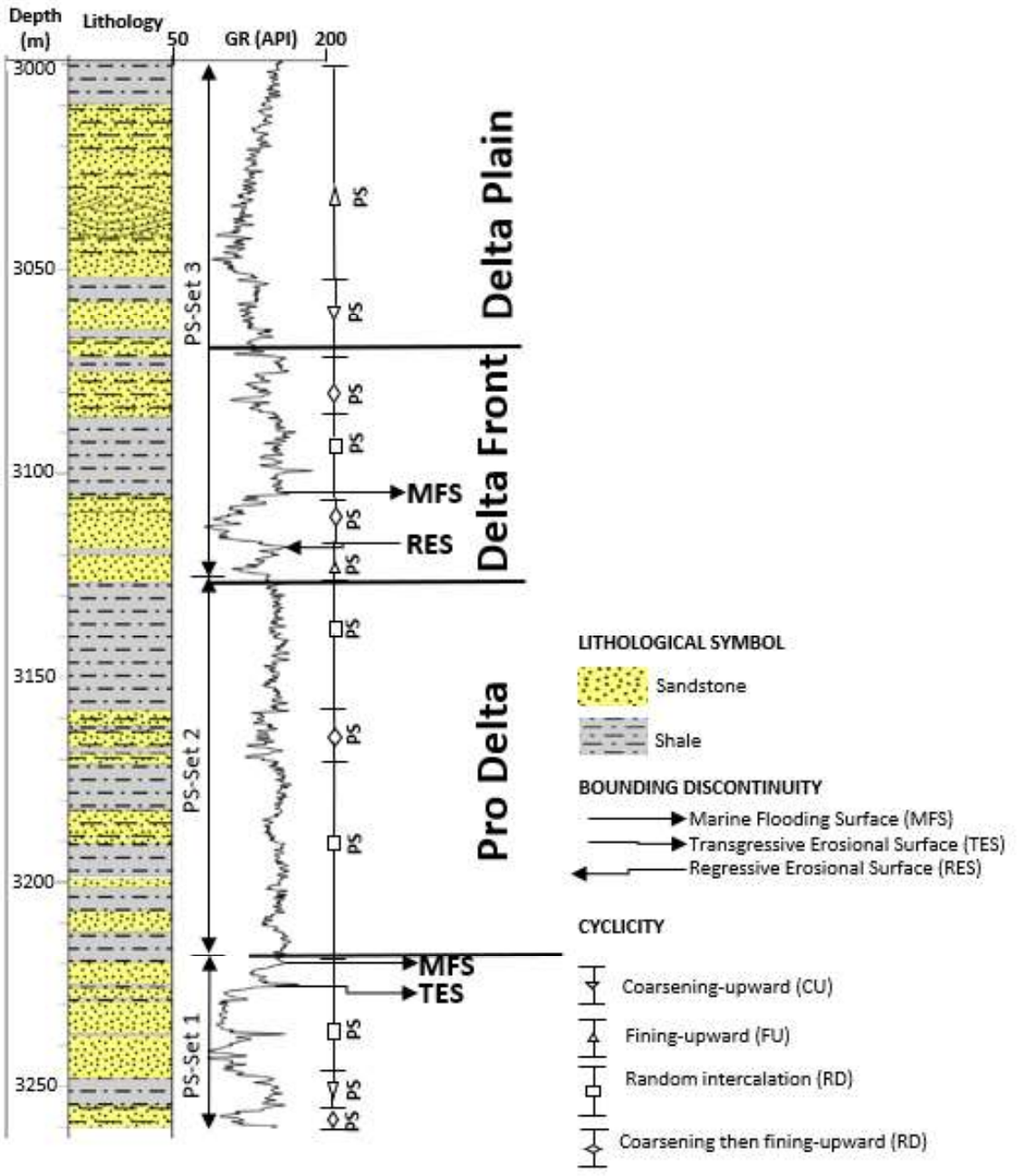

Figure 4.9 Different types of bounding discontinuities, para-sequence set, para sequence have been identified from the gamma ray log response in Srikail-4 well ranges from 3000-3260 m depth. (Here MFS-Marine flooding surface, TES-Transgressive erosional surface, RES-Regressive erosional surface, PS-Set-Para sequence Set and PS-Para sequence).

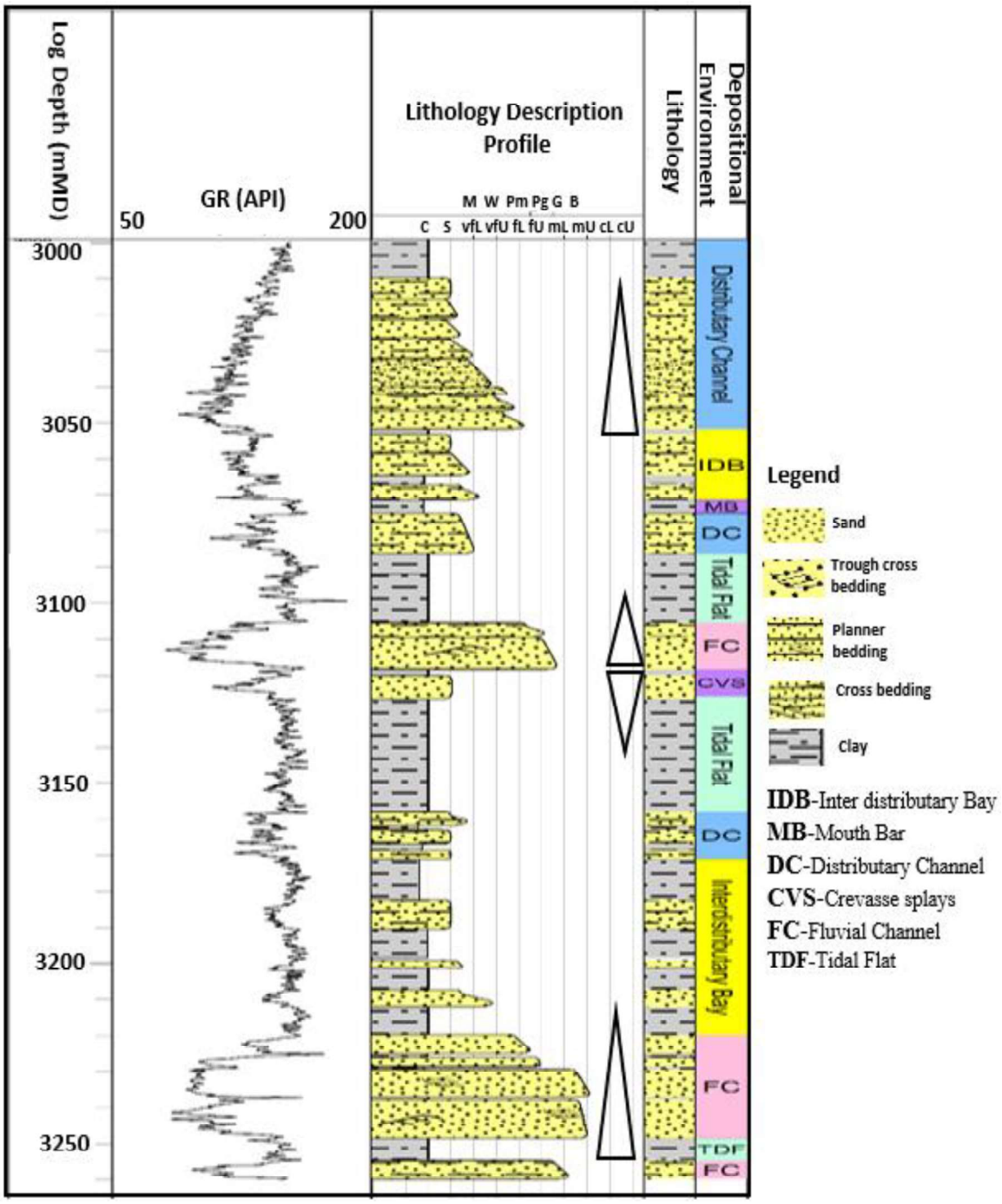

Figure 4.10 Different depositional environments have been identified from gamma ray log of well-4 (IDB-Inter Distributary Bay, MB-Mouth Bar, DC-Distributary Channel, CVS-Crevasse Splays, FC-Fluvial Channel and TDF-Tidal Flat.

4.5 Depositional System with Lithofacies

Based on core and wireline log analysis two depositional systems have been identified in the study area (Srikail gas field) of Bengal Basin and they are tide dominated delta and lacustrine prodelta (Figure 4.11). Different sedimentary facies from the core sample and different log motives from gamma ray log of well-4 have been used for the analysis. This analysis has been performed aiming to study the cyclicity of the sedimentation, vertical change in depositional pattern, energy variation during deposition and sedimentary facies cross ponding to the environment and sub-environment for the core and log data. Three lithofacies association and different electro-facies have already been identified from core and log data (Table 4.1). Each of this lithofacies provide the specific depositional environment regarding the general idea about water depth, depositional system where they have been accumulated.

4.5.1 Tide Dominated Delta

Tide dominated delta is composed of fluvial dominated delta plain, delta plain, proximal delta front and distal delta front which have been identified from the combination of core data and log motives (Figure 4.11).

Fluvial dominated delta plain:

Fluvial lithofacies association represents 22.5% of the studied succession and it is composed of three architectural elements (Figure 4.12). They are fluvial channel (FC), crevasse splays (CVS) and flood plain deposits (FPL).

Formation	Depositional Environment	Sub-Environment	Microfacies	Abbreviation	Geometry fro Gamma ray		
					Curve shape	Lithofacies	Curve samples
Bhuban	Tide Dominated Delta	Fluvial dominated delta plain	Flood plain	FPL	Linear Shape	Fm, F1, Ln	
			Crevasse splays	CVS	Funnel Shape	Wb, Srm	
			Fluvial Channel fill	FC	Box or Bell Shape	Sh, St, Sp, Ms	
		Delta plain	Distributary channel	DC	Box of Bell Shape	Sp, St	

Formation	Depositional Environment	Sub-Environment	Micro facies	Abbreviation	Geometry fro Gamma ray		
					Curve shape	Lithofacies	Curve samples
Bhuban	Tide dominated Delta	Proximal Delta Front	Distributary Channel	DC	Box of Bell	Sp, St	
			Mouth Bar	MB	Funnel	Wb, Srm	
		Distal Delta Front	Interdistributary Bay	IDB	Linear	Fm, F1, Ln	
			Lagoon Mud	LM	Linear	Fm, F1, Ln	

Formation	Depositional Environment	Sub-Environment	Micro facies	Abbreviation	Geometry fro Gamma ray		
					Curve shape	Litho facies	Curve samples
Bhuban	Lacustrine/ Prodelta	Prodelta/ Shallow Lacustrine	Sheet Sand	SS	Interfinger	Fm, F1, Ln	
		Sub lacustrine fan	Sub-lacustrine distributary channel	SLDC	Bell	Wb, Srm	
		Semi-deep lacustrine	Lacustrine Mudstone	LM	Linear	Fm, F1, Ln	

Figure 4.11 Shows different depositional systems in Bhuban formation of Surma group interpreted based on core sample analysis and wireline log analysis. In this figure different lithofacies their depositional environments and sub-environments have been combined.

Fluvial channel: Channel fills deposits are mainly sandstone which is medium to coarse grained, moderately sorted, sub-angular to sub-rounded. It is identified by box and bell shape log motives from gamma ray log. Most of the reservoir zones of the studied gas field is channel fills and they are composed of planar (Sp) to trough (St) cross-bedded sandstone and parallel laminate sandstone (Sh), massive sandstone (Ms) is also common.

Crevasse splay: Crevasse splay is composed of wavy bedded sandstone (Wb) facies and flasser bedded sandstone facies (Srm) which is identified by the funnel shape geometry in gamma ray log. The thinness of this facies is ranges for 3 to 7 m and they are fine to medium grained. Heterogenous structure between the deposits reflects the chaotic flow condition, various flood events and rapid sedimentation.

Delta plain

Delta plain is composed of multiple distributary channels and flood plain. It is relatively thin in the studied gas area which covers 12.09% of the total succession (Figure 4.12).

Distributary channel: Distributary channel deposits are characterized by fine to medium grained, moderate to well sorted sandstone. Parallel (Sp) and trough (St) cross bedded sandstone facies are the common lithofacies in delta plain. It shows the bell shape geometry in the gamma ray log.

Flood plain: Flood plain deposits are mainly fine to medium grained and composed shale and claystone facies (Fm), sandstone with siltstone (F1) and shale with lenticular structure (Ln). It is identified by linear geometry in gamma ray log and represents the lower hydrodynamic condition.

Delta Front:

Delta front deposits have been identified in the studied area of Bengal Basin which is divided into two parts, proximal delta front and distal delta front. Total four depositional sub-environments have been identified based on lithofacies association those are Distributary channel (DC), Mouth bar (MB), Inter distributary bay (IDB) and Lacustrine mudstone (LM). Proximal delta plain deposits cover 19.3% and distal delta plain covers 16.92% of the total studied sedimentary succession (Figure 4.12).

Distributary channel: Distributary channels of proximal delta plain is characterized by medium to fine grained sandstone which is rounded to sub-rounded and moderately sorted. Planner (Sp) and trough (St) cross bedded sandstone facies are common in this depositional environment. Gamma ray log motif shows bell and box shape with high variation (Figure 4.11).

Mouth bar: Mouth bar (MB) deposits are fine to coarse grained, rounded to sub-rounded and poorly sorted sandstone. Small scale cross bedded sandstone (Sp), wavy bedded sandstone (Wb) facies are common in this type of deposit. It shows the funnel shape geometry and over all coarsening upward sequence in gamma ray log response.

Interdistributary bay: Shale with claystone (Fm), Sandstone with siltstone (F1) and shale with sandstone lenses (Ln) are the main facies in the interdistributary bay sub-depositional environment. Gamma ray log shows linear shaped geometry (Figure 4.11).

Prodelta:

Sheet sand, massive blocky mudstone, siltstone and overlying massive sandstone are the main characteristics of prodelta deposits. This sub-depositional environment contains shale

with claystone (Fm), sandstone with siltstone (F1) and shale with sandstone lenses (Ln) facies. Sand sheet ranges from 2 to 5 meters in thickness. They show interfinger geometry in gamma ray log. Prodelta deposits cover 10.59% of the total studied succession (Figure 4.12).

4.5.2 Lacustrine System

Shale and mudstone are the main characteristics of lacustrine sub-environment. In the study area, shale and mudstone are bluish grey in color, they are moderately hard and blocky. This type of facies is deposited in semi-deep to deep lacustrine or in prodelta. It is composed of sub-lacustrine fan and semi-deep lacustrine environment.

Sub-lacustrine environment: Sub-lacustrine deposits are characterized by the sheet sand with thickness of 2 to 5 meters. These sandstones are fine to medium grained, sub-rounded to sub-angular and moderately sorted. Gamma ray log shows the frequent change on motif and gives interfingering geometry. It contains 6.54% of the total studied succession (Figure 4.12).

Semi-deep lacustrine environment: Semi-deep lacustrine sub-environment is characterized by lagoonal mud which represents the calm and quite depositional environment. In the gamma ray log, this deposit shows linear shaped geometry with some interfingering nature due to the sheet sand. Semi-deep lacustrine mud covers 18.7% of the total studied sequence (Figure 4.12).

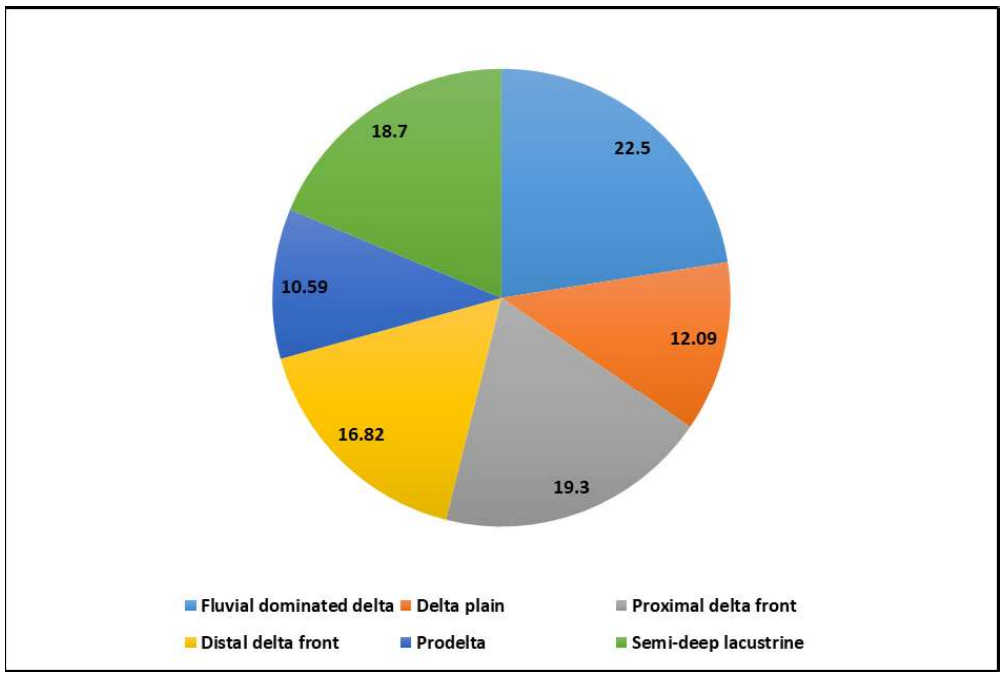

Figure 4.12 Pie chart shows percentage of contribution of different sub-depositional environment in the studied Bhuban formation, Surma group of Srikail gas field in Bengal Basin where deltaic depositional environment shows the maximum contribution.

4.6 Interpretation and discussion

Detailed analysis of various facies and facies associations, their internal stratification pattern, shows that the Surma Group sediments in the studied field were deposited in sub-tidal and intertidal environment of tide dominated deltaic setting. Cross bedded sandstone is an indication of strong reversal current and which is possible in tide-dominated environment. Mud layer bundles resemblance to tidal bundles also indicate the influence of tide dominated depositional environment (Alam et al., 2003). The facies association, wavy bedded sandstone (Wv), lenticular bedded (Ln) and flaser bedded sandstone (Figure 4.3a, Figure **4.3**c & Figure **4.5**b) which are common in the studied core samples are main the criteria for recognizing the intertidal depositional between coastal setting (Klein, 1985).

Variable hydrodynamic conditions of deposition are frequently observed through intermittent association of high and low energy stratification patterns in the core sample which is a typical example of tide dominated environmental deposits (Rahman et al., 2009). In many meso- and macro-tidal coastal settings, tide dominated environments are very likely to occur. For instance, several kilometers wide tidal flats of inter-tidal environments can occur closed to lagoons, in estuaries, behind the barrier island and in tide-dominated deltas (Tucker, 2001).

The huge thickness of the Surma Group sediments encountered in the sub-surface of Bengal basin with their various facies' associations indicates tidal influence. They are thought to have been deposited in shallow marine shelf and tide dominated delta system with the influence of different transgressive and regressive events due to subsidence and relative sea-level changes (Sultana, 2001).

The evidence of deltaic regime with strong tidal influence throughout the history of the Surma Group are also evident from the electrofacies sequence analysis. Various small cyclic patterns of parasequence (PS), parasequence set (PS-set) of large-scale cyclic pattern, regressive and transgressive erosional surface, and marine flooding surface were identified from the log response of studied well (Srikail well-4 from 2650-3260 m). Different log motifs have been identified. These include bell shape which represents the fining upward sequence (FU) deposited during transgressive event in a retrograding distributary channel, funnel shape representing the coarsening upward sequence (CU) deposited during regressive event in fluvial channel of a prograding delta (Figure 4.7). Cylindrical log pattern represents the aggradational parasequence. Bow of egg shape gamma ray log response represents the channel- floodplain, sub-tidal and intertidal

depositional environments. Based on lithofacies and facies association from the core and gamma ray log, it can be inferred that the study area has been developed in shallow marine shelf and tide dominated delta system. Different depositional environments with their lithological description are illustrated in the (Figure 4.10). A conceptual depositional model illustrating the depositional environment and sub-environment correlating with the facies and their association that has been encountered in the studied Srikail gas field has been developed (Figure 4.13). According to the depositional model, the study area is located on the upper delta plain where sediments have been deposited in distributary channels forming crevasse splay. The sediments are medium to fine grain deposited in proximal part of delta that represents the higher hydrodynamic condition than the distal. Distal part of the delta is characterized by enormous distributary channels and mouth bar deposits. Pro-deltaic deltaic part is mostly shale dominated with minor sandstone deposits where influence of tide is prominent. Among the depositional environments of deltaic setting fluvial channel sands, deposited in upper delta plain shows the best reservoir quality in terms of porosity and permeability. The D-lower and E-sand have been deposited in fluvial channels those show the better reservoir quality than D-upper which has been deposited in deltaic distributary channels.

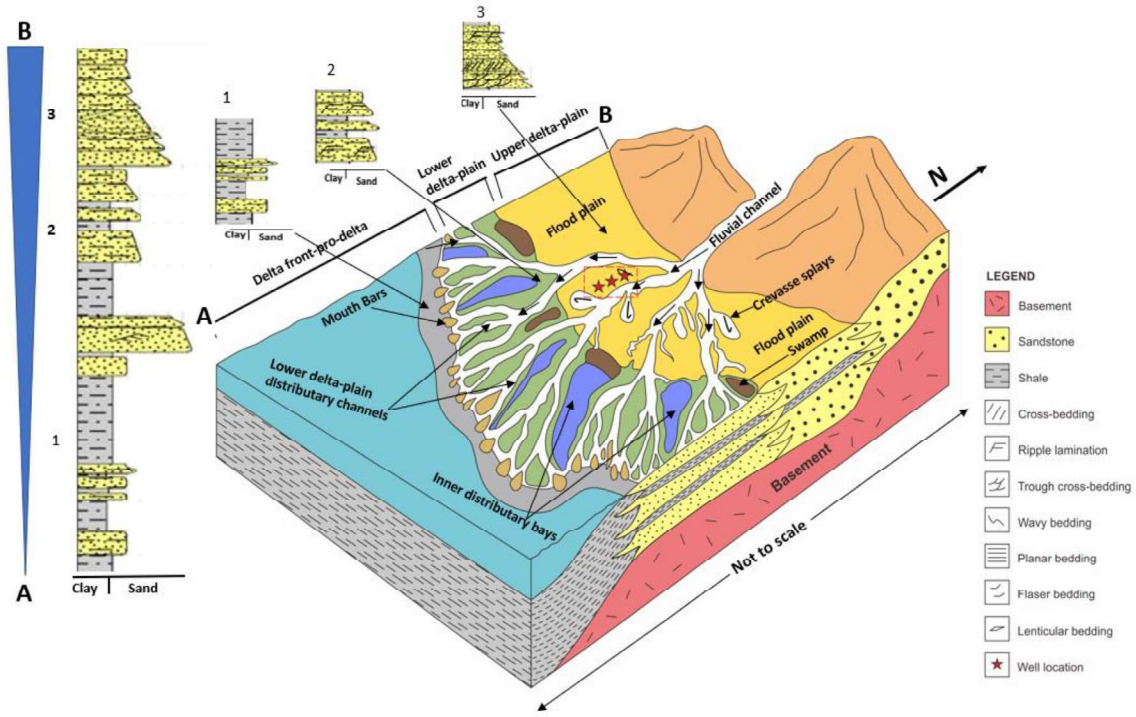

Figure 4.13 Conceptual depositional illustrating different depositional environment and sub-environment and their lateral relationship identified in studied Srikail gas field from core and wireline log analysis. Marked area shows the present well location of studied gas field.

CHAPTER 5

PETROPHYSICAL ANALYSIS

5.1 Wireline Log Analysis

In this study, three prospective zones: D-Upper, D-Lower and E-Sands have been interpreted, based on basic wireline logs (gamma ray, resistivity, neutron porosity and density) of wells-3 and -4. Interpretation includes determination of lithology, gross thickness of hydrocarbon bearing zones, their net thickness, shale volume (V_{sh}) calculation, average porosity and water saturation (S_w) determination (Figure 5.1 and Figure **5.2**). A summary of the results is shown in (Table 5.1). Based on the petrophysical evaluation, shale content is a major control in reservoir quality as suggested by inverse relation with porosity (Figure 5.3). The cross plot has been constructed using density porosity and gamma value of the three gas bearing zones (Figure 5.3 a, b and c). Shale-rich sands can cause compartments within the reservoir zones. D-upper zone is segmented by inter bedded shale layer as shown in (Figure 5.1 and Figure 5.2). It is also proved by the ratio lower net to gross thickness (Table 5.1).

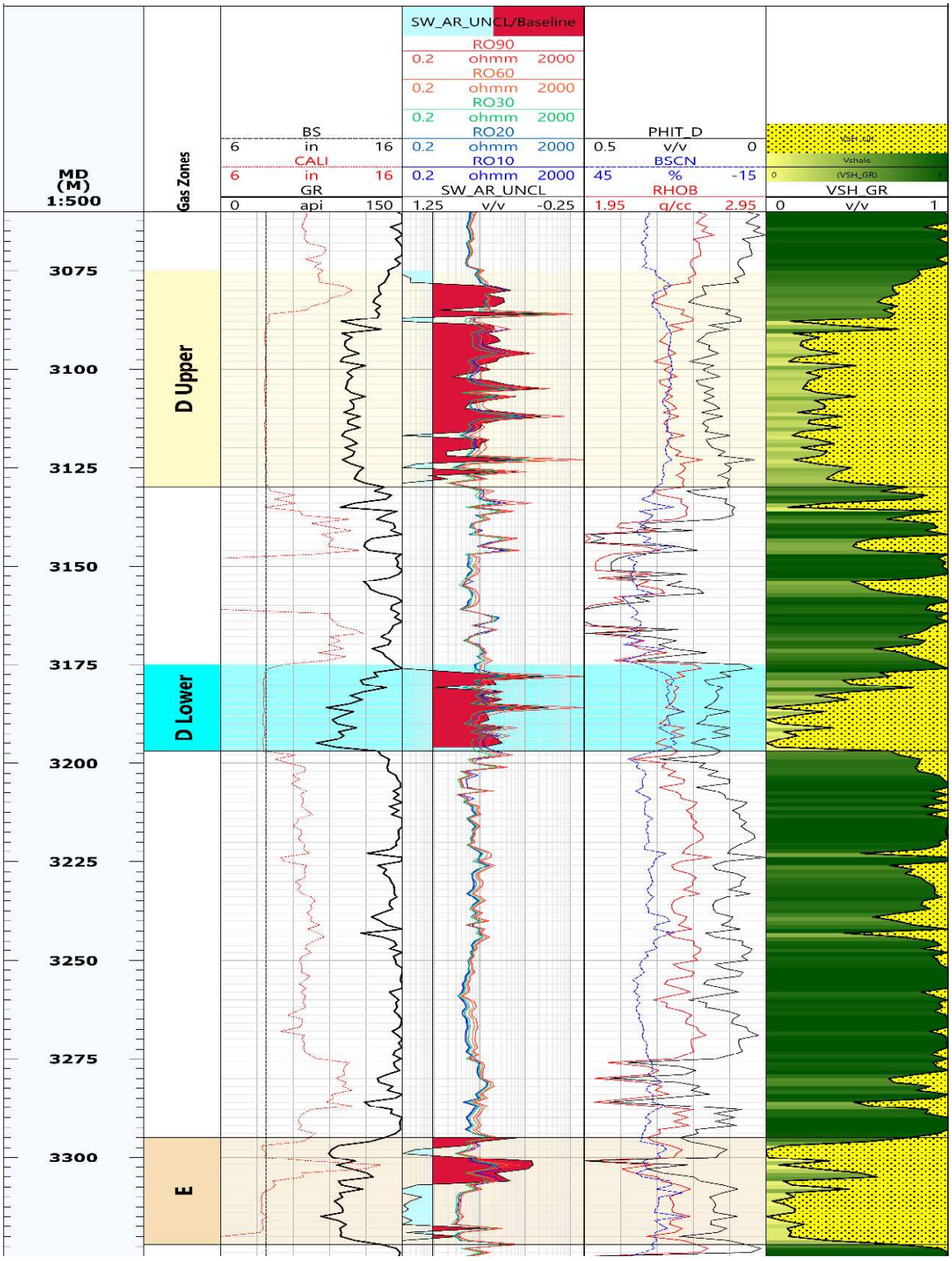

Figure 5.1 Wireline log interpretation of Srikail well-3. Different colored zones represent the reservoir gas sands (D-upper, D-lower and E-sand), red shaded area shows the gas saturated area.

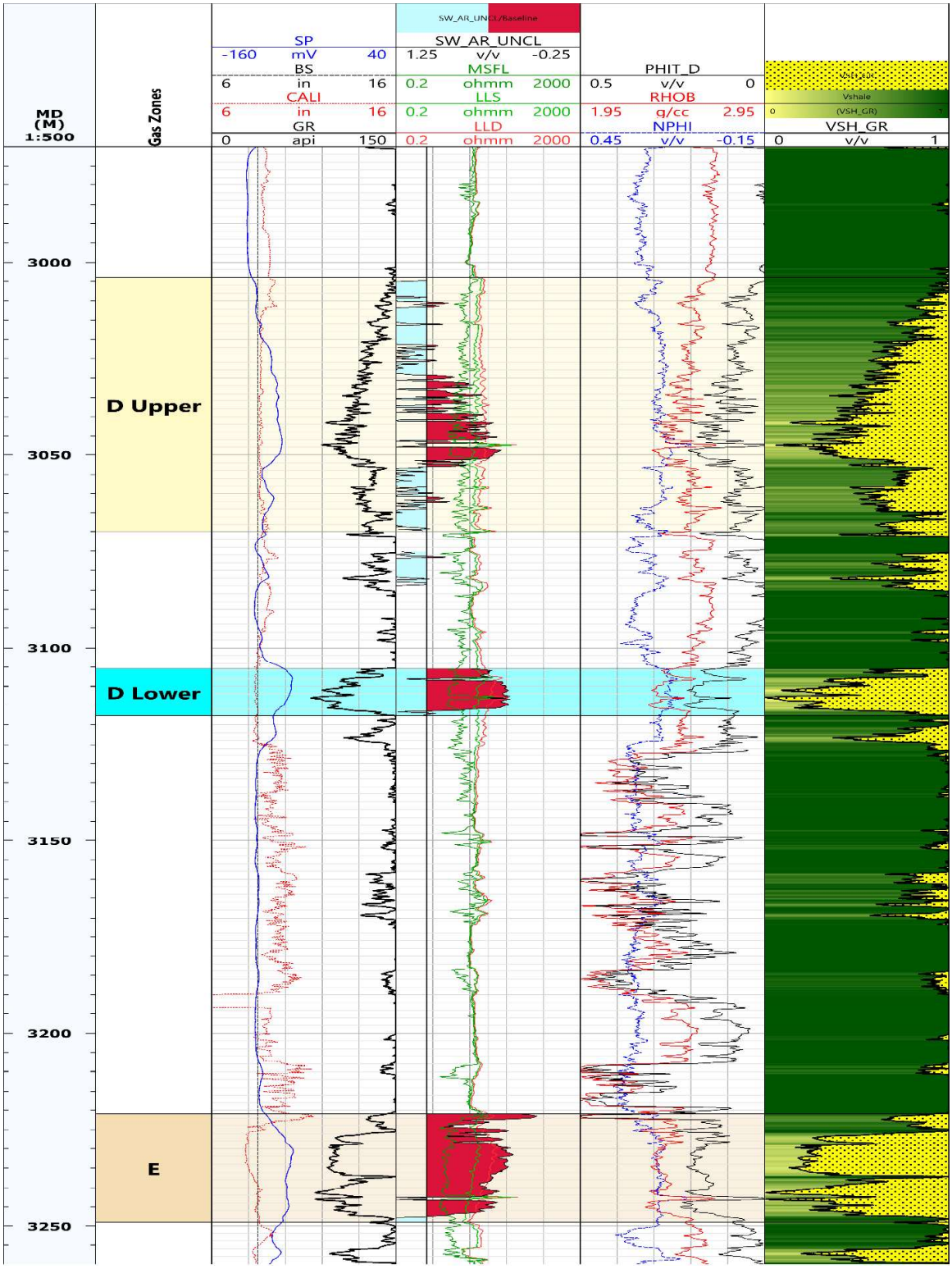

Figure 5.2 Wireline log interpretation of Srikail well-4. Different colored zones represent the reservoir gas sands (D-upper, D-lower and E-sand), red shaded area shows the gas saturated area.

Table 5.1 Results of wireline log data interpretation of prospective zones (D-Upper, D-Lower and E- sand) of well-3 and 4.

Zone	Well	Gross Thickness (m)	Net Thickness (m)	Net to Gross Ratio	Avg. V_{sh} (v/v)	Avg. Porosity (v/v)	Avg. S_w (v/v)
D Upper	W-3	51.26	29.813	0.58	0.277	0.155	0.509
	W-4	20.27	9.171	0.45	0.388	0.154	0.55
D Lower	W-3	25.35	15.664	0.62	0.216	0.15	0.49
	W-4	11.18	6.762	0.60	0.26	0.176	0.387
E Sand	W-3	11.20	6.569	0.59	0.114	0.195	0.466
	W-4	25.95	15.568	0.60	0.285	0.176	0.443

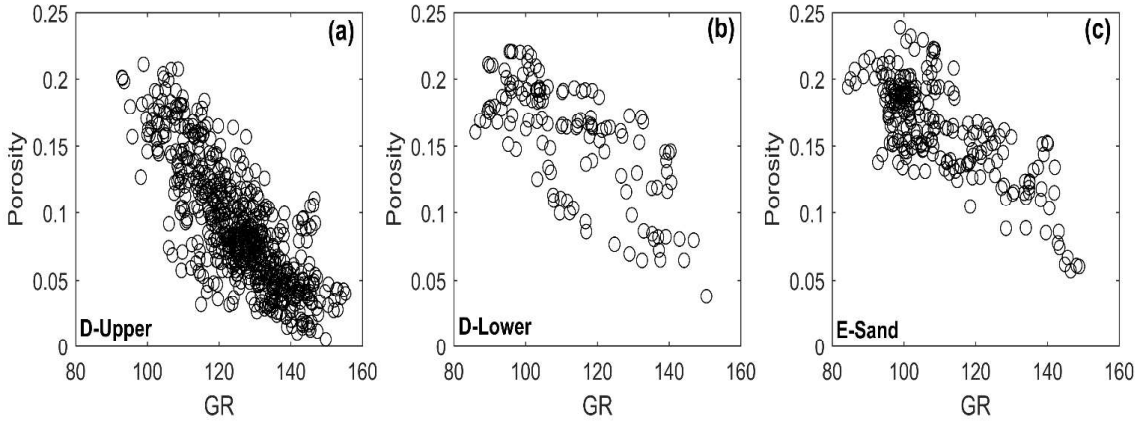

Figure 5.3 Cross plot of calculated porosity vs gamma value of gas bearing zones a. D-upper; b. D-lower and c. E-sand of Srikail wells. Which shows the inverse relationship between porosity and gamma value.

5.2 Core Porosity and Permeability

5.2.1 Porosity

Core porosity varies from 8% to 20% in the studied reservoir samples of Srikail wells

Table 5.2). The wireline log analysis revealed similar range of porosity from 8% to 19.5% in the three reservoir zones. Two major ranges of porosity were obtained from statistical analysis (R_1: 13.44-16.44%, R_2: 16.44-19.44%) of the core data (Figure 5.4a). Two types of pores were identified from thin section and SEM analyses: intergranular primary pores (Figure 6.6a), intragranular secondary pores developed by feldspar dissolution (Figure 6.5b; Figure **6.6**a). In the studied reservoir zones of Srikail wells, primary pores are the most abundant pore types. Intragranular secondary porosity was developed due to the dissolution of detrital feldspar and rock fragments (Figure 6.5f). Most of the secondary pores are ineffective because they are occupied by clay minerals (Figure 6.5b). Authigenic clays and other phyllosilicate minerals like muscovite and biotite have moderate control (r^2 = 0.57 and 0.55 respectively) on core porosity (Figure 5.5a, c) but more impact (r^2 = 0.63 and 0.73 respectively) on intergranular porosity (Figure 5.5b, d).

5.2.2 Permeability

Core Permeability of the studied samples ranges from 0.1 mD to 111 mD with an average of 40 mD. Three major ranges of permeability were obtained from statistical analysis (R_1: 1-21 mD, R_2: 21-41 mD, R_3: 61-81 mD) (Figure 5.4b). Core porosity-permeability cross plots show that permeability increases with porosity although a noticeable scatter could be observed (Figure 5.7a). Although porosity values of most samples range between 8% and 20%, permeability varies by around 2 orders of magnitude (from 0.8 to 118 mD). Such scatter might be explained by the variable ductile grains and clay contents which are inversely related to permeability (Figure 5.5e and f). There is a less effect of authigenic clay and other cements on permeability (r^2 = 0.30) (Figure 5.5e), whereas muscovite and

biotite contribute more to permeability reduction (r^2 = 0.59) (Figure 5.5f). There is one sample that clearly deviates from the overall trend (Figure 5.5e &f; labeled A). This sample has much lower permeability compared with other samples that have similar clay or ductile grains content. This might be explained by the presence of a shale lamination in the middle of the sample which will not be captured by the QEMSCAN result (done on surface), yet it can reduce the vertical permeability drastically (Figure 5.6).

Table 5.2 Measured core porosity and permeability of D-Upper and D-Lower Sand of well-3 and E-Sand of well-4.

Zone	Sample ID	Depth (m)	Porosity (%)	Permeability (mD)
D-Upper	S-3-3084	3084	7.44	0.1
	S-3-3085	3085	10.58	0.6655
	S-3-3087	3087	18.56	73.24
	S-3-3088	3088	16.15	4.24
	S-3-3089	3089	17.85	33.03
	S-3-3090	3090	17.21	4.77
	S-3-3091	3091	15.55	2.46
D-Lower	S-3-3179	3179	15.72	33.31
	S-3-3180	3180	15.71	10.03
	S-3-3181	3081	18.17	22.61
	S-3-3182	3082	17.44	75.69
	S-3-3183	3083	16.98	71.24
	S-3-3185	3185	17.02	68.18
	S-3-3186	3186	15.2	35.45
E-Sand	S-4-3228	3228	19.57	104.14
	S-4-3229	3229	17.28	76.09
	S-4-3230(a)	3230	18.05	89.15
	S-4-3230(b)	3230	19.88	84.46
	S-4-3231	3231	15.95	1.3
	S-4-3232	3232	17.99	49.44
	S-4-3233	3233	19.83	111.66
	S-4-3234	3234	15.83	14.3
	S-4-3235	3235	16.23	25.94
	S-4-3236	3236	14.97	16.83

5.3 Comparison of Porosity and Permeability Data with Other Fields

Porosity and permeability data of the Bhuban Formation from the Titas and Bakhrabad gas fields has been compared with data of Srikail gas field of this study (Figure 5.7b). Data of this study fits within the overall porosity-permeability relationship but shows relatively lower porosity and permeability values compared to those of the Bakhrabad and Titas gas fields. The shallower burial depth for the formation at the Titas and Bakhrabad gas fields may explain the higher porosity and permeability values compared with Srikail field (this study). With the increasing depth, compaction increases, and grains are rearranged thus reducing the porosity and permeability.

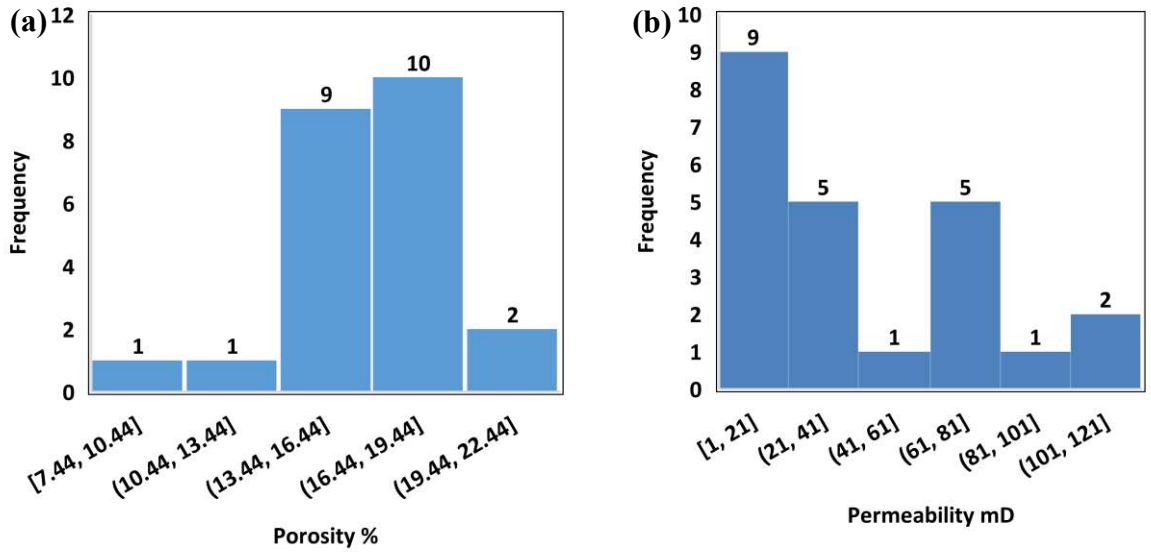

Figure 5.4 Histogram diagram shows a. porosity distribution, two porosity range (R_1: 13.44-16.44%, R_2: 16.44-19.44%) b. permeability distribution, three permeability range (R_1: 1-21 mD, R_2: 21-41 mD, R_3: 61-81 mD) of Bhuban formation in Srikail gas field.

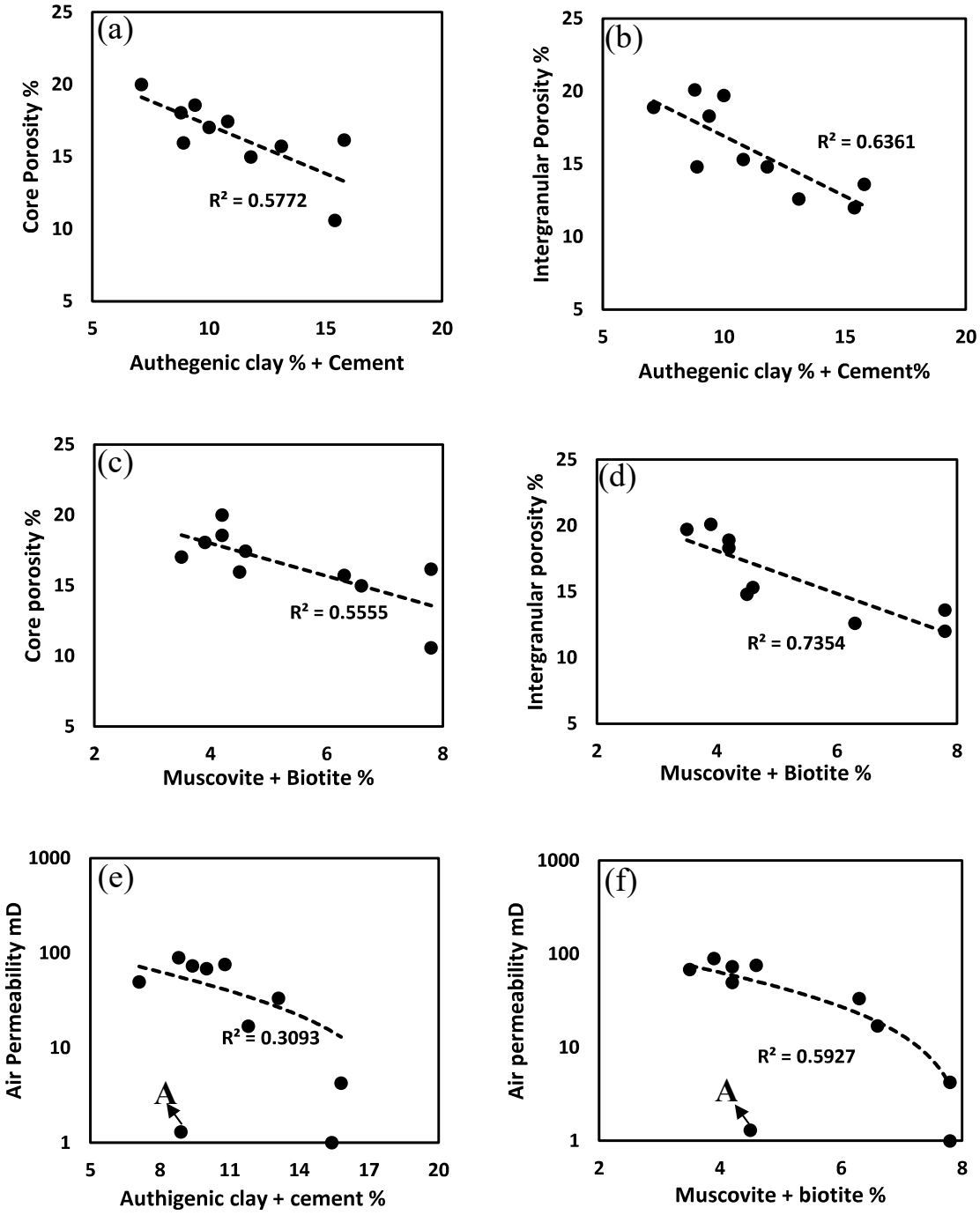

Figure 5.5 Mineralogical controls on core porosity and permeability a. Core porosity versus authigenic clay + cement; b. Intergranular porosity versus authigenic clay + cement; c. Core porosity versus muscovite + biotite; d. Intergranular porosity versus muscovite + biotite; e. Air permeability versus authigenic clay + cement; f. Air permeability versus muscovite + biotite. Sample with high porosity, low permeability is denoted by A which is due to thin shale lamina in sample no S-4-3285.

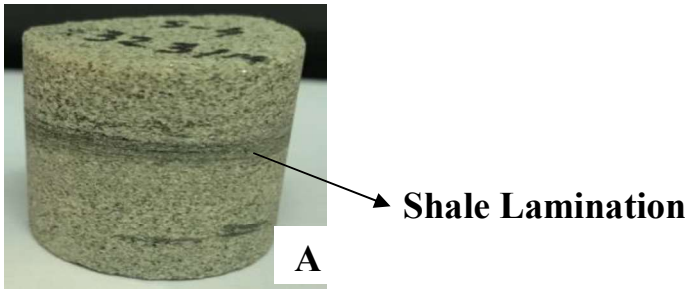

Figure 5.6 Thin layer of shale in E-Sand at 3231 m depth which is responsible for low permeability with high porosity. In the cross plot the point has been marked as A.

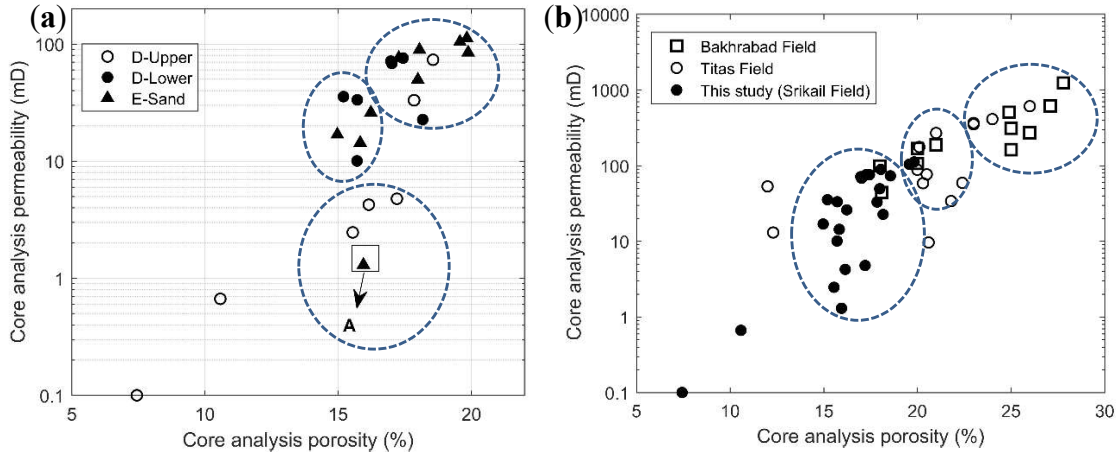

Figure 5.7 Porosity versus permeability cross plot a. D-upper, D-lower and E-sand of studied field; higher porosity obtained in D-upper and E-sand than D-upper b. Nearest Srikail gas field (this study), Bakhrabad and Titas gas field (data from Rahman et al. 2016), higher porosity and permeability found in both Bakhrabad and Titas gas field than Srikail gas field.

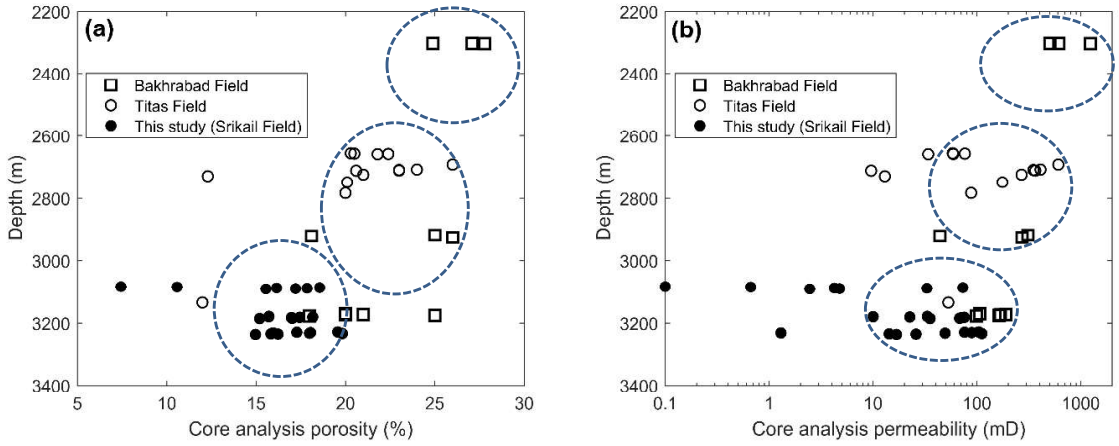

Figure 5.8 a. Porosity versus depth and b. permeability versus depth for samples from Surma Group sandstone in Srikail Field (this study) and Bakhrabad and Titas Fields (data from Rahman et al. 2016). Both porosity and permeability decrease with the increment of burial depth in Bakhrabad and Titas gas field as well as studied Srikail gas field.

CHAPTER 6

PETROGRAPHY, DIAGENESIS AND MINERALOGY

6.1 Lithological Composition and Fabrics

Petrographic analysis results of sandstones are presented in Table 6.1. A modal analysis of was carried out on the sandstones encountered in the investigated Srikail wells, using the Folks (1980) classification scheme (Figure 6.1a). The sandstones are predominantly subarkosic in composition. A QFL provenance plot was made following Weltje (2006). According to this plot, sandstones derived from continental block (Figure 6.1b). The sandstones are predominantly medium to fine grained, moderate to well sorted. Dominant grain contact types are long, point, concavo-convex with few sutured contacts (Figure 6.2c, d).

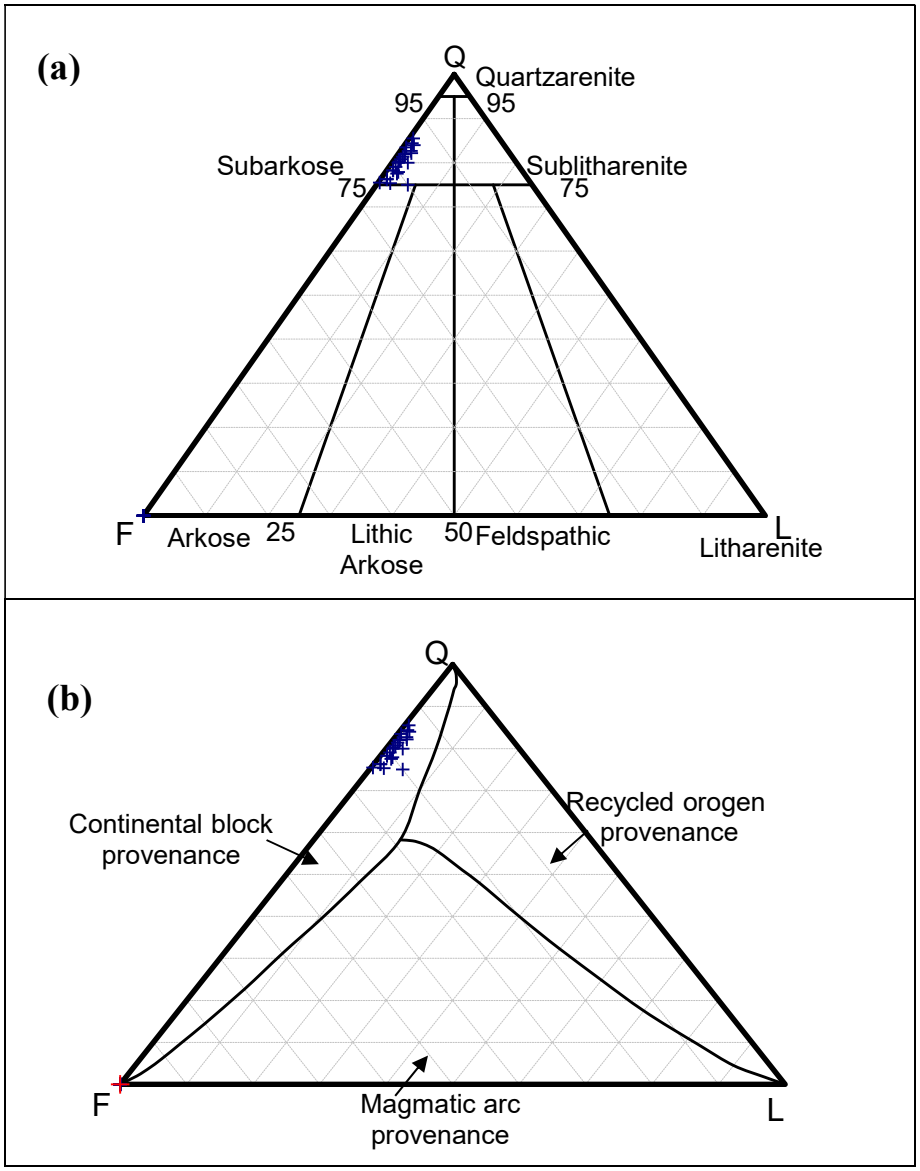

Figure 6.1 QFL triangular diagram shows a. The classification of sandstone of wells SKL-3 and 4 of the Bhuban Formation, Srikail Gas Field, Bengal Basin, Bangladesh according to Folks, 1980 McBride, (1991); b. the provenance of reservoir sandstone of wells SKL-3 and 4 of the Bhuban Formation, Srikail Gas Field, Bengal Basin, Bangladesh; modified after Weltje (2006).

Table 6.1 Petrographic and core porosity-permeability values of core sample from well-3 and 4 of Srikail gas field. Folks sandstone classification method has been used for point counting (Folks, 1980). Quartz, Feldspar and Lithic grains have been considered as 100 percent of the volume. (m-medium, fin-fine, crs- coarse, mod-moderate, wl- well, rd- rounded, ang- angular, lg- long, pt- point, conx- concave).

		Texture				Minerals									
Well	Sample ID	Grain Size ≥20%	Sorting	Roundness	Grains contact	Quartz	Feldspar	Lithic	Matrix %	Cement%	Muscovite/ Mica %	Cement Type	Visual Porosity %	Core Porosity %	Core Permeability (mD)	Classification
SKL-3	S-3-3083	m-fin	mod	sub-rd-sb-ang	lg, pt, conx	83.28	15.72	1.72	15	3	1	Si, Fe, Cly	10	not found	0	Sub Arkose
SKL-3	S-3-3084	fin-m	mod	sb-rd	lg, conx	80	17.5	2.5	30	5	3	Si, Fe, cly,cal,dol	3	7.44	0.1	Sub Arkose
SKL-3	S-3-3085	m-fin	mod-wl	sb-rd-rd	lg, pt, conx	80.77	18.23	1	5	2	0.5	Si, Fe, cly,cal,dol	10	10.58	0.6655	Sub Arkose
SKL-3	S-3-3087	m-fin	mod-wl	sub-rd-rd	pt	82.19	15.81	2	2	1	0.5	Si, Fe, cly,dol	20	18.56	73.24	Sub Arkose
SKL-3	S-3-3088	fin-m	mod	sb-ang-sb-rd	lg-pt	82	17	1	10	3	2	Si, Fe, cly	15	16.15	4.24	Sub Arkose
SKL-3	S-3-3089	fin-vf	mod-wl	sb-rnd-rnd	conx, pt	84.42	14.58	1	3	2	1	Si, Fe, cly	15	17.85	33.03	Sub Arkose
SKL-3	S-3-3090	fin-m	mod-wl	sb-rd-sb-ang	lg, pt, conx	83.49	16.01	0.5	5	2	3	Si, Fe, cly	20	17.21	4.77	Sub Arkose
SKL-3	S-3-3091	fin-m	mod-pr	sb-rd	L	80	19	1	15	4	5	Si, Fe, cly	10	15.55	2.46	Sub Arkose
SKL-3	S-3-3179	m-fin	mod	sb-rd-rd	pt, conx	85.53	13.85	0.62	3	3	0.5	Si, Fe, cly,dol	16	15.72	33.31	Sub Arkose
SKL-3	S-3-3180	fin-m	md-wl	sb-rd	pt, lg, conx	81.41	17.59	1	5	2	0.5	Fe, Si, cly	15	15.71	10.03	Sub Arkose
SKL-3	S-3-3181	fin-vfin	mod-wl	sb-rd-sb-ang	pt, lg, conx	84	14.5	1.5	5	5	1	Fe, cly, Si	15	18.17	22.61	Sub Arkose
SKL-3	S-3-3182	m-fin	mod	sb-rd-sb-ang	pt, conx	77.49	20.51	1	3	3	1	Fe, Si, cly	18	17.44	75.69	Sub Arkose
SKL-3	S-3-3183	m-fin	mod	sb-rd-rd	pt, lg, conx	77.9	20.1	2	3	2	0.5	Si, Fe, cly	19	16.98	71.24	Sub Arkose
SKL-3	S-3-3185	m-crs	mod	sd-rd-sb ang	pt, conx	77.5	19.5	1	3	3	2	Fe, Si, cly	18	17.02	68.18	Sub Arkose

Well	Sample ID	Grain Size ≥20%	Sorting	Roundness	Grains contact	Quartz	Feldspar	Lithic	Matrix %	Cement%	Muscovite/ Mica %	Cement Type	Visual Porosity %	Core Porosity %	Core Permeability (mD)	Classification
SKL-3	S-3-3186	m-fin	md-wl	sb-rd-sb-ang	pt, lg, conx	75	20	5	7	3	1	Si, Fe, cly	15	15.2	35.45	Sub Arkose
SKL-4	S-4-3228	m-fin	md	sb-rd-sb-ang	lg, conx, pt	78.3	20.7	1	2	1	1	Si, Fe, cly	20	19.57	104.14	Sub Arkose
SKL-4	S-4-3229	m-fin	md	sb-rd-sb-ang	pt, lg, conx	77.54	20.46	2	2	1	1	Si, Fe, cly	19	17.28	76.09	Sub Arkose
SKL-4	S-4-3230(a)	m-fin	md-wl	sb-rd-sb-ang	pt, lg, conx	80.3	18.7	1	1	1	1	Si, Fe, cly	20	18.05	89.15	Sub Arkose
SKL-4	S-4-3231	m-fin	mod-wl	sb-ang-sb-rnd	lg, conx, pt	75.33	22.67	2	3	2	1	Si, Fe, cly, cal, dol	19	15.95	1.3	Sub Arkose
SKL-4	S-4-3232	m-fin	mod-wl	sb-rnd-rnd	lg, conx, pt	82	17	1	1	1	1	Si, Fe, cly, cal, dol	20	17.99	49.44	Sub Arkose
SKL-4	S-4-3233	m-fin	mod-wl	sb-rnd-sb-ang	lg, conx, pt	82	17	1	1	1	2	Si, Fe, cly	20	19.83	111.66	Sub Arkose
SKL-4	S-4-3234	f-m	mod-wl	sb-rd-rd	lg-pt	76.32	22.68	1	3	2	3	Si, Fe, cly	16	15.83	14.3	Sub Arkose
SKL-4	S-4-3235	f-m	wl	sb-rd-rd	lg, conx	76.2	22.8	1	3	3	2	Si, Fe, cly	16	16.23	25.94	Sub Arkose
SKL-4	S-4-3236	f-m	m-wl	sb-sb-ang	lg, conx, pt	75.49	24.26	0.25	5	3	2	Si, Fe, cly,cal,dol	15	14.97	16.83	Sub Arkose

Table 6.2 QEMSCAN analysis of 10 thin sections shows the area percentage of minerals. Thin sections were made from the same sample which were selected for SEM analysis.

Well	Sample No	Quartz	K-Feldspar	Albite	Muscovite	Biotite	Chlorite	Illite	Smectite	Kaolinite	Calcite	Dolomite	Pyrite	Heavy Minerals	Porosity	Others
SKL-3	S3-3085	48	5.3	10.1	2.7	5.1	6.3	5.6	0.1	1.4	1.4	0.5	0.1	0.4	12	0.8
SKL-3	S3-3087	53.4	4.2	9.5	1.8	2.4	5.2	2.8	0.2	0.7	0.1	0.4	0	0.6	18.3	0.5
SKL-3	S3-3088	47.4	5.2	9.4	3.4	4.4	9.3	4.4	0.2	0.9	0.3	0.6	0.1	0.5	13.6	0.3
SKL-3	S3-3179	51.6	4.9	10.1	2.9	3.4	8.6	3.2	0.2	1.1	0	0	0	0.6	12.6	0.8
SKL-3	S3-3182	53.4	4.5	10.3	2	2.6	7.2	2.8	0.2	0.6	0	0	0	0.4	15.3	0.5
SKL-3	S3-3185	50.5	5.2	9.4	1.4	2.1	5.2	2.8	0.1	0.7	0	0	1.2	0.3	19.7	1.4
SKL-4	S4-3230	50.5	5.5	10.3	1.8	2.1	5.5	2.8	0.1	0.3	0	0	0.1	0.4	20.1	0.4
SKL-4	S4-3231	54.8	5.5	10.8	2.3	2.2	5.4	2.8	0.2	0.4	0.1	0	0	0.3	14.8	0.4
SKL-4	S4-3233	52.9	5.2	10.5	2	2.2	3.8	2.7	0.1	0.4	0	0	0.1	0.2	18.9	1
SKL-4	S4-3236	51.3	4.8	10.1	3.2	3.4	7	3.5	0.2	0.9	0.1	0.1	0	0.4	14.8	0.3

Quartz representing an average of 74% of the total grains, is the most common detrital constituent in the analyzed samples (Table 6.1). The quartz grains are predominantly monocrystalline with minor amount of polycrystalline grains. Feldspar (avegage:15.5%) is the second most abundant grain in the samples. It is mainly represented by plagioclase with a minor amount of K-feldspar. Rock fragments are dominated by metamorphic lithic grains and they are mainly micaceous phyllite and schist/gneiss. Sedimentary lithic grains are also common in the samples. Detrital mica (muscovite and biotite) is rare to common, ranging from 1.5-5% (Figure 6.2 a &b). The mica grains are generally platy and locally deformed when sandwiched between detrital grains. Quartz, and feldspar also appear to have undergone fracturing (Figure 6.2c). QEMSCCAN analysis shows that heavy minerals including zircon, garnet, rutile and tourmaline occur in traces, accounting for an average of 0.5% (Table 6.2).

6.2 Diagenetic Constituents and Features

Silica and clay minerals (chlorite, illite-smectite and kaolinite) are the main diagenetic minerals present as cements in the Bhuban Formation of Srikail wells. XRD data showed their common presence in air dried, glycolated and 550 ºC heated diffractograms as well as in XRD diffractogram of the powdered samples (Figure 6.3c, d). Diagenetic features like Quartz overgrowth Figure 6.2e; Figure 6.5c, b; Figure 6.6a and feldspar dissolution (Figure 6.2c, f,; Figure **6.5**b, f and Figure **6.6**c, d) are common in thin section and SEM analyses. Chlorite rims are also revealed by SEM analysis (Figure 6.5g). Trace amount of pyrite crystals are also found in SEM analysis (Figure 6.6c, d, e). As shown by the QEMSCAM analysis, calcite and dolomite occur as minor in amount cements in the

samples (Table 6.2). In the subsequent section, the diagenetic constituents are described according to their abundance.

6.3 Clay Minerals as Cement

As revealed by QEMSCAN, XRD and SEM analyses the most common clay minerals encountered in the reservoir sandstones of Srikail wells are chlorite, illite, and kaolinite. They represent 13% of the total minerals in the QEMSAN analysis (Table 6.1). XRD analysis of powdered samples also confirm the presence of clay minerals (Figure 6.3c). XRD spectral of the separated clay fraction of these sandstones gives chlorite (47%) and illite (42%) are the most abundant while kaolinite (10%) and smectite (1%) are common to rare (Figure 6.3d).

Chlorite

Chlorite is the dominant cement in these sandstones, and it is extensively developed in intergranular pore networks and occurs as pore lining constituents (Figure 6.6b). It also forms rim around the detrital grains (Figure 6.5g). Energy dispersive spectrum (EDS) shows that chlorite is rich in iron (Figure 6.5h). In this sandstone, detrital grains are coated by chlorite inhibiting quartz overgrowth (Figure 6.6b). Chlorite consists of small microcrystalline, irregular to pseudo hexagonal plates, aligned in a grain perpendicular form, occasionally enclosed by quartz overgrowth. Occasionally, chlorite forms as replacement of lithic grains and feldspar.

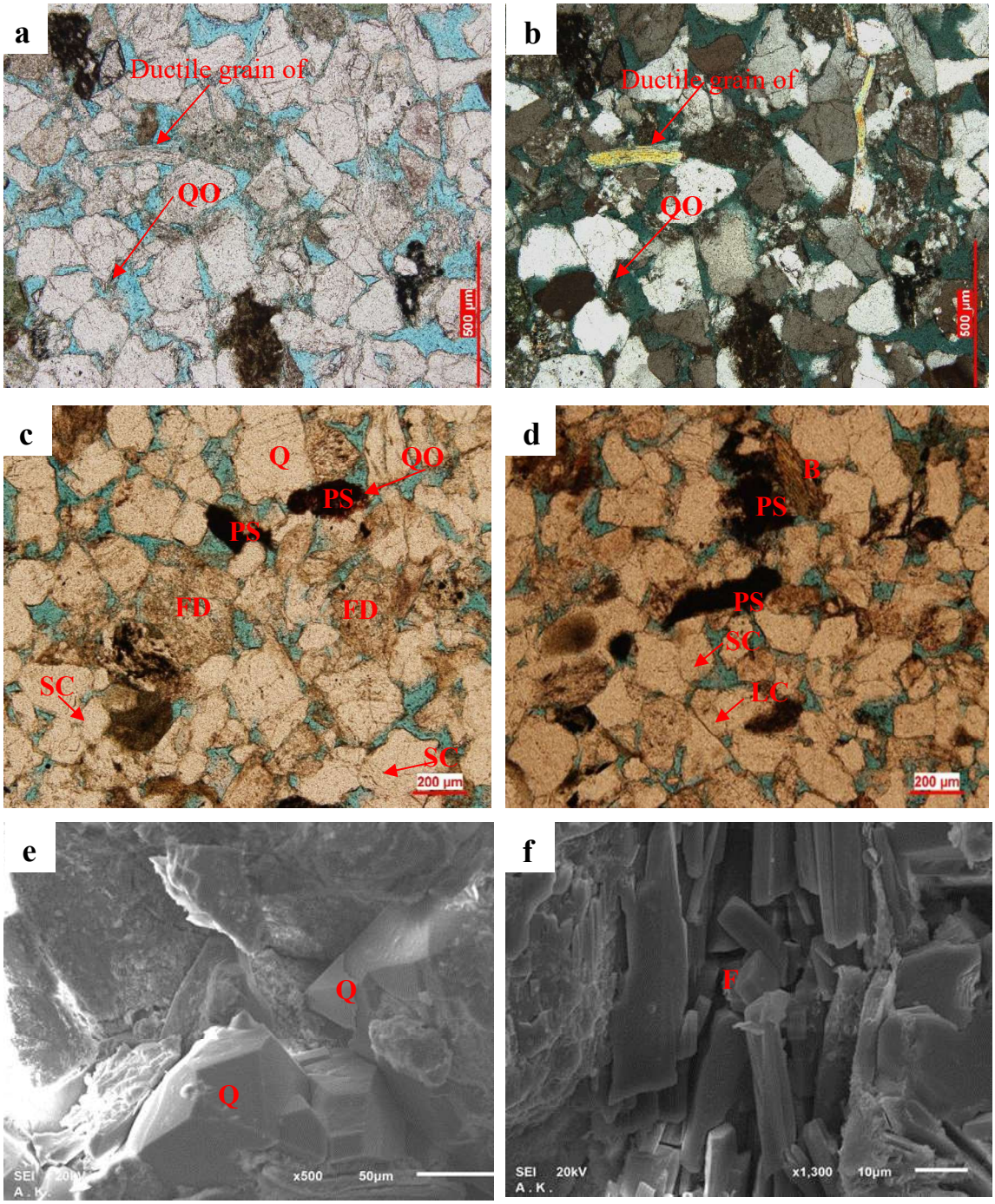

Figure 6.2 a. Microphotograph shows ductile grain of muscovite occluding pore space and isolating others grain to reduce permeability and quartz over growth (QO); b. Ductile grain in cross polarized light; c. Micrograph shows fractured quartz surface (FQ), Quartz over growth (QO), Feldspar dissolution features (FD), pseudo-matrix and suture grain contact (SC); d. Biotite grain (B) occluding the pores, Pseudo matrix (PS), long (LC) and suture grain contact (SC); e. Scanning electron micrograph shows quartz crystal (Q) and quartz over growth (QO); f. Broken feldspar crystal (F).

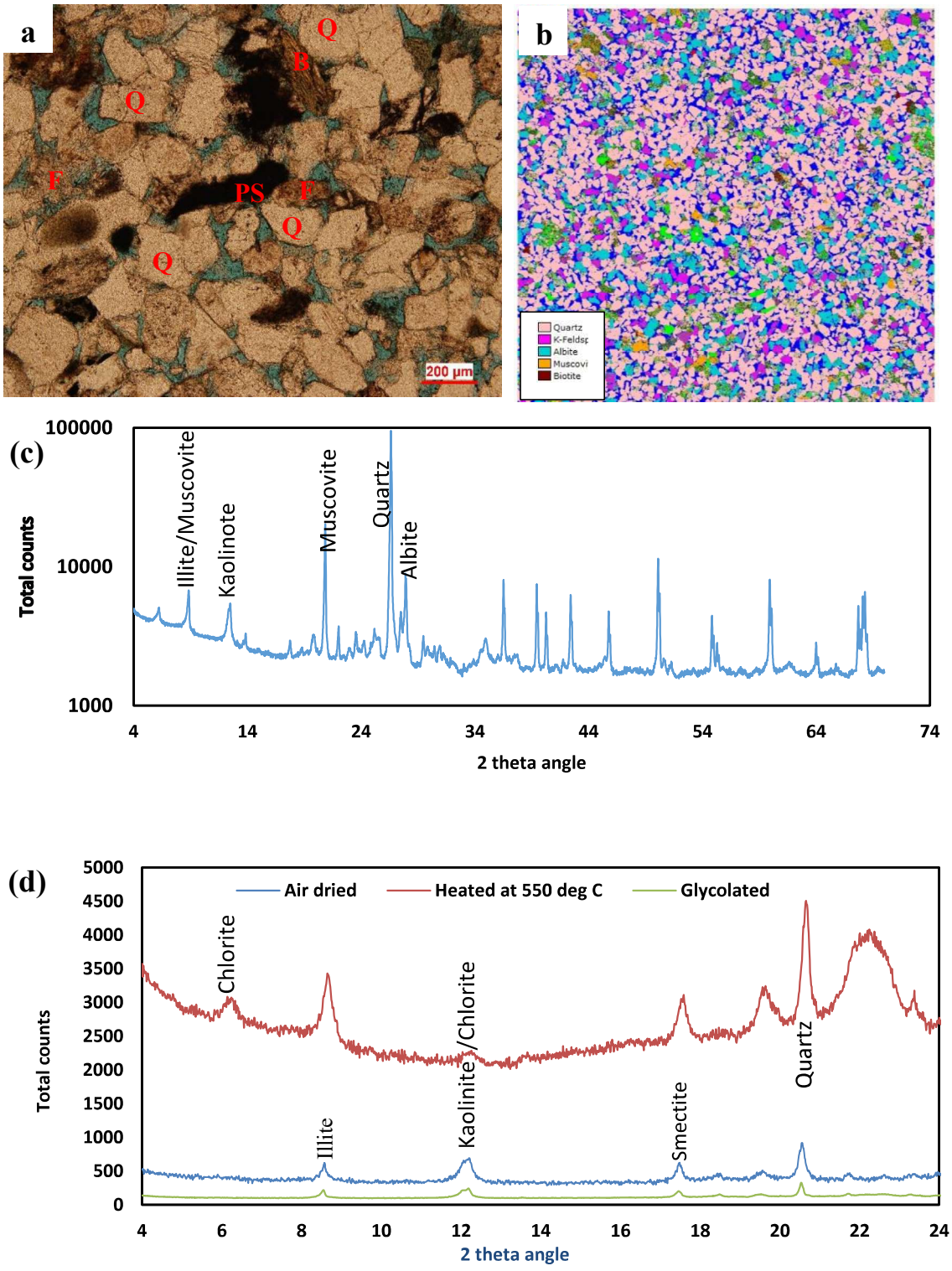

Figure 6.3 Shows the main framework minerals of Bhuban sandstone a. thin section shows quartz (Q), feldspar (F), Pseudo-matrix (PS) and biotite (B); b. QEMSCAN colormap of main framework minerals (different color code used for individual minerals); c. XRD spectra shows highest intensity in quartz and feldspar (sample-s3-3085) d. XRD spectra of separated clay from sand stone, air dried, glycolated and heated at 550 ºC at depth 3084m.

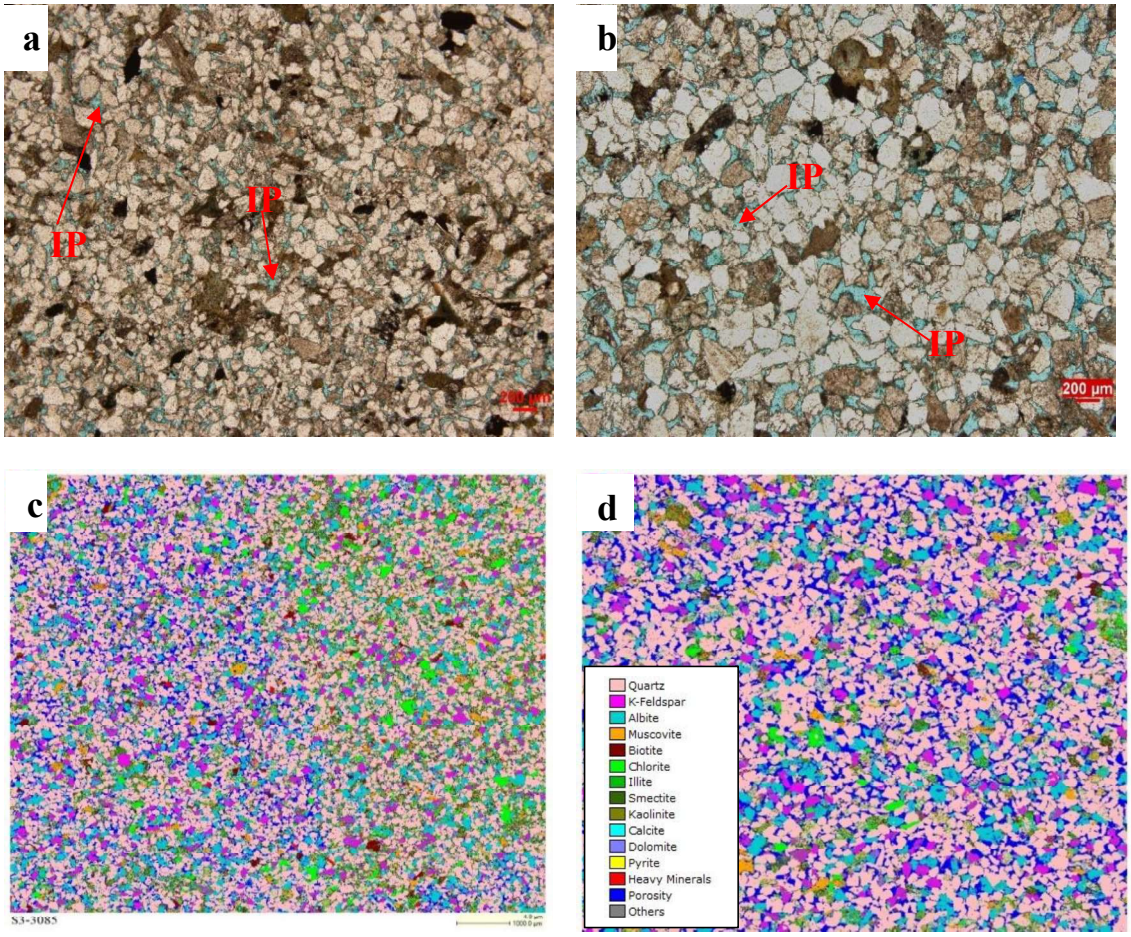

Figure 6.4 Shows thin section and QEMSCAN image of a. Microphotograph of S3-3088 of D-upper sand; fine to medium grained, moderately sorted sandstone shows low intergranular porosity (IP); b. Microphotograph of S4-3233 of E-sand; medium to fine grained, moderately sorted sandstone shows higher intergranular porosity (IP); c. Scan image of S3-3088 of D upper sand showing high concentration of clay minerals; d. Scan image of S4-3233 of E sand showing low concentration of clay minerals.

Illite

The second most abundant clay mineral in this sandstone is fibrous illite. Mixed layer of illite and smectite is common with lath-like crenulated morphology and with honey comb-like crystals (Figure 6.5). Illite-smectite, occurs locally as pore lining coating grains, and as an alteration product of detrital micas when they are pore filling.

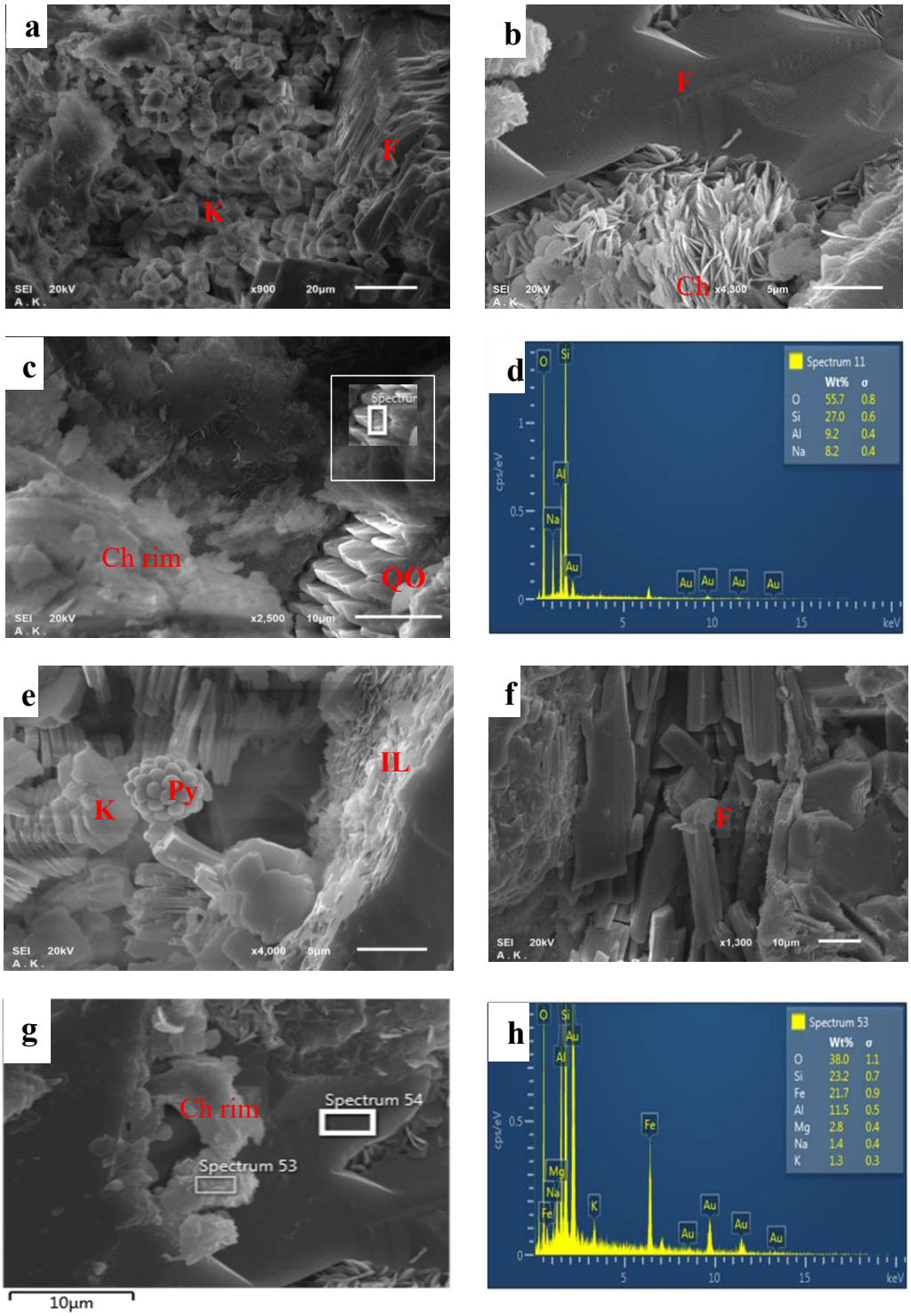

Figure 6.5 Scanning electron micrographs of sandstones (sub-arkose) shows (a) Kaolinite (Ka) booklet structure, feldspar dissolution; (b) Pore filling chlorite (Ch) and well-developed feldspar overgrowth (FO); c. Chlorite rim (Ch-rim) and quartz overgrowth (QO). d. EDS spectrum of quartz cement shows high concentration of silica (Si); e. Booklet structure of kaolinite clay (Ka) with micropore (MP), pyrite crystal (Py) and Illite (IL); f. Feldspar dissolution feature (FD); g. Chlorite rim (Ch-rim) with micro pore (MP); h. EDS of chlorite rim rich in Iron.

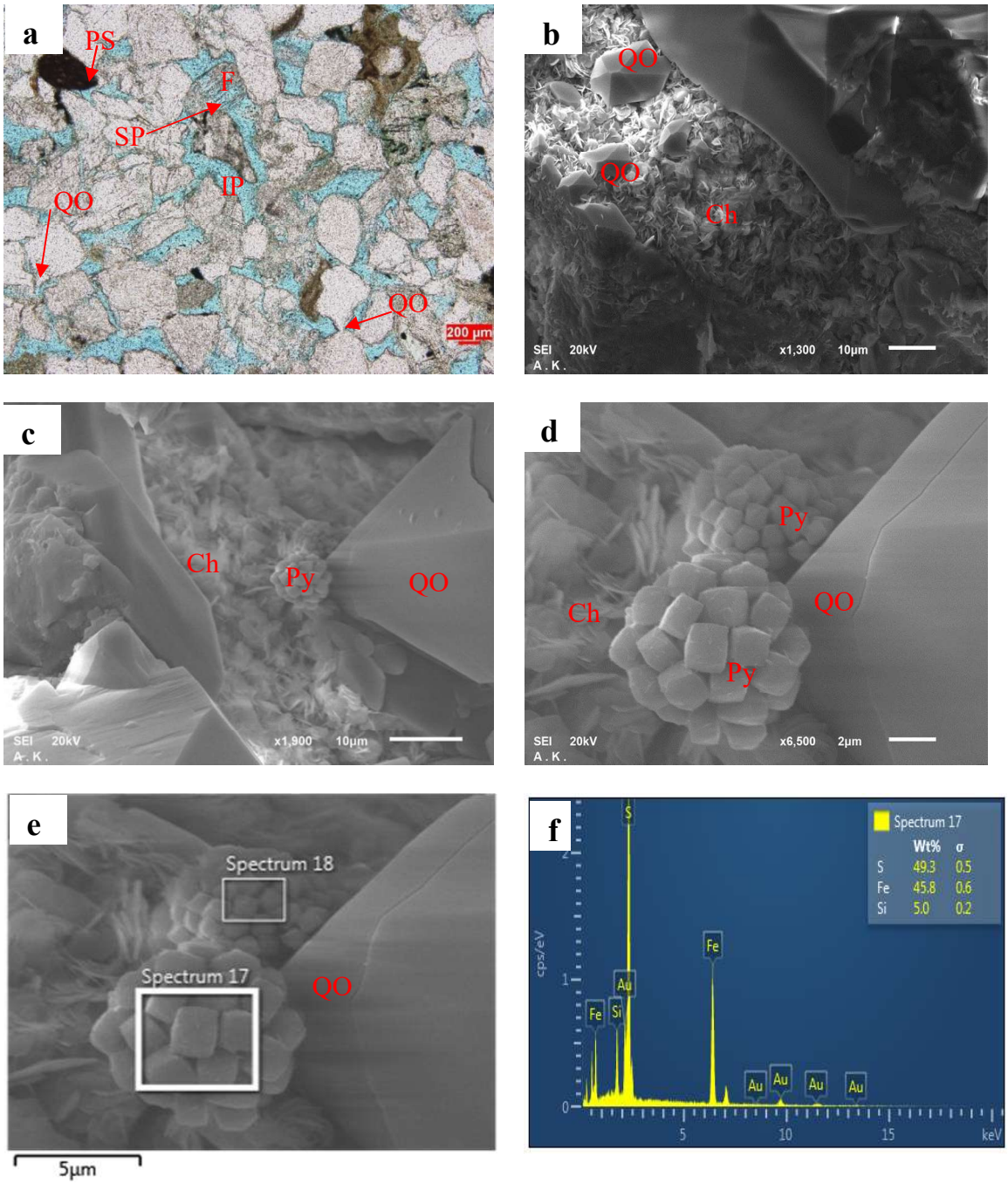

Figure 6.6 Shows a. Photomicrograph of moderately sorted, rounded to sub-rounded, sub-arkose sandstone shows intergranular porosity (IP) and feldspar dissolution features (FD) that increased the secondary porosity (SP); quartz over growth (QO) lining pore throats; pseudo-matrix that decreases permeability b. Scanning electron micrographs of sandstones shows quartz over growth (QO) and hindering chlorite (Ch); c. Quartz overgrowth (QO), pyrite crystal (Py) and chlorite (Ch); d. Chlorite (Ch), pyrite crystal (Py), and quartz overgrowth (QO); e & f. Marked area and EDS spectrum of pyrite crystal rich in iron.

Kaolinite

Vermicular aggregate of kaolinite cement is found in primary pores. It occurs as stack of booklet in close association with secondary pores in feldspar grain (Figure 6.5a). Euhedral crystals and clusters of vermicular kaolinite locally filled the intergranular pores. In some samples blocky habits are also noticed (Figure 6.5e).

6.4 Quartz Overgrowth and Silica Cement

Silica cement ranges from trace to approximately 5% in this reservoir. It occurs as quartz overgrowth around the detrital quartz grain (Figure 6.2; Figure **6.5**c; Figure 6.6b, c, d). Small euhedral crystals of silica precipitated by the growth of the quartz overgrowths towards the center of the pores, are locally developed in primary pores (Figure 6.5c)., Silica cement is better developed in the large intergranular pore networks, and it totally filled the pores (Figure 6.6c). Pores are totally occluded where quartz overgrowth encloses kaolinites and chlorite plates. In some cases, quartz overgrowth is inhibited by chlorite rim (Figure 6.6b).

6.5 Minor Cement

Calcite, dolomite and pyrite were observed as minor cements in the sandstones. Framboidal aggregates of pyrite are revealed in SEM image (Figure 6.5e; Figure **6.6**c, d, e). Energy dispersive spectrum (EDS) analysis confirms their presence in the samples. Calcite and dolomite cements are not common in all the sandstone samples. They are only locally developed (Table 6.2).

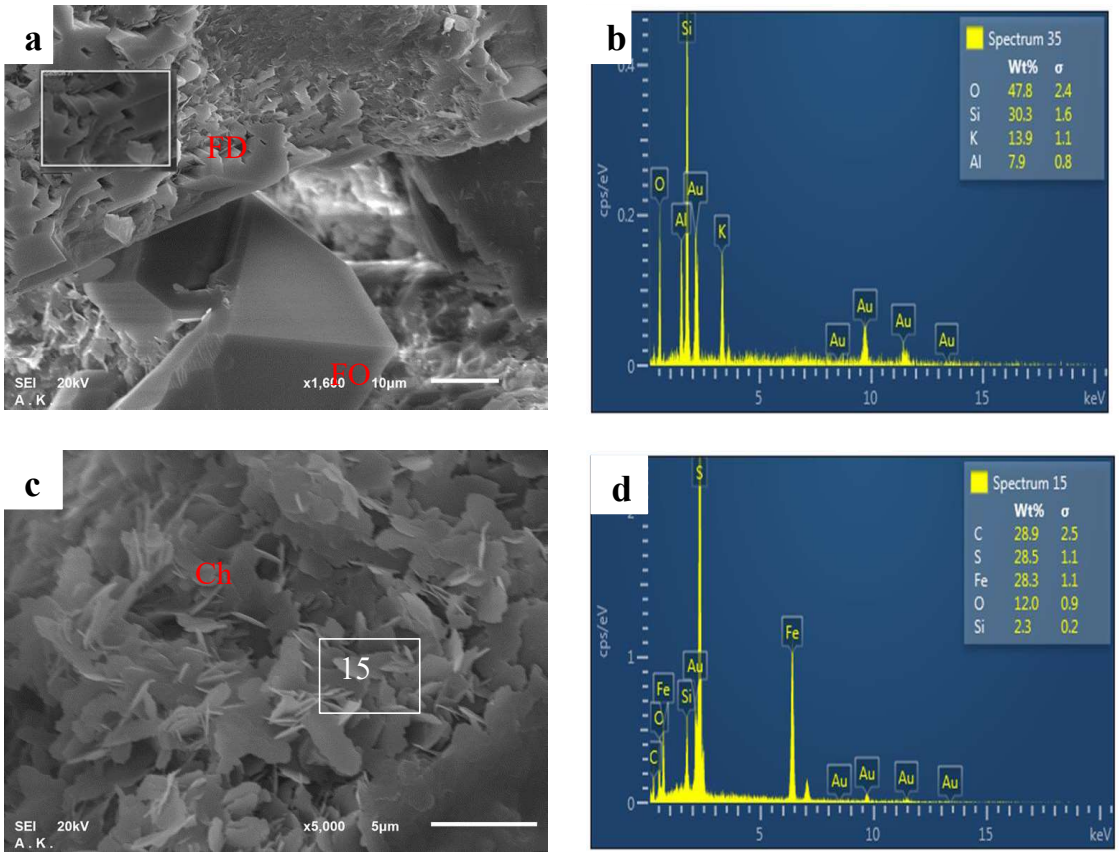

Figure 6.7 Shows a. feldspar dissolution features (FD) and feldspar overgrowth (FO); b. Energy dispersive spectrum (EDS) of feldspar rich in potassium and aluminum; c. Pore filling chlorite (Ch) at 3228 m; d. Energy dispersive spectrum of chlorite rich in sulfur and iron.

6.6 Paragenetic Sequence

A paragenetic sequence has been prepared for the Bhuban formation of the Surma group based on the diagenetic features and constituents that were identified from the petrographic analysis of the studied field data (Figure 6.8).

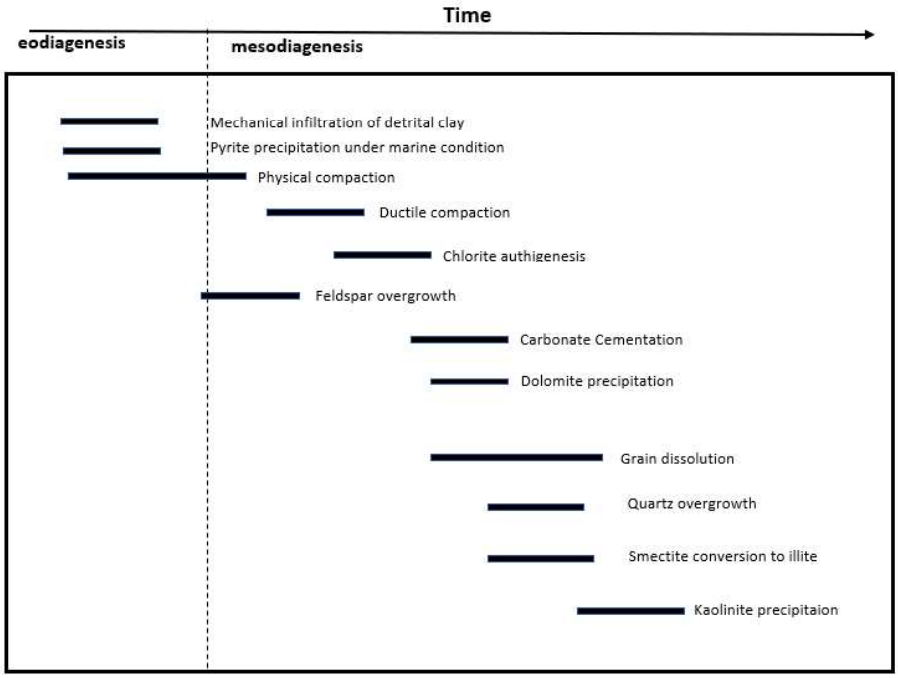

Figure 6.8 Paragenetic sequence for Bhuban formation of Surma group sediments which has been constructed based on studied field data.

CHAPTER 7

GEOCHEMICAL ANALYSIS

7.1 Introduction

Geochemical analysis is an analytical technique that can be used to explain diagenetic activity. Diagenetic process like alteration of minerals, formation of clay minerals, quartz overgrowth etc. can be explained. In this study, twenty-nine samples were taken for the geochemical analysis from the studied core intervals of the Bhuban formation from Srikail gas field. X-ray Fluorescence and high-resolution SPECTRAL CORE GAMMA (SGR) have been used for this analysis.

7.2 XRF & SGR Analysis

The major elements identified from the XRF analysis are Si, Al, Fe, K, Mg, Ca, S and Ti; (Table 7.1 & Figure 7.1). Silica (Si) concertation is highest in every sample indicating that quartz is the main rock forming minerals. The presence of Al and K indicates the presence of feldspar. The trace elements are Cr, Mn, Ni, Cu, Zn, Ga, Rb, Sv, Y Zr, Nb and Pb (Table 7.2 & Figure 7.1). Radioactive elements such as Th, U and K were quantitatively analyzed by high-resolution SPECTRAL CORE GAMMA (Table 7.3).

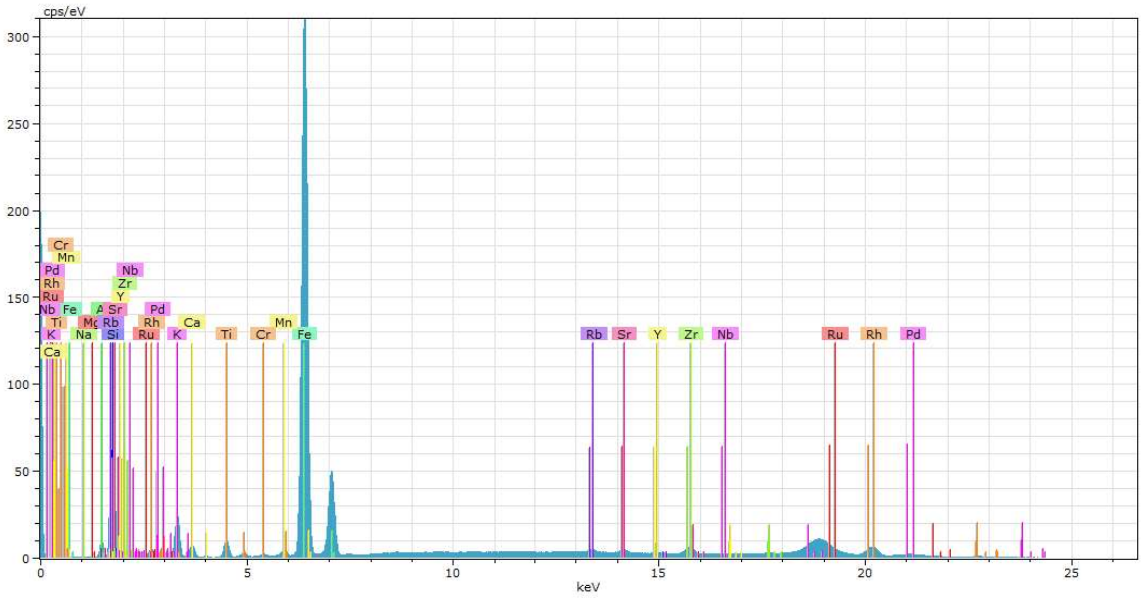

Figure 7.1 XRF spectrum of core sample (S4-3231) shows the Major and Trace element in Bhuban Formation.

Table 7.1 Major elements obtained from XRF analysis from studied core sample of Bhuban Formation. Concentration of elements are in $\mathbf{W_t}$%.

Sample Id	Si	Al	K	Fe	Mg	Ca	S	Ti
S-3-3083	52.02	12.15	12.59	15.53	1.65	2.09	1.64	1.23
S-3-3084	43.83	13.91	13.16	18.01	2.01	2.24	4.49	1.46
S-3-3085	55.06	11.29	11.59	14.19	1.41	3.19	0.53	1.23
S-3-3086	51.50	12.33	12.37	14.90	1.70	2.32	2.54	1.26
S-3-3087	66.69	7.58	9.41	10.87	0.77	1.42	0.84	1.15
S-3-3088	55.31	10.98	11.68	15.36	1.74	1.89	0.70	1.12
S-3-3089	59.43	9.38	10.78	13.56	1.24	1.86	1.07	1.43
S-3-3090	52.38	11.23	11.83	14.90	1.69	2.18	3.30	1.31
S-3-3091	57.65	9.69	10.52	14.79	1.49	1.66	1.96	1.14
S-3-3092	64.76	8.24	10.40	11.75	0.90	1.36	0.00	1.24
S-3-3178	52.12	12.32	10.47	18.53	1.51	0.75	2.05	1.21
S-3-3179	62.60	8.62	9.57	14.47	0.81	0.83	0.75	1.02

Sample Id	Si	Al	K	Fe	Mg	Ca	S	Ti
S-3-3180	59.84	9.54	9.86	13.98	0.90	0.96	1.92	1.46
S-3-3181	63.37	7.91	8.63	14.73	0.69	0.87	0.39	1.60
S-3-3182	65.21	8.30	9.17	13.02	0.81	0.92	0.27	0.95
S-3-3183	65.25	8.14	9.49	12.95	0.72	0.96	0.09	0.82
S-3-3184	35.51	14.93	12.14	24.22	2.11	1.04	7.69	1.46
S-3-3186	63.80	7.89	10.69	9.14	0.44	1.54	4.46	0.67
S-4-3228	64.55	8.45	10.46	12.53	0.65	0.87	0.00	1.27
S-4-3229	65.08	8.47	10.49	11.88	0.77	0.77	0.00	1.03
S-4-3230	65.47	8.17	9.42	12.60	0.70	0.89	0.00	1.28
S-4-3231	60.14	10.09	12.31	13.22	1.08	0.84	0.00	0.87
S-4-3232	62.51	9.24	11.55	12.49	0.91	0.83	0.00	0.94
S-4-3233	64.39	8.33	12.50	11.22	0.51	0.93	0.00	0.75
S-4-3234	61.56	9.53	10.79	13.57	0.97	0.83	0.33	0.96
S-4-3235	65.61	8.25	9.65	10.82	0.69	2.29	0.00	1.07
S-4-3236	62.86	8.75	10.90	12.38	0.77	1.22	0.00	1.85

Table 7.2 Trace elements obtained from XRF analysis from studied core sample of Bhuban Formation. Concentration of elements are in ppm.

Sample Id	Cr	Mn	Ni	Cu	Zn	Ga	Rb	Sr	Y	Zr	Nb	Pb
S-3-3083	520	1310	272	105	424	115	777	721	94	1558	199	69
S-3-3084	444	1173	304	86	431	125	919	790	130	1053	219	45
S-3-3085	648	1879	294	123	377	121	764	896	109	1559	237	61
S-3-3086	594	1377	280	85	379	98	725	725	84	1096	199	76
S-3-3087	749	1094	276	96	238	69	483	631	70	1467	195	57
S-3-3088	566	1192	313	111	440	105	778	765	104	811	222	89
S-3-3089	637	1465	293	85	354	111	699	849	111	1736	246	80

Sample Id	Cr	Mn	Ni	Cu	Zn	Ga	Rb	Sr	Y	Zr	Nb	Pb
S-3-3090	498	1180	270	140	363	130	774	770	102	1362	218	66
S-3-3091	467	1354	301	105	385	95	652	628	65	829	193	30
S-3-3092	780	1226	294	81	361	107	522	672	69	1265	203	24
S-3-3178	577	1250	316	109	376	110	728	697	92	1040	216	4
S-3-3179	735	1730	287	95	308	99	533	624	82	1225	206	49
S-3-3180	842	1271	287	136	278	91	422	471	102	2320	166	18
S-3-3181	1056	1417	253	123	263	100	458	575	453	5138	237	54
S-3-3182	692	1355	252	89	266	91	507	616	83	1143	193	19
S-3-3183	648	2733	280	109	278	86	479	687	71	1220	186	46
S-3-3184	447	1670	285	146	438	127	884	722	98	1247	229	5
S-3-3186	714	1290	211	172	226	77	408	539	24	991	170	14
S-4-3228	807	1002	244	180	244	105	458	651	63	1199	229	40
S-4-3229	566	998	260	86	274	84	471	695	38	760	183	28
S-4-3230	609	1467	228	124	260	74	443	692	120	1634	197	12
S-4-3231	506	1339	291	104	338	96	610	716	38	935	178	97
S-4-3232	652	1012	311	145	263	132	597	742	94	1988	207	65
S-4-3233	512	1639	261	143	247	109	588	887	34	618	200	58
S-4-3234	710	1329	282	85	307	122	610	738	58	753	205	26
S-4-3235	676	1859	266	103	262	90	507	711	72	2083	224	18
S-4-3236	700	1102	253	171	261	112	534	636	66	1822	268	41

Table 7.3 Concentration of K, Ur and Th obtained from SGR analysis of studied core sample of Bhuban formation.

Sample Id	K-fraction	U (ppm)	Th (ppm)
S3-3085	0.01056	5.10750	3.90300
S3-3087	0.00913	11.32800	20.04000
S3-3088	0.00778	4.10250	13.69900

Sample Id	K-fraction	U (ppm)	Th (ppm)
S3-3089	0.01301	6.26250	14.53100
S3-3090	0.00199	1.49900	2.95350
S3-3091	0.00347	2.14300	3.90800
S3-3092	0.00148	2.77900	2.50850
S3-3179	0.00369	1.02900	2.73750
S3-3180	0.00498	0.71150	7.92100
S3-3181	0.00263	1.52150	1.79750
S3-3182	0.00510	1.24450	2.30950
S3-3183	0.00579	1.20400	5.96550
S3-3184	0.01424	4.69412	6.57444
S3-3185	0.00371	1.82000	2.15800
S3-3186	0.00331	0.87800	2.17400
S4-3228	0.00394	1.57300	3.14400
S4-3229	0.00417	1.18900	2.21700
S4-3230	0.00229	1.36800	2.46950
S4-3231	0.00522	0.76650	2.55800
S4-3232	0.00282	0.92200	2.28050
S4-3233	0.00277	1.62450	3.55000
S4-3234	0.00437	1.62950	3.13900
S4-3235	0.00499	0.84600	2.25000
S4-3236	0.00259	0.85750	3.00550

Major oxides obtained from XRF analysis include SiO_2, Al_2O_3, K_2O, Fe_2O_3, MgO, CaO, TiO_2 and Na_2O. Presence of minerals such as quartz, feldspar and clay are indicated by SiO2, K2O, and Al2O3, respectively (Table 7.4).

Table 7.4 Major Oxides obtained from the XRF analysis of core sample of Bhuban formation.

Sample Id	SiO2	Al2O3	K2O	Fe2O3	MgO	CaO	TiO2	Na2O
S-3-3083	64.03	14.79	7.15	8.65	1.86	1.29	0.88	0.46
S-3-3084	56.93	17.63	7.96	10.85	2.35	1.50	1.12	0.33
S-3-3085	66.59	13.56	6.43	7.68	1.58	1.93	0.85	0.77
S-3-3086	63.87	15.13	7.04	8.32	1.94	1.44	0.90	0.48
S-3-3087	77.56	8.89	4.68	5.33	0.85	0.77	0.72	0.69
S-3-3088	66.89	13.15	6.50	8.36	1.94	1.15	0.79	0.64
S-3-3089	71.35	11.20	5.80	7.15	1.38	1.10	0.97	0.64
S-3-3090	65.28	13.81	6.69	8.33	1.93	1.35	0.94	0.59
S-3-3091	70.10	11.65	5.75	7.96	1.67	1.00	0.79	0.56
S-3-3092	75.84	9.68	5.36	5.95	0.94	0.76	0.80	0.65
S-3-3178	64.38	14.96	6.04	10.52	1.69	0.48	0.89	0.46
S-3-3179	74.00	10.14	5.05	7.49	0.89	0.48	0.69	0.69
S-3-3180	72.06	11.43	5.27	7.36	1.01	0.56	0.99	0.86
S-3-3181	74.81	9.27	4.57	7.60	0.75	0.51	1.07	0.75
S-3-3182	75.83	9.68	4.69	6.54	0.88	0.52	0.61	0.76
S-3-3183	75.86	9.48	4.85	6.49	0.79	0.54	0.53	0.84
S-3-3184	48.66	19.60	7.90	16.00	2.54	0.76	1.24	0.23
S-3-3186	76.94	9.63	5.38	4.60	0.50	0.85	0.43	0.87
S-4-3228	74.94	9.85	5.38	6.30	0.71	0.49	0.82	1.00
S-4-3229	75.46	9.89	5.32	5.92	0.85	0.43	0.66	0.99
S-4-3230	75.98	9.52	4.80	6.29	0.76	0.50	0.82	0.83
S-4-3231	71.00	11.92	6.55	6.87	1.19	0.48	0.58	0.88
S-4-3232	73.23	10.87	6.00	6.37	1.00	0.47	0.61	0.86
S-4-3233	75.26	9.81	6.40	5.63	0.56	0.51	0.48	0.80
S-4-3234	72.50	11.22	5.69	7.00	1.06	0.48	0.64	0.89

Sample Id	SiO2	Al2O3	K2O	Fe2O3	MgO	CaO	TiO2	Na2O
S-4-3235	75.97	9.64	4.84	5.33	0.76	1.25	0.67	0.87
S-4-3236	73.82	10.29	5.66	6.28	0.84	0.69	1.21	0.65

All the weight percentages of the major oxides are plotted against depth to detect the variation of oxides in core sample of studied gas field (Figure 7.2). From the plot, MgO, CaO and TiO_2 are not affected by diagenetic process very much while SiO2, Al_2O_3, K_2O, Na_2O_3 and Fe_2O_3 shows the maximum variation that is related to the diagenetic processes. Through this diagenetic process, at the expense of feldspar, clay minerals are formed.

From the cross plot of Na_2O vs K_2O, an increasing trend of K_2O is observed; an indication of diagenetic process (Figure 7.3). Formation clay minerals illite and montmorillonite can be explained by the variation in Fe_2O_3+MgO vs Na_2O_3/K_2O in sandstone with an overall increasing trend (Figure 7.4).

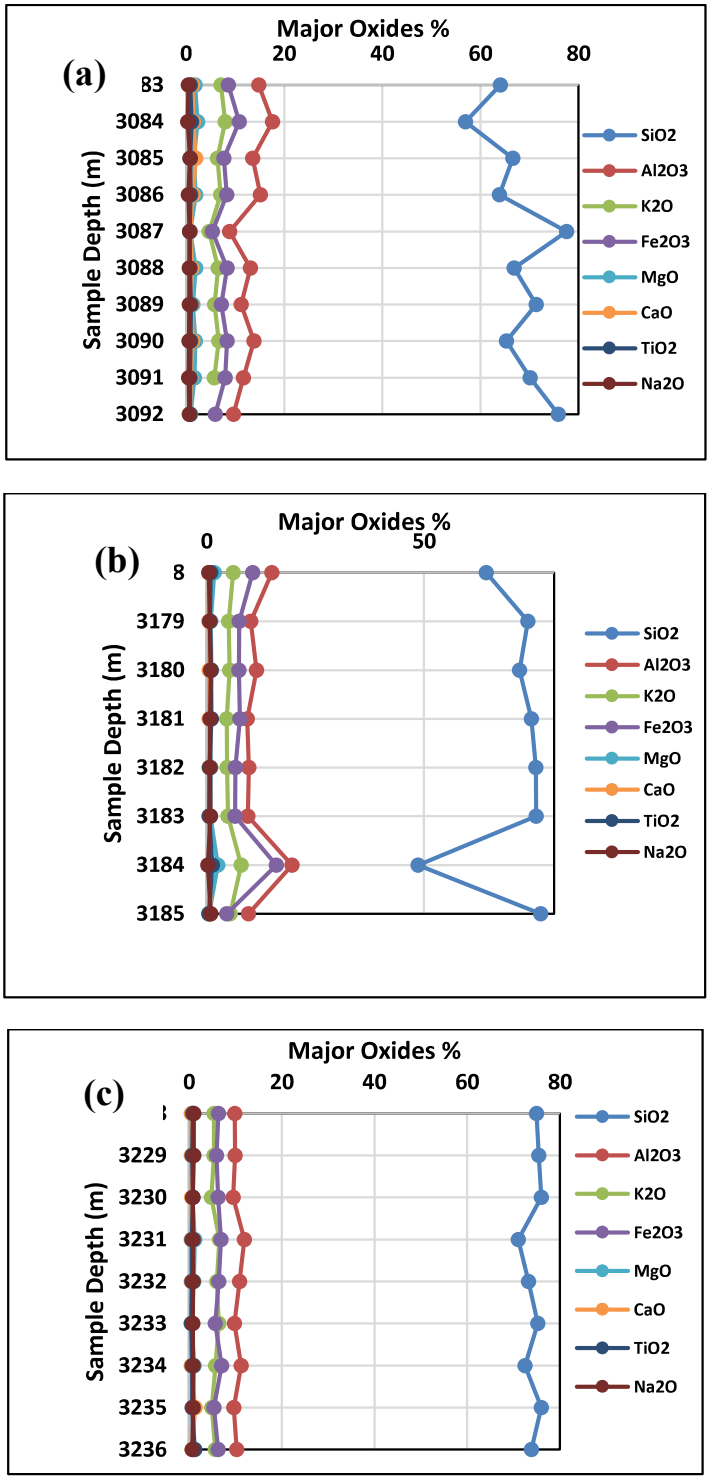

Figure 7.2 All the oxides has been plotted against the sample depth; (a) D-upper ; (b) D-lower and (e) E-sand of studied gas field. Change of Al_2O_3, K_2O, Fe_2O_3 against SiO_2 represents the diagenetic process.

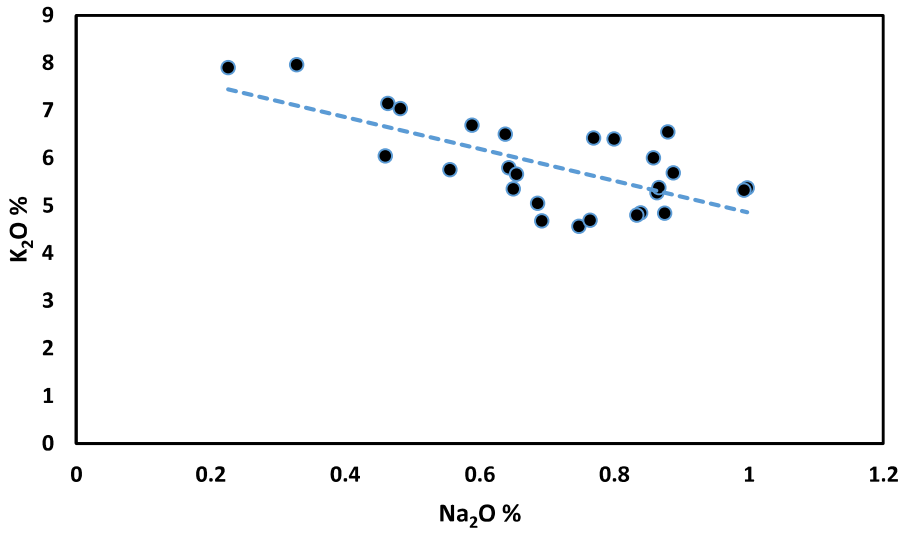

Figure 7.3 Cross plot K_2O vs Na_2O of all core samples where increasing trend of K_2O indicates the formation of mica and muscovite through diagenetic process.

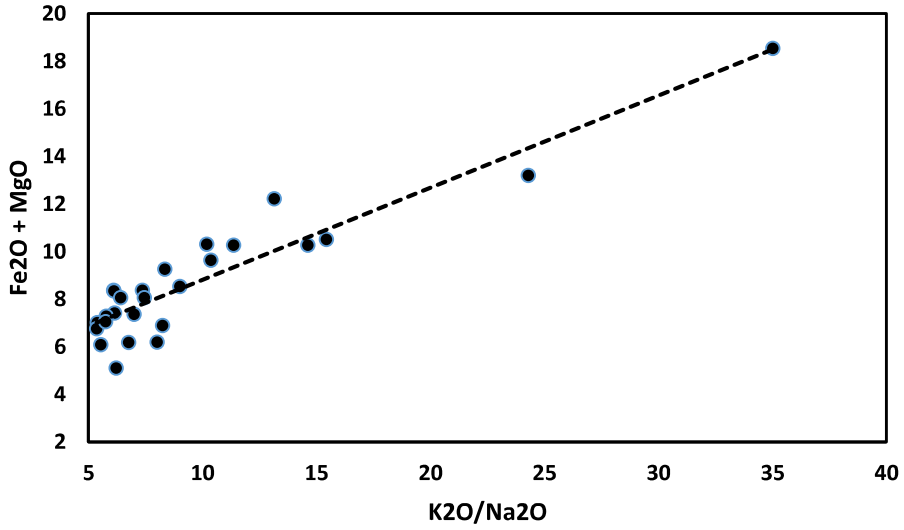

Figure 7.4 Cross plot of K_2O/Na_2O vs Fe_2O_3+MgO where formation of clay minerals, illite, montmorillonite can be explained through the increasing trend.

Increasing trend of Ti2O in the cross plot Fe2O3+MgO vs TiO2 can be explained by the presence of Sphene in Bhuban formation (Figure 7.5).

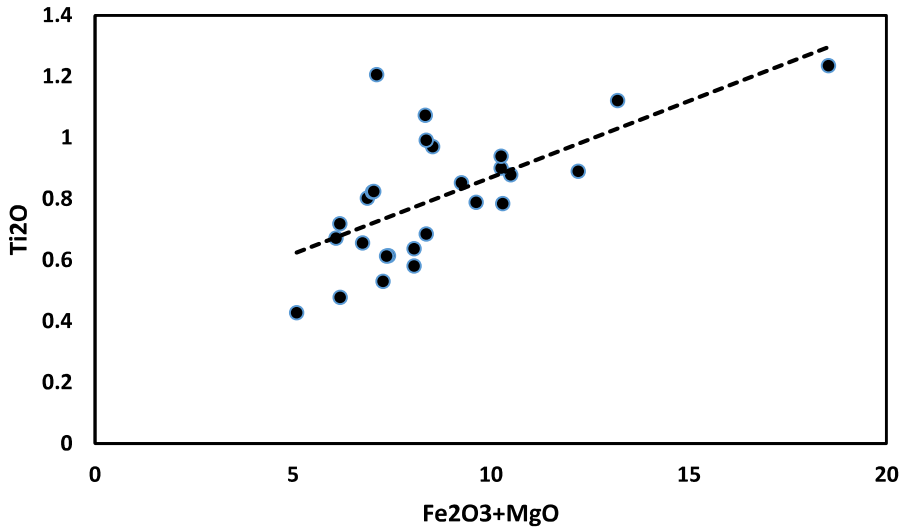

Figure 7.5 Cross plot of Fe2O3+MgO vs Ti2O of analyzed core sample.

From the cross plot of Al_2O_3/SiO_2 vs Fe_2O_3+MgO, an increasing trend of Al_2O_3/SiO_2 is observed from which it can be explained that silicate minerals like, feldspar are converting into clay minerals and mica is converting to chlorite through the diagenetic processes Figure 7.6.

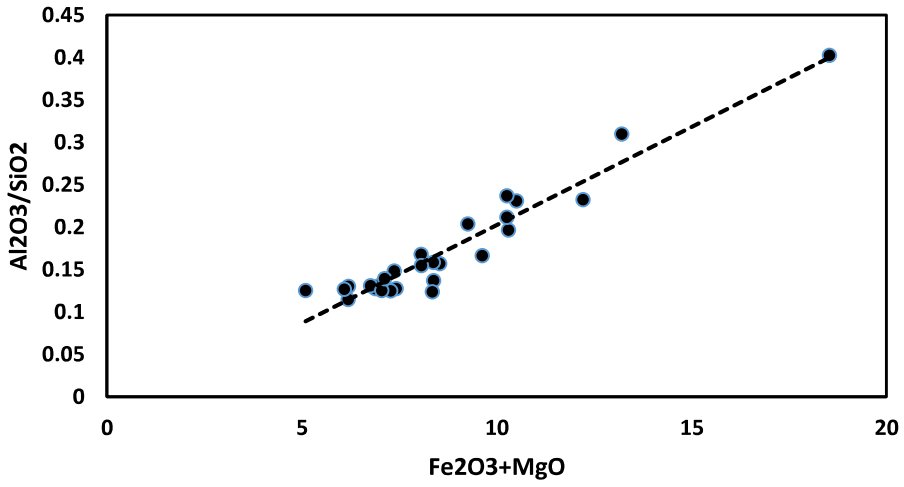

Figure 7.6 Cross plot of Fe_2O_3+MgO vs Al_2O_3/SiO_2 where increasing trend indicates that silicate mineral like feldspar is converting into clay minerals and mica in chlorite through the diagenetic processes.

In the sedimentary rocks, the ratio of Th/U is of interest because it can reveal weathering and recycling process of sediments (McLennan et al., 1993). Recycling process causes the loss of U which leads to an increase in Th/U ratio. The ratio of Th/U values are between 3.5 and 4.0 in most of the upper crustal rocks (McLennan et al., 1993). In the Surma Group sandstone Th/U ratio, range from 3.06 to 6.26 and varies from 4.88 to 7.33 in the shale (Rahman et al., 2017b). In this study area the Th/U ratio ranges 1 to 6 which indicates that this sediment has been derived from recycling of the crust (Figure 7.7).

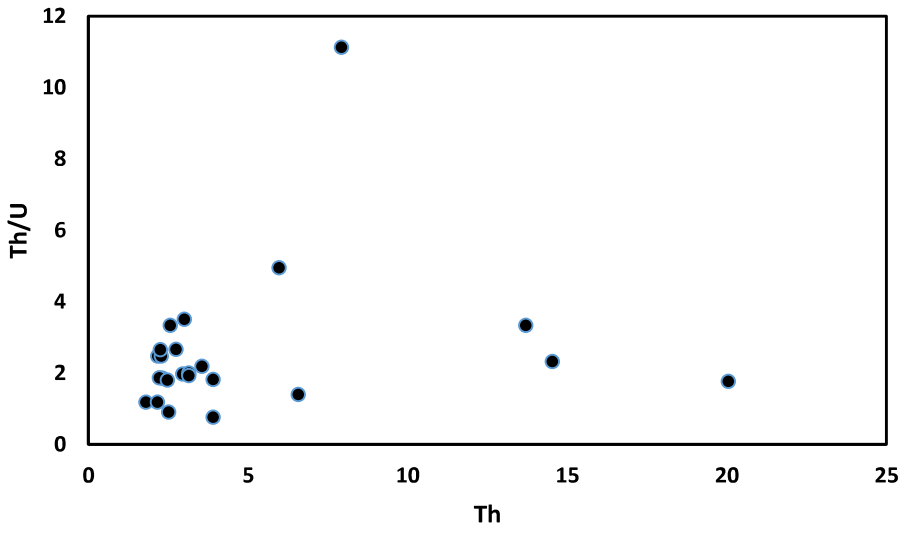

Figure 7.7 Cross plot between Th/U vs Th of studied core sample which indicate that studied sediments are derived through the recycling of the crust.

CHAPTER 8

INTERPRETATION AND DISCUSSION

8.1 Introduction

Eight lithofacies and three lithofacies associations were identified based on grain textures and sedimentary structures from the core sample analysis of studied Srikail gas field (Table 4.1). Total of six parasequence sets, twenty-five para-sequence and different bounding surfaces have also been identified from gamma ray log analysis which represents the change in depositional environment locally and basin wide. Based on wireline log analysis of well-3 and well-4, three prospective gas zones have been identified: D-upper; D-lower and E-sand and they are belonging to Bhuban formation. Although D-upper has the largest net thickness, both D-lower and E-sand have better reservoir quality in terms of higher porosity, gas saturation and lower shale volume (Figure 5.1; Figure **5.2**, Table 5.1). Additionally, permeability in the D-lower and E-sands are higher than in the D-upper (Figure 5.7). Facies analysis, the diagenetic events and controls on reservoir quality of the Bhuban formation in Srikail Field are discussed in the following section.

8.2 Lithofacies and Electro facies

From the core and gamma ray log analysis, three distinct lithofacies associations and six para-sequence set were identified. Lithofacies associations are mainly composed of

different facies which reflects the different depositional environments in which they were been deposited. Parasequence sets are comprised of different small para-sequence and they are bounded by different bounding surfaces like, transgressive erosional surface, regressive erosional surface and marine flooding surface which reflect the major as well as small depositional changes in the depositional environment.

8.2.1 Lithofacies

Detailed analysis of various facies and facies association based on internal stratification pattern, indicates that the sediments of the studied formations have been deposited in sub-tidal and intertidal environment of tide dominated deltaic setting. The presence of cross bedded sandstone is an indication of strong reversal current and which is possible in tide-dominated environment. Mud layer bundles resemblance to tidal bundles also indicate the influence of tide dominated depositional environment (Alam et al., 2003). The wavy bedded sandstone (Wv), lenticular bedded (Ln) and flaser bedded sandstone facies (Figure 4.3a, c; Figure **4.5**b) which are more common in the studied core samples are main criteria for recognizing the intertidal deposition environment in coastal setting (Klein, 1985). Variable hydrodynamic conditions of deposition are frequently observed through intermittent association of high and low energy stratification patterns in the studied core samples which is a typical example of tide dominated environment deposits (Rahman et al., 2009). In many meso and macro-tidal coastal settings, tide dominated environments are very likely to occur. For instance, several kilometers wide tidal flats of inter-tidal environments can occur closed to lagoons, in estuaries, behind the barrier island and in tide-dominated deltas (Tucker, 2001).

The huge thickness of Surma Group sediments encountered in the sub-surface of Bengal basin with their various facies' associations indicates tidal influence. They are thought to have been deposited in shallow marine shelf and tide dominated delta system with the influence of different transgressive and regressive events due to subsidence and relative sea-level changes (Sultana, 2001).

8.2.2 Electro facies

The evidence of deltaic regime with strong tidal influence throughout the history of the Surma Group are also evident from the electrofacies sequence analysis. Various small cyclic patterns of parasequences (PS), para-sequence sets (PS-set) of large-scale cyclic patterns, regressive, transgressive, erosional and marine flooding surfaces were identified from the log response of studied well (Srikail well-4 from 2650-3260 m). Different log motifs like bell shape which represents the fining upward sequence (FU) deposited during transgressive event in retrograding distributary channel were identified. Funnel shape representing coarsening upward sequence (CU) deposited during regressive event in fluvial channel of a prograding delta was also recognized (Figure 4.7). A cylindrical log pattern identified from the logs represents aggradational parasequence. Bow of egg shape gamma ray log response represents channel- floodplain, sub-tidal and intertidal depositional environments.

Based on lithofacies and facies associations from the core and gamma ray log, it can be inferred that the study area has been developed in tide dominated delta system. According to the depositional model, present study area is located on the upper delta plain where sediments have been deposited in distributary channels forming crevasse splay (Figure 4.13). The sediments are medium to fine grain deposited in proximal part of the delta that

represents the higher hydrodynamic condition than the distal. Distal part of the delta is characterized by enormous distributary channels and mouth bar deposits. Pro-deltaic part is mostly shale dominated with minor sandstone deposits where influence of tide is prominent. Among the depositional environments of deltaic setting, fluvial channel sands, deposited in upper delta plain shows the best reservoir quality in terms of porosity and permeability. In between the reservoir zones of Srikail gas field, the D-lower and E-sands deposited in fluvial channels, show better reservoir quality than the D-upper which was deposited in deltaic distributary channels.

8.3 Control of Depositional Environment on Reservoir Quality

There is a strong influence of depositional environment on the reservoir quality of Bhuban Formation in reservoir zones of studied gas field. From lithofacies analysis and GR log response of the reservoir intervals, several depositional sub environments including fluvial channels, distributary channels, crevasse splays, tidal flat, interdistributary bay and mouth bar were identified (Figure 4.10). The best quality reservoir sand has been deposited as fluvial channel deposits (Figure 4.2b, c). These sandstones are massive, low angle cross bedded, clean, medium to fine grained, moderate to well sorted, limited interbedded shale layer as barrier and with low matrix content (Figure 4.2c). These sandstones were deposited in high energy fluvial channel environment. D-lower and E-sands are the fluvial channel deposits which have low V_{sh} value, (0.216 in well-3, 0.26 in well-4 for D-lower sand and 0.114 in well-3, 0.28 in well-4 for E-sand). In contrast, the very fine-grained distributary channel fill sandstone deposited in low energy settings, has higher clay content (V_{sh} value 0.277 in well-3 and 0.388 in well-4 for D-upper sand) and lower reservoir quality as found in D-upper. The difference in the depositional environments between D-upper and E-sands

was reflected on their grains sizes and consequently pore sizes. Larger grain sizes in the fluvial deposits (Figure 6.4a) compared to the finer grained sandstone (Figure 6.4b) resulted in larger pores sizes and thus larger permeability in D-lower and E-sand compared to D-upper (Figure 5.7a). Higher clay content (Vsh) in D-sand compared to E-sand (Table 5.1; Figure 5.1;Figure **5.2**) is responsible for the lower quality of D-upper sand. The presence of shale laminae between the sand have compartmentalized the reservoir zones. This can be inferred from the low net to gross ratio values (0.58 in well-3 and 0.45 in well-4) of D-upper sand. As observed in sample S-4-3231of E-sand, thinly laminated shale has a prominent effect in reducing the permeability than the porosity (Figure 5.6).

8.4 Diagenetic Events

Mechanical infiltration of detrital clay and its mixed layer occurred immediately after deposition. They are present in the form of localized argillaceous matrix distributed on the detrital grain surfaces. The grain coated clays are developed due to the mechanical infiltration where the sediments are exposed to the surface (Matlack et al., 1989; Moraes and De Ros, 1990; Moraes and De Ros, 1992) or it may also occur due to bioturbation processes (McIlroy, 2003; Needham et al., 2005; Richard et al., 2006). The grain coating clays in the studied core samples are mostly illite and chlorite (Figure 6.5b, e; Figure **6.6**b). Authigenic chlorite significantly inhibits the development of quartz overgrowth by creating continuous grain coatings like in other sedimentary basins (Bloch and Clay, 2002). Worden, (2003) stated that chlorite mostly develops at temperature greater than 60 or 70 ºC. Reservoir temperature in the studied horizon in the Srikial gas field is 100 ºC which implies that chlorite was likely formed in the early diagenetic stage. Chlorite in the investigated sandstone might have been formed by diagenetic replacement of biotite and

transformation of gain coating clay minerals. Fe and Mg in the chlorite were likely derived from biotite grains and lithic fragments formed in deltaic or estuarine environment like the Fe source of Niger Delta (Panel et al., 1988; Ehrenberg, 1993). The Surma Group sandstone has been widely interpreted to have been deposited in a prograding deltaic setting (e.g. Johnson and Alam, 1991). The breakdown of ferromagnesian alumino-silicate minerals and iron oxides in reducing alkaline pore water was likely the source for necessary components for this early diagenetic formation of chlorite (Land and Dutton, 1978).

Development of framboidal pyrite (Figure 6.6c, d) reveals the influence of near-surface low temperature and presence of sulphate reducing bacteria in sulphate-rich marine pore water (Berner, 1980). The presence of this mineral suggests the influence of reducing marine conditions.

Thin section petrographic analysis reveals that long, concavo-convex and suture are the dominant contact types between the grains of the investigated samples (Figure 6.2c, d). This suggests that the Surma Group sandstones have experienced moderate to high degrees of compaction. The presence of other mechanical compaction features such as mica bending, ductile deformation of lithic grain and brittle fracturing of quartz and feldspar grains (Figure 6.2a, b, f) indicate the effect of compaction in these sandstones. Feldspar overgrowth observed in few samples as euhedral crystal on feldspar grains, which is likely developed by the dissolution and precipitation of detrital feldspars (Figure 6.7a).

Dissolution of feldspar grains is a prominent diagenetic feature in the studied sandstone samples Figure 6.6a. Honeycomb texture created by partial dissolution of feldspar grains (Mcdonald, 1979) suggests that the dissolution of metastable minerals and grains in the

Bhuban sandstone, is the main mechanism for secondary porosity development (Figure 6.7a). Formation of kaolinite and quartz overgrowth was facilitated by the leaching and dissolution of detrital grains in the subsequent stage of diagenesis. Secondary porosity in this formation may be developed due to calcite and feldspar dissolution as they are susceptible to the presence of acidic fluids.

Quartz overgrowth is also a pore occluding processes identified in the sandstone reservoirs of the Srikail gas field (Figure 6.2e; Figure **6.6**b, d). Silica cement can be sourced from a number of origins; though it is still being debated whether they are sourced externally or internally (Worden and Morad, 2009). Fault controlled fluid flow or the neighboring shale sediments may be the external source of authigenic silica precipitation in the Bhuban Sandstone. Paleochannel filled by mud which is the lateral seal for the reservoirs of Srikail gas field, likely serves as the external source of fluid flow in the sequence. Intergranular pressure solution might have also acted as the internal source for the silica (Schmid et al., 2004).

The occurrence of hair-like with spiny termination grain coating illite indicates a diagenetic as opposed to detrital origin (Morad, Ketzer, and De Ros, 2000). Illite typically forms at ≥ 90 ºC during progressive burial. It is formed through the transformational or infiltration by clays (Inoue, 1986). Potassium source is needed for the illitization of smectite and in this case alteration of feldspar in the studied samples probably supplied the required potassium (Morad, 1994; Ehrenberg (2), 1993).

Kaolinite was probably formed by the alteration of detrital feldspar grains as it is closely associated with degraded feldspar grains (Figure 6.5a, e). Feldspar alteration in low saline

or low pH acidic formation water favors the formation of kaolinite. During the maturation of organic matter, acidic water may possible generate at the depth in adjacent shale (Rahman and McCann, 2012). An influx of CO_2 from the source rock is thought to be responsible for the growth of carbonate minerals and is associated with the alteration of feldspar grains to kaolinite due to acid buffering by the feldspar and clay reaction (Worden et al., 2000).

8.5 Diagenetic Controls on Reservoir Quality

Diagenetic controls on the reservoir quality can be explained by the effect of mechanical compaction through porosity and permeability changes after deposition due to the grain rearrangements and ductile deformation of grain. Alteration of minerals, and formation of authigenic clays also affect the reservoir quality by blocking the pore space through reduction of porosity and permeability and increasing porosity through feldspar dissolution.

8.6 Mechanical Compaction

Bulk sediment volume is reduced due to the mechanical compaction during progressive burial of the sediments. It generally occurs in a variety of ways such as through the simple process of grain reorganization, a change in fabric, or packing (e.g., simple cubic packing or hexagonal rhombohedral packing) with the increasing depth. An initial porosity of 45% in sediments can be reduced to 26% due to post depositional repacking (Klimentidis et al., 2002). Ductile minerals such as muscovite and biotite reduce the porosity and permeability by blocking interconnected pores due to the mechanical compaction of the sediments. This

effect can be seen from the cross plot of porosity and permeability with the total percentage of ductile minerals (Figure 5.5c, d, f).

All though there is not any distinctive effect of mechanical compaction is observed in the porosity and permeability data in the three reservoir zones of the studied wells. The effect of mechanical compaction due to increasing depth on the sandstone reservoirs was obtained by the porosity and permeability plot of the nearest Bakhrabad and Titas gas fields with studied field against depth (Figure 5.8 a, b). The comparison suggests that mechanical compaction is the main porosity and permeability reduction process in the sandstone of Bhuban Formation. Reduction of porosity and permeability with the increasing depth have also been reported by Islam, (2009) and Rahman et al. (2016).

8.7 Control of Diagenetic Clay Minerals

The most significant process affecting porosity and permeability after compaction, is the pore filling clay minerals (Figure 6.5a, b). Chlorite growing into the secondary pore reduces its effectiveness by blocking the pores. However, on the hand, chlorite coating of grains, also inhibits quartz overgrowth development towards the cores of the pores (Figure 6.5b) preserving the porosity. This has been reported in many basins around the world (Dowey, Hodgson, & Worden, 2012). Illite is the second dominant clay mineral in the reservoir sand of studied gas field obtained (Table 6.2). It reduces both the porosity and permeability by blocking the pore throats. Authigenic kaolinite developed due to feldspar dissolution, also locally reduces the porosity and it also affects the porosity by re-distributing the secondary porosity Figure 6.2a. Effect of authigenic clay concentrations and those of the other cements (e.g., silica) on porosity and permeability of reservoir

sandstones in Srikail gas field can be seen in the cross plot of authigenic clay and other cements percentages against porosity and permeability (Figure 5.5a, b, e & f).

8.8 Comparison Between Surma Group and Other Miocene Sandstones

Analysis of Miocene sandstones of petroliferous basins around the world such as in southeast Asia, central Europe, Gulf of Mexico and California, in terms of reservoir quality and diagenetic processes has shown several common features that are due to rapid sedimentation rate.

Ductile deformation due to mechanical compaction plays an important role in controlling the reservoir quality of different Miocene reservoirs of the world including those of the Surma Group. In some parts of the Gulf of Mexico, mineralogically immature Miocene sediments have the tendency to undergo ductile deformation (Dutton et al., 2012). The same tendency has been reported in SE Asia (Worden et al., 2000) and in central Europe (Gier et al., 2008). Due to the high rate of sediment accumulation, sediments are rapidly deposited and are less winnowed out, not well arranged or cleaned-up to attain textural and mineralogical maturity before deposition. Example of high sedimentation rate with concomitant rapid deposition has been reported in the North Sea's Brent Group (Giles et al., 1992) where the accumulation rate was higher than the usual depositional rate .

Although calcite and dolomite cements are less prominent in the study area, calcite cementation has more effect than dolomite cementation on the Surma Group sandstone in other locations. This is also common in most Miocene sandstones in SE Asia, Gulf of Mexico, central Europe and California (Dutton et al., 2012; Fayek et al., 2001; Gier et al.,

2008; James et al., 1987; Yamin Ali, 1995). Like in the Surma Group sandstone, authigenic clay minerals such as smectite-illite, kaolinite, are also common in these basins.

Similar to the Surma Group, silica cement and quartz overgrowth are also common in other Miocene sandstones. The development of quartz cement in the Surma Group sandstones, is prominent from 2300 m depth to onward at (85-115 ºC). Quartz cement concentration at same depth in the Surma Group sandstone, is similar to those of central Europe (Gier et al., 2008) and SE Asia (Worden et al, 2000). At greater depth, with high temperature, concentration of quartz cement proportion increases (Dutton et al., 2012; Worden et al., 2000). (Gier et al., 2008) has reported lack of quartz cement at more than 100 ºC may be due to the lack of available time for growing quartz cement.

CHAPTER 9

SUMMARY AND CONCLUSION

9.1 Summary

The aims of this study were to characterize the producing and prospective gas bearing zones and investigate controls on reservoir heterogeneity and quality of Miocene Bhuban formation of Neogene Surma group at the Srikail gas field, Bengal basin, Bangladesh. This study has been done by combining interpretation of wireline logs from two wells with petrophysical and petrographical analysis of core samples collected from three gas bearing zones of Srikail wells (well-3 and 4).

Methodology for this study includes core description, facies analysis from both core and wireline log, wireline log interpretation using Techlog software, determination of depositional environment from gamma ray log petrographic analysis including thin section study, Scanning Electron Microscopy (SEM). Mineralogical analysis has been performed by XRD, XRF, SGR analysis and QEMSCAN analysis.

Three gas bearing zones D-upper, D-lower and E-sand have been identified from wireline log interpretation. According the wireline log and core analysis, in between three reservoir zones of studied gas field D-lower and E-sand has the better quality than D-upper sand in terms of porosity and permeability due to the variation of depositional environment.

The reservoir sandstone of the study field is medium to fine grained, moderate to well sorted which has been deposited fluvial to deltaic environment. According to the Folks 1980 sandstone classification this sandstone is sub-arkosic arenite.

This study concludes that facies variation due to depositional environment as well as diagenetic process are the controlling factors for maintaining the reservoir quality in the studied field. Good reservoir quality with 15-20% porosity and 30-100 mD permeability are medium to fine grained, moderate to well sorted, with low ductile mineral content and less interbedded clay layer. Fluvial channel sands are the best quality reservoir. Reservoir sandstones are not uniformly distributed. They are compartmentalized by the interbed layer of shale which is prominent in the log response as well. Though mechanical compaction is not the main control for reservoir quality in this study field but compared with the other filed it is the main control for Bhuban formation of Surma group. This effect becomes intense with the higher concentration of ductile grains for reducing the porosity and permeability. Authigenic clays like illite, kaolinite and chlorite play also an important role for reducing the reservoir quality. Illite reduces the porosity and permeability by blocking pore throats and kaolinite growth due to feldspar dissolution reduces the secondary porosity. Quartz overgrowth is also a quality reducing factor in the reservoir zones as quartz cement grows at ≥100 ºC and the reservoir temperature in the Srikail gas field recorded 100 ºC during well testing operation as well as in wireline log record. It reduces the porosity and permeability by lining the pore throats.

9.2 Conclusions

1) Studied reservoir horizons of Srikail gas field belong to Bhuban Formation of Surma Group and they contain sub-arkosic sandstone.

2) Analysis of core sample and wireline logs revealed that sediments of studied gas field have been deposited in tide dominated deltaic and shallow marine depositional environment.

3) Three facies association has been identified from the core analysis in which Medium Grain Facies (MF) and Coarse Grain Facies (CF) have the better reservoir quality.

4) In between three reservoir zones of Srikail gas field (D-upper, D-lower and E-sand), E sand has better reservoir quality (Porosity-17.6-19.5%, Permeability-30-111mD) compared to others. Both its log and core plug measured porosities are higher than those of the other two reservoirs zones. Its core measured permeability is also higher than in the other zones.

5) Fluvial channel sands show the best reservoir quality with more than 15% porosity and 30-100 mD permeability. They are medium to fine grained, moderate to well sorted and with low ductile and clay mineral content.

6) Reservoir sandstones of Buban formation, Neogene Surma group are not uniformly distributed. They are compartmentalized by the interbed shale layers.

7) Though mechanical compaction is not the main control for reducing the porosity and permeability in studied three reservoir zone but regionally it is the main factor that become intense with the increasing proportions of ductile mineral grains.

8) Authigenic clays like illite, kaolinite and chlorite have important controls on reservoir quality in this field. Illite reduces the porosity and permeability by blocking pore throats,

kaolinite reduces porosity by blocking intergranular space and chlorite kills the secondary porosity grows due to feldspar dissolution.

9) Quartz overgrowth is also observed in the reservoir zones as silica cement reduce the porosity and permeability by lining the pore throats which has minor effect on reservoir quality.

References

Alam, M., Alam, M. M., Curray, J. R., Chowdhury, M. L. R., & Gani, M. R. (2003). An overview of the sedimentary geology of the Bengal Basin in relation to the regional tectonic framework and basin-fill history. *Sedimentary Geology*, *155*(3–4), 179–208. https://doi.org/10.1016/S0037-0738(02)00180-X

Ali, M. Y. (1995). Carbonate cement stratigraphy and timing of diagenesis in a Miocene mixed carbonate-clastic sequence, offshore Sabah, Malaysia: constraints from cathodoluminescence, geochemistry, and isotope studies. *Sedimentary Geology*, *99*(3-4), 191-214.

Berner, R. A. (1980). *Early Diagenesis: A Theoretical Approach*. Princeton University Press, Princeton.

Bloch, S., Clay, W. (2002). *Origin and predictability*. *2*(2), 301–328.

Boles, J. R., & Ramseyer, K. (1987). Diagenetic carbonate in Miocene sandstone reservoir, San Joaquin basin, California. *AAPG Bulletin*, *71*(12), 1475-1487.

Bowles, E., Hossain, Z., 2015. Onshore Gas-Bangladesh. In: CEAPEX conference, Singapore, 1-3.

Curiale, J. A., Covington, G. H., Shamsuddin, A. H. M., Morelos, J. A., Shamsuddin, A. K. M., Curiale, J. A., & Corporation, U. (2002). *in Bangladesh*. *4*(4), 625–652.

Dickinson, W. R. (1985). Interpreting provenance relations from detrital modes of sandstones. In *Provenance of arenites* (pp. 333-361). Springer, Dordrecht.

Dowey, P. J., Hodgson, D. M., & Worden, R. H. (2012). Pre-requisites, processes, and prediction of chlorite grain coatings in petroleum reservoirs: A review of subsurface examples. *Marine and Petroleum Geology*, *32*(1), 63–75. https://doi.org/10.1016/j.marpetgeo.2011.11.007

Dutton, S. P., Loucks, R. G., & Day-Stirrat, R. J. (2012). Impact of regional variation in detrital mineral composition on reservoir quality in deep to ultradeep lower Miocene sandstones, western Gulf of Mexico. *Marine and Petroleum Geology*, *35*(1), 139–153. https://doi.org/10.1016/j.marpetgeo.2012.01.006

El-Deek, I., Abdullatif, O., & Korvin, G. (2017). Heterogeneity analysis of reservoir porosity and permeability in the Late Ordovician glacio-fluvial Sarah Formation paleovalleys, central Saudi Arabia. *Arabian Journal of Geosciences*, *10*(18). https://doi.org/10.1007/s12517-017-3146-2

El Hajj, H., Suzart, W., Al Tammar, M., Al-Ghamdi, T., & Al-Abdullatif, A. (2015). Significance of clay mineralogy for reservoir quality prediction. *3rd EAGE/AAPG Workshop on Tight Reservoirs in the Middle East*, (October 2015), 13–15. https://doi.org/10.3997/2214-4609.201414105

Ehrenberg, S. N. (1993). Preservation of anomalously high porosity in deeply buried sandstones by grain-coating chlorite: examples from the Norwegian continental shelf. *AAPG Bulletin*, *77*(7), 1260-1286.

Fayek, M., Harrison, T. M., Grove, M., Mckeegan, K. D., Coath, C. D., & Boles, J. R. (2001). In situ Stable Isotopic Evidence for Protracted and Complex Carbonate Cementation in a Petroleum Reservoir, North Coles Levee, San Joaquin Basin,

California, U.S.A. *Journal of Sedimentary Research*, *71*(3), 444–458. https://doi.org/10.1306/2dc40954-0e47-11d7-8643000102c1865d

Folk, R. L. (1980). *Petrology of Sedimentary Rocks*.

Gani, M. R., Alam, M. M. (2003). Sedimentation and basin-fill history of the Neogene clastic succession exposed in the southeastern fold belt of the Bengal Basin, Bangladesh: A high-resolution sequence stratigraphic approach. *Sedimentary Geology*, *155*(3–4), 227–270. https://doi.org/10.1016/S0037-0738(02)00182-3

Gier, S., Worden, R. H., Johns, W. D., & Kurzweil, H. (2008). Diagenesis and reservoir quality of Miocene sandstones in the Vienna Basin, Austria. *Marine and Petroleum Geology*, *25*(8), 681–695. https://doi.org/10.1016/j.marpetgeo.2008.06.001

Giles M. R. , Stevenson, S., Martin, S.V., Cannon, S. J. C., Hamilton, P. J. (1992). The reservoir properties and diagenesis of the Brent Group: a regional perspective. *Geological Society, London*, *61*(Special), 289–327.

Grotzinger, J. P. (1986). Cyclicity and paleoenvironmental dynamics Rocknest platform, northwest Canada. *Geological Society of America Bulletin*, *97*(10), 1208–1231. https://doi.org/10.1130/0016-7606(1986)97<1208:CAPDRP>2.0.CO;2

Harrison III, C. W., & Dutton, S. P. (1991). Reservoir Characterization of the Frontier Tight Gas Sand, Green River Basin, Wyoming. In *Low Permeability Reservoirs Symposium*. Society of Petroleum Engineers

Hippler, S. J., Neal, J. E., Alramahi, B., Becker, S., & Klimentidis, R. E. (2013). Advanced analytical capabilities for optimizing exploitation of unconventional resources.

Society of Petroleum Engineers - International Petroleum Technology Conference 2013, IPTC 2013: Challenging Technology and Economic Limits to Meet the Global Energy Demand, *6*, 4686–4692. https://doi.org/10.2523/iptc-17042-ms

Imam, M. B., & Shaw, H. F. (1987). Diagenetic controls on the reservoir properties of gas bearing Neogene Surma Group sandstones in the Bengal Basin, Bangladesh. *Marine and petroleum geology*, *4*(2), 103-111.

Islam, M. A. (2009). Diagenesis and reservoir quality of Bhuban sandstones (Neogene), Titas Gas Field, Bengal Basin, Bangladesh. *Journal of Asian Earth Sciences*, *35*(1), 89–100. https://doi.org/10.1016/j.jseaes.2009.01.006

Johnson, S. Y., & Nur Alam, A. M. (1991). Sedimentation and tectonics of the Sylhet trough, Bangladesh. *Geological Society of America Bulletin*, *103*(11), 1513–1527. https://doi.org/10.1130/0016-7606(1991)103<1513:SATOTS>2.3.CO;2

Keller, W. D., Reynolds, R. C., & Inoue, A. (1986). Morphology of clay minerals in the smectite-to-illite conversion series by scanning electron microscopy. *Clays and Clay Minerals*, *34*(2), 187-197.

Khanam, F., Rahman, M. J. J., Alam, M. M., Abdullah, R. (2017). Facies characterization of the Surma Group (Miocene) sediments from Jalalabad gas field, Sylhet trough, Bangladesh: Study from cores and wireline log. *Journal of the Geological Society of India*, *89*(2), 155–164. https://doi.org/10.1007/s12594-017-0579-x

Klein, G. D. (1985). *Sandstone depositional models for exploration of fossil fuels* (3rd ed.). D. Reidal Publ. Co., Holland,.

Klimentidis, R. E., Paxton, S. T., & State, O. (2002). Intergranular Volume. *AAPG Bulletin*, *c*(12), 2047–2067.

Land, L. S., & Dutton, S. P. (1978). Diagenetic Mineralogy Detrital Mineralogy. *Society*, *48*(4), 1167–1176.

Lietz, J. K. (1982). Prospects and constraints of oil exploration in Bangladesh. *Society of Petroleum Engineers - Offshore South East Asia Show, SEA 1982*.

Mahgoub, M. I., Padmanabhan, E., Abdullatif, O. M. (2016). Sedimentological reservoir characteristics of the Paleocene fluvial/lacustrine Yabus Sandstone, Melut Basin, Sudan. *Journal of African Earth Sciences*, *123*, 75–88. https://doi.org/10.1016/j.jafrearsci.2016.06.018

Matlack, K. S., Houseknecht, D. W., Applin, K. R. (1989). Emplacement of clay into sand by infiltration. *Journal of Sedimentary Petrology*, *59*(1), 77–87. https://doi.org/10.1306/212F8F21-2B24-11D7-8648000102C1865D

Maurice E. Tucker. (2001). *Sedimentary Petrology: An Introduction to the Origin of Sedimentary Rocks* (3rd ed.). Wiley-Blackwell.

McIlroy, R. H. W., S. J. N. (2003). Faeces, clay minerals and reservoir potential. *Journal of the Geological Society*, (160), 489–493.

McBride, E. F. (1991). Petrology of the sedimentary rocks. *Geomorphology*, *4*(2), 156–157. https://doi.org/10.1016/0169-555x(91)90027-8

McLennan, S. M., Hemming, S., McDaniel, D. K., & Hanson, G. N. (1993). Geochemical approaches to sedimentation, provenance, and tectonics. *Special Papers-Geological Society of America*, 21-21.

Miah, M. I. (2014). Porosity assessment of gas reservoir using wireline log data: A case study of bokabil formation, Bangladesh. *Procedia Engineering*, *90*(January), 663–668. https://doi.org/10.1016/j.proeng.2014.11.789

Morad, S., Ketzer, J. M., & De Ros, L. R. (2000). Spatial and temporal distribution of diagenetic alterations in siliciclastic rocks: Implications for mass transfer in sedimentary basins. *Sedimentology*, *47*(SUPPL. 1), 95–120. https://doi.org/10.1046/j.1365-3091.2000.00007.x

Morad, S., & De Ros, L. F. (1994). Geochemistry and diagenesis of stratabound calcite cement layers within the Rannoch Formation of the Brent Group, Murchison Field, North Viking Graben (northern North Sea)—comment. *Sedimentary Geology*, *93*(1-2), 135-141.

Moraes, M. A. S., & De Ros, L. F. (1990). Infiltrated clays in fluvial Jurassic sandstones of Reconcavo Basin, northeastern Brazil. *Journal of Sedimentary Petrology*, *60*(6), 809–819. https://doi.org/10.1306/212F928C-2B24-11D7-8648000102C1865D

Moraes, M. A. S., & De Ros, L. F. (1992). Depositional, Infiltrated and Authigenic Clays in Fluvial Sandstones of the Jurassic Sergi Formation, Recôncavo Basin, Northeastern Brazil. *Origin, Diagenesis, and Petrophysics of Clay Minerals in Sandstones*, (June), 197–208. https://doi.org/10.2110/pec.92.47.0197

Morton-Thompson, D., & Woods, A. M. (Eds.). (1993). *Development geology reference manual: AAPG methods in exploration series, no. 10* (No. 10). AAPG.

Murkute, Y. A. (2001). Kamthi sandstones: Grain size distribution and depositional processes. *JOURNAL-GEOLOGICAL SOCIETY OF INDIA*, *58*(5), 435-440.

Needham, S. J., Worden, R. H., & McIlroy, D. (2005). Experimental Production of Clay Rims by Macrobiotic Sediment Ingestion and Excretion Processes. *Journal of Sedimentary Research*, *75*(6), 1028–1037. https://doi.org/10.2110/jsr.2005.078

Panel, G.S., Odin, J.P., Debenay, J. P., Masse, A. (1988). Chapter B4 The Verdine Facies Deposits Identified in 1988. *Developments in Sedimentology*, *45*, 131–158.

Raaf , J.E.M. and Boersma, J. R. (1971). Tidal deposits and their sedimentary structures. *Geologie En Mijnbouw*, *50*, 479–503.

Rahman, M. J. J., & Worden, R. H. (2016). Diagenesis and its impact on the reservoir quality of Miocene sandstones (Surma Group) from the Bengal Basin, Bangladesh. *Marine and Petroleum Geology*, *77*(September 2017), 898–915.

Rahman, M. J. J., Faupl, P., & Alam, M. M. (2009). Depositional facies of the subsurface Neogene Surma Group in the Sylhet Trough of the Bengal Basin, Bangladesh: Record of tidal sedimentation. *International Journal of Earth Sciences*, *98*(8), 1971–1980.

Rahman, M. J. J., & McCann, T. (2012). Diagenetic history of the Surma Group sandstones (Miocene) in the Surma Basin, Bangladesh. *Journal of Asian Earth Sciences*, *45*, 65–78.

Rahman, M. J. J., Xiao, W., McCann, T., & Songjian, A. (2017a). Provenance of the Neogene Surma Group from the Chittagong Tripura Fold Belt, southeast Bengal Basin, Bangladesh: Constraints from whole-rock geochemistry and detrital zircon U-Pb ages. *Journal of Asian Earth Sciences*, *148*(September 2016), 277–293.

Rahman, M. J. J., Xiao, W., McCann, T., & Songjian, A. (2017b). Provenance of the Neogene Surma Group from the Chittagong Tripura Fold Belt, southeast Bengal Basin, Bangladesh: Constraints from whole-rock geochemistry and detrital zircon U-Pb ages. *Journal of Asian Earth Sciences*, *148*(September), 277–293. https://doi.org/10.1016/j.jseaes.2017.09.010

Rahman, M Julleh Jalalur, Faupl, P., & Alam, M. M. (2009). *Depositional facies of the subsurface Neogene Surma Group in the Sylhet Trough of the Bengal Basin , Bangladesh : Record of tidal sedimentation Depositional facies of the subsurface Neogene Surma Group in the Sylhet Trough of the Bengal Basin , Bangladesh*. (December). https://doi.org/10.1007/s00531-008-0347-7

Reading, H. G. (1986). *Sedimentary Environment and Facies*.

Reineck, H.E., Singh, I. B. (1980). *Depositional Sedimentary Environments*.

Samad, A., Rahman, J. J., & Woobaidullah, A. S. M. (2015). *Reservoir Characterization of Different Gas Fields in Eastern Fold Belt of Bangladesh*. *5*(2).

Schmid, S., Worden, R. H., & Fisher, Q. J. (2004). Diagenesis and reservoir quality of the Sherwood Sandstone (Triassic), Corrib Field, Slyne Basin, west of Ireland. *Marine and Petroleum Geology*, *21*(3), 299–315.

Schmidt, V., & McDonald, D. A. (1979). The role of secondary porosity in the course of sandstone diagenesis.

Sultana, D. N. and A. (2001). Facies Analysis of the Neogene Surma Group Succession in the Subsurface of the Sylhet Trough, Bengal Basin, Bangladesh. *Bangladesh Geoscience Jour*, *6*, 53–74.

Uddin, A., & Lundberg, N. (2004). Miocene sedimentation and subsidence during continent-continent collision, Bengal basin, Bangladesh. *Sedimentary Geology*, *164*(1–2), 131–146. https://doi.org/10.1016/j.sedgeo.2003.09.004

Van Wagoner, J. C., Mitchum, R. M., Campion, K. M., & Rahmanian, V. D. (1990). Siliciclastic sequence stratigraphy in well logs, cores, and outcrops: concepts for high-resolution correlation of time and facies.

Weltje, G. J. (2006). Ternary sandstone composition and provenance: an evaluation of the 'Dickinson model'. *Geological Society, London, Special Publications*, *264*(1), 79-99.

Worden, R. H., & Morad, S. (2009). Quartz Cementation in Oil Field Sandstones: A Review of the Key Controversies. *Quartz Cementation in Sandstones*, 1–20. https://doi.org/10.1002/9781444304237.ch1

Worden, R. S. M. (2003). *Clay Mineral Cements in Sandstones*.

Worden, R. H., Needham, S. J., & Cuadros, J. (2006). The worm gut; a natural clay mineral factory and a possible cause of diagenetic grain coats in sandstones. *Journal of Geochemical Exploration*, *89*(1-3 SPEC. ISS.), 428–431.

Worden, S. A. B. and R. H. (2000). Geochemical modelling of diagenetic reactions in a sub-arkosic sandstone. *Clay Minerals*, *35*(1), 57–67.

Zahid, K. M., & Barbeau, D. L. (2012). Constructing Sandstone Provenance and Classification Ternary Diagrams Using An Electronic Spreadsheet. *Journal of Sedimentary Research*, *82*(2), 131–132. https://doi.org/10.2110/jsr.2012.12

Zhang, P., Lee, Y. Il, & Zhang, J. (2015). Diagenesis of tight-gas sandstones in the lower cretaceous denglouku formation, songliao basin, NE China: Implications for reservoir quality. *Journal of Petroleum Geology*, *38*(1), 99–114. https://doi.org/10.1111/jpg.12600

Vitae

Name : Kazi Faiz Alam

Nationality : Bangladeshi (by born)

Date of Birth :8/10/1982

Email : alamfaiz906@gmail.com

Address : Manager (Geology), Geological Division, 10th floor, BAPEX Bhaban, 4-Karwan bazar, Dhaka-1205, Bangladesh.

Academic Background : Bachelor in Geological Sciences from Jahangirnagar University, Savar, Dhaka, Bangladesh.

Research Interest: Reservoir characterization, well site geology, NMR

Publications :

- Alam, K., El-Husseiny, A., Abdullatif, O., & Babalola, L. (2019, June). Petrophysical Evaluation of Prospective Reservoir Zones in Srikail Gas Field, Bengal Basin Bangladesh. In 81st EAGE Conference and Exhibition 2019 (Vol. 2019, No. 1, pp. 1-5). European Association of Geoscientists & Engineers.

- Cavity and Fracture Detection Using GPR and EM Methods: Comparison with Surface Features of the Rus Formation, KFUPM campus, Saudi Arabia. Geophysical Research Abstracts, Vol. 21, EGU2019-12650, 2019, EGU General Assembly 2019.